NPS-62-90-009

NAVAL POSTGRADUATE SCHOOL
Monterey, California

THESIS

AN ANALYSIS OF MLAYER: A MULTILAYER TROPOSPHERIC PROPAGATION PROGRAM

by

Lean-Weng Yeoh

June 1990

Thesis Advisor: Hung-Mou Lee

Prepared for: The Chief of Naval Operations (OP-03B)
Pentagon
Washington, DC 20350

NAVAL POSTGRADUATE SCHOOL
Monterey, California

Rear Admiral Ralph W. West, JR.
Superintendent

Harrison Shull
Provost

This report was prepared in conjunction with research conducted for the Chief of Naval Operations (OP-3B), Pentagon, Washington, DC 20350 and funded by the Naval Postgraduate School.

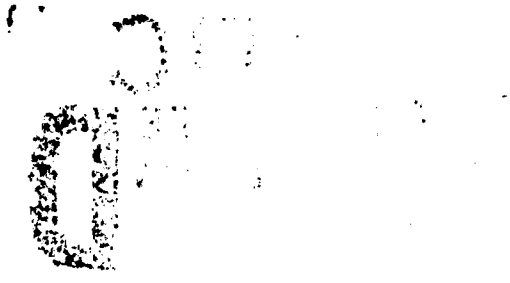

Released by:

Richard L. Elster, for

Dean of Faculty and Graduate Studies

DISCLAIMER NOTICE

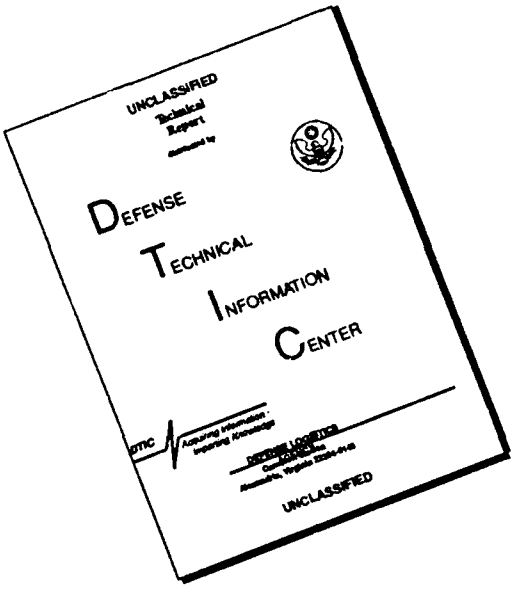

THIS DOCUMENT IS BEST QUALITY AVAILABLE. THE COPY FURNISHED TO DTIC CONTAINED A SIGNIFICANT NUMBER OF PAGES WHICH DO NOT REPRODUCE LEGIBLY.

Unclassified

security classification of this page

REPORT DOCUMENTATION PAGE

1a Report Security Classification: Unclassified	1b Restrictive Markings
2a Security Classification Authority	3 Distribution Availability of Report: Approved for public release; distribution is unlimited.
2b Declassification Downgrading Schedule	
4 Performing Organization Report Number(s)	5 Monitoring Organization Report Number(s)
6a Name of Performing Organization: Naval Postgraduate School; 6b Office Symbol (if applicable): EC	7a Name of Monitoring Organization: Office of the Chief of Naval Operations (OP-03B)
6c Address (city, state, and ZIP code): Monterey, CA 93943-5000	7b Address (city, state, and ZIP code): Pentagon, Washington, D.C. 20350
8a Name of Funding Sponsoring Organization: Naval Postgraduate School; 8b Office Symbol (if applicable): EC	9 Procurement Instrument Identification Number: O&MN, Direct Funding
8c Address (city, state, and ZIP code): Monterey, CA 93943-5000	10 Source of Funding Numbers: Program Element No | Project No | Task No | Work Unit Accession No

11 Title (include security classification): AN ANALYSIS OF MLAYER : A MULTILAYER TROPOSPHERIC PROPAGATION PROGRAM. (Unclassified)

12 Personal Author(s): Lean-Weng Yeoh

13a Type of Report	13b Time Covered	14 Date of Report (year, month, day)	15 Page Count
Master's Engineer's Thesis	From To	June 1990	158

16 Supplementary Notation: The views expressed in this thesis are those of the author and do not reflect the official policy or position of the Department of Defense or the U.S. Government.

17 Cosati Codes			18 Subject Terms (continue on reverse if necessary and identify by block number)
Field	Group	Subgroup	Tropospheric duct propagation, computer program documentation.

19 Abstract (continue on reverse if necessary and identify by block number)

MLAYER, a computer program, was developed by the Naval Ocean Systems Center (NOSC) for calculating the signal levels of electromagnetic waves propagating in a multilayer tropospheric waveguide environment over seawater. The program is an extension of the XWVG which is a trilinear ducting program. Modifications of the XWVG were carried out to handle multilayer tropospheric ducts.

A number of modifications and improvements on the program made over the past several years were not documented. A detailed documentation of MLAYER was also not available. The objective of this study is to develop a technical documentation for MLAYER using the program as baseline. The study aims to put together the theoretical formulations (specific to MLAYER) into a complete self-contained document. This is to facilitate potential users with better appreciation of the capabilities, limitations, approximations and assumptions used in the mathematical modelling techniques. As far as possible, the same terminologies and functional variables used by Baumgartner (in the XWVG development) and by Pappert (in the MLAYER development) are adopted to enable one to relate this document to the program. Step-by-step derivation of certain equations was carried out and checked for compatibility with the algorithm in the program. An in-depth scrutiny of each program element was also conducted and a description for each is provided. As a result of a detailed analysis of the respective algorithm in the program, the documentation for the evaluation of the modal function was eventually prepared. Additional materials were gathered from technical reports and papers to supplement the development of this document.

The MLAYER supporting programs (Microsoft program maintenance utility "makefiles") were modified to enable the program to run on Microsoft FORTRAN version 5.0. MLAYER was tested and ran successfully on Microsoft FORTRAN version 5.0. and C compilers version 5.0.

20 Distribution Availability of Abstract	21 Abstract Security Classification	
☒ unclassified unlimited ☐ same as report ☐ DTIC users	Unclassified	
22a Name of Responsible Individual: Hung-Mou Lee	22b Telephone (Include Area code): (408) 646-2846	22c Office Symbol: EC Lh

DD FORM 1473,84 MAR

83 APR edition may be used until exhausted
All other editions are obsolete

security classification of this page

Unclassified

Approved for public release; distribution is unlimited.

An Analysis of MLAYER : A Multilayer Tropospheric Propagation Program.

by

Lean-Weng Yeoh
Ministry of Defence, Singapore
B.ENG.(Hons), National University of Singapore, 1983
MSc(EE), National University of Singapore, 1987

Submitted in partial fulfillment of the requirements for the degrees of

MASTER OF SCIENCE IN ELECTRICAL ENGINEERING
and
ELECTRICAL ENGINEER

from the

NAVAL POSTGRADUATE SCHOOL
June 1990

Author: _____
Lean-Weng Yeoh

Approved by: _____
Hung-Mou Lee, Thesis Advisor

_____
Richard W. Adler, Second Reader

_____
John P. Powers, Chairman,
Department of Electrical and Computer Engineering

_____
Dean of Faculty and Graduate Studies

ABSTRACT

MLAYER, a computer program, was developed by the Naval Ocean Systems Center (NOSC) for calculating the signal levels of electromagnetic waves propagating in a multilayer tropospheric waveguide environment over seawater. The program is an extension of the XWVG which is a trilinear ducting program. Modifications of the XWVG were carried out to handle multilayer tropospheric ducts.

A number of modifications and improvements on the program made over the past several years were not documented. A detailed documentation of MLAYER was also not available. The objective of this study is to develop a technical documentation for MLAYER using the program as baseline. The study aims to put together the theoretical formulations (specific to MLAYER) into a complete self-contained document. This is to facilitate potential users with better appreciation of the capabilities, limitations, approximations and assumptions used in the mathematical modelling techniques. As far as possible, the same terminologies and functional variables used by Baumgartner (in the XWVG development) and by Pappert (in the MLAYER development) are adopted to enable one to relate this document to the program. Step-by-step derivation of certain equations was carried out and checked for compatibility with the algorithm in the program. An in-depth scrutiny of each program element was also conducted and a description for each is provided. As a result of a detailed analysis of the respective algorithm in the program, the documentation for the evaluation of the modal function was eventually prepared. Additional materials were gathered from technical reports and papers to supplement the development of this document.

The MLAYER supporting programs (Microsoft program maintenance utility "makefiles") were modified to enable the program to run on Microsoft FORTRAN version 5.0. MLAYER was tested and ran successfully on Microsoft FORTRAN version 5.0. and C compilers version 5.0.

Table of Contents

List of Tables

List of Figures

ACKNOWLEDGEMENTS

The author wishes to express his sincere gratitude to Professor Hung-Mou Lee for his professional guidance, invaluable advice and moral support throughout the thesis preparation period. Credit is also given to Dr. Richard A. Pappert and Mr. Ken Anderson of NOSC for making available the MLAYER program, technical reports and papers relevant to MLAYER.

Finally, special thanks are due to Professors Richard W. Adler and John P. Powers for their review and constructive suggestions to the thesis work.

I. INTRODUCTION

Propagation of radio waves through the troposphere is strongly affected by the complex nature of this propagation medium. The effects on radio wave propagation are due to changes in the refractive index with height, absorption by the atmosphere and its constituent gases, attenuation and scattering due to climatic conditions.

Although weather conditions could result in attenuation of radio wave transmission through the absorption of energy by gases, water vapour or scattering by rain, certain meteorological conditions can lead to an enhancement of signal strength. This peculiar phenomenon known as ducting is due to the inversions of the refractive index profile. Propagation in a tropospheric duct can result in an unusual increase in range.

To predict the anomalous propagation effects, knowledge of the characteristics of the refractive index and its effects on propagated fields is required. In the mathematical formulation of the model, the concept of modified index of refraction is used to describe wave propagation over a flat earth.

In a uniform atmosphere with constant index of refraction, electromagnetic waves travel in straight lines over the curved surface of the earth. This situation is unaltered if the earth is considered as flat and the rays curved, provided the relative curvature between the earth and the rays is preserved. To account for the upward bending of rays over the flat earth, the constant index of refraction is transformed to a modified index which increases with height and is given by

$$m(z) = n + \frac{z}{a} \quad , \tag{1}$$

where n is the index of refraction, z is the height above the surface of the earth and a is the radius of the earth. Equation 1 is still valid in a stratified atmosphere where the index of refraction is a function of height. In this case, n is replaced by n(z) in Equation 1.

The modified index concept allows one to transform a spherically stratified refractive structure into a planar layer by preserving the relative curvature between the normal of the radio-wavefront and the earth's surface. Therefore wave propagation over a spherical earth can be reduced to that over a flat earth if the index of refraction is replaced by the modified index of refraction. For $z/a \ll 1$, the angle of inclination of a ray

at any point in space and the distance (optical length) along the ray path will remain invariant in the transformation.

The flat-earth approximation is adopted in MLAYER [Ref. 1 and 2]. This approximation considerably simplifies the mathematical solution of the problem. The accuracy of the flat-earth approximation was investigated by Pekeris [Ref. 3]. It was found that for a standard atmosphere, the fractional error in the height gain function is approximately

$$e = \frac{2\pi\sqrt{6}}{5} \frac{z^{5/2}}{\lambda a^{3/2}} \quad . \tag{2}$$

Equation 2 shows that the flat-earth approximation will break down at high frequency and at great height above the earth's surface. For example, a 10 GHz signal at a height of 2000 m will give a fractional error of approximately 114%. The work of Pekeris also indicates that the flat-earth approximation is valid to within two percent for ranges up to about one-half of the radius of the earth [Ref. 3] .

As typical values of m(z) differ from unity by about 300 parts per million, it is sometimes more convenient to introduce the modified refractivity to describe the phenomena involved in the formation of tropospheric ducts. The modified refractivity is defined as

$$M(z) = [m(z) - 1] \times 10^6 \quad . \tag{3}$$

In this program, the modified refractivity profile of the troposphere is modelled as a series of continous piecewise linear segments (see Figure 1).

The linear approximation simplifies mathematical manipulations to a large extent. In general, any complicated profile can be approximated by several linear segments and the accuracy of the modelling can be improved by increasing the number of linear segments and reducing the thickness of each layer.

If $M_i(z)$ is the value of the modified refractivity in the i^{th} layer, then for a linear modified refractivity profile,

$$M_i(z) = M(z_i) + \frac{dM_i}{dz}(z - z_i) \quad ; \qquad z_i \leq z \leq z_{i+1} \quad . \tag{4}$$

From Equation 3, the square of the modified index of refraction is

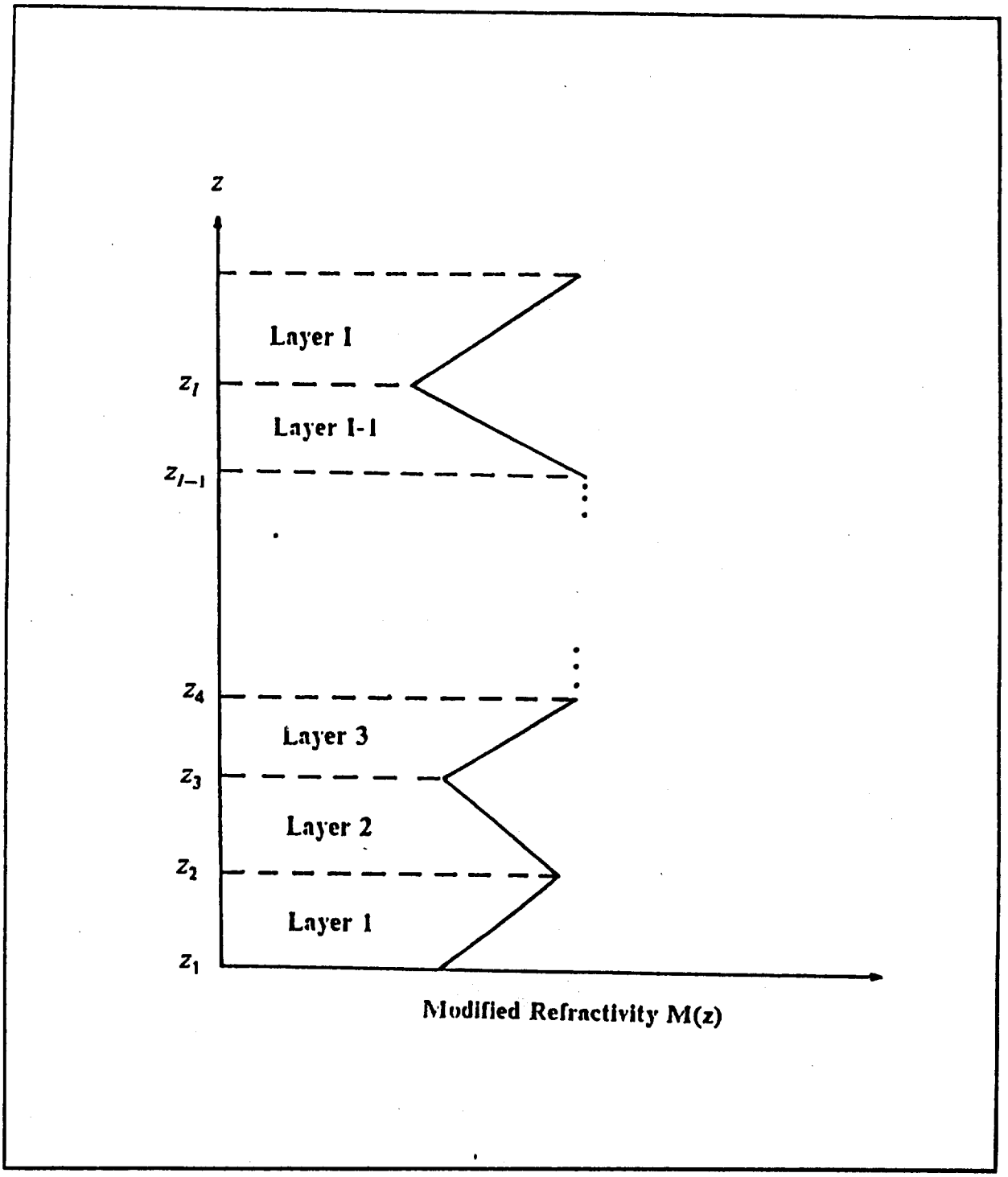

Figure 1. Multiple piecewise linear modified refractivity profile

$$m_i^2(z) \simeq 1 + 2 \times 10^{-6} M_i(z) - j\eta_i \quad , \tag{5}$$

where η_i is introduced to account for attenuation of the signal due to the absorption by atmospheric gases. The derivative of $m_i^2(z)$ is given by

$$\begin{aligned} \frac{d}{dz}\{m_i^2(z)\} &\simeq 2 \times 10^{-6} \frac{dM_i(z)}{dz} - j\frac{d\eta_i}{dz} \\ &\equiv \alpha_i \quad . \end{aligned} \tag{6}$$

Equations 4, 5 and 6 will be used in the mathematical model to represent the characteristics of the propagation medium.

MLAYER also incorporates in the solution of the modal function, the effects of surface roughness, atmospheric absorption and the variation of the complex index of refraction of seawater as a function of temperature, salinity and frequency.

The program uses the Shellman-Morfitt complex root-finding routine to locate the modes that propagate in the tropospheric ducts. This routine attempts to find all waveguide modes with attenuation rates below a user-specified value.

Overflow problems commonly encountered in the evaluation of the modal function are avoided by performing numerical computations with extended complex arithmetic.

II. MATHEMATICAL FORMULATION OF THE MODEL

A. HORIZONTALLY POLARIZED WAVE PROPAGATION

In formulating the problem, the flat-earth approximation with modified index of refraction is adopted. The cylindrical coordinate system, (r, ϕ, z), is used. The vertical height, z, is measured from the surface of the flat-earth.

A horizontally polarized source may be approximated as a radiating magnetic dipole oriented in the z direction and located at r = 0 and $z = z_T$. The magnetic Hertz vector associated with the dipole is given by

$$\vec{\Pi}(r, z) = \Pi(r, z)\,\hat{z} \quad , \tag{7}$$

where $\Pi(r, z)$ satisfies the following equation:

$$\nabla^2 \Pi(r, z) + k^2 m^2(z)\,\Pi(r, z) = -4\pi\,\{\delta(x)\,\delta(y)\,\delta(z - z_T)\} \quad , \tag{8}$$

where k is the wave number in free space, $\delta(.)$ is the Dirac delta function and z_T is the location of the source. The right hand side of Equation 8 corresponds to a point source of strength -4π located at r = 0 and $z = z_T$. The time dependence $e^{j\omega t}$ is assumed throughout this thesis.

The electric and magnetic field can be expressed in terms of the Hertz vector as

$$\vec{E} = -j\omega\mu_0 \vec{\nabla} \times \vec{\Pi} \tag{9}$$

and

$$\vec{H} = \vec{\nabla} \times \vec{\nabla} \times \vec{\Pi} \quad , \tag{10}$$

where μ_0 is the free space permeability. Solution to Equation 8 can be represented as a contour integral:

$$\Pi(r, z) = \frac{1}{2} \int_C \rho d\rho H_0^{(2)}(r\rho) f(\rho, z) \quad , \tag{11}$$

where $H_0^{(2)}(r\rho)$ is the zeroth-order Hankel function of the second kind and $f(\rho, z)$ is the height gain function. The contour of integration, C, as shown in Figure 2 can be deformed into C_1 and C_2, also shown in Figure 2.

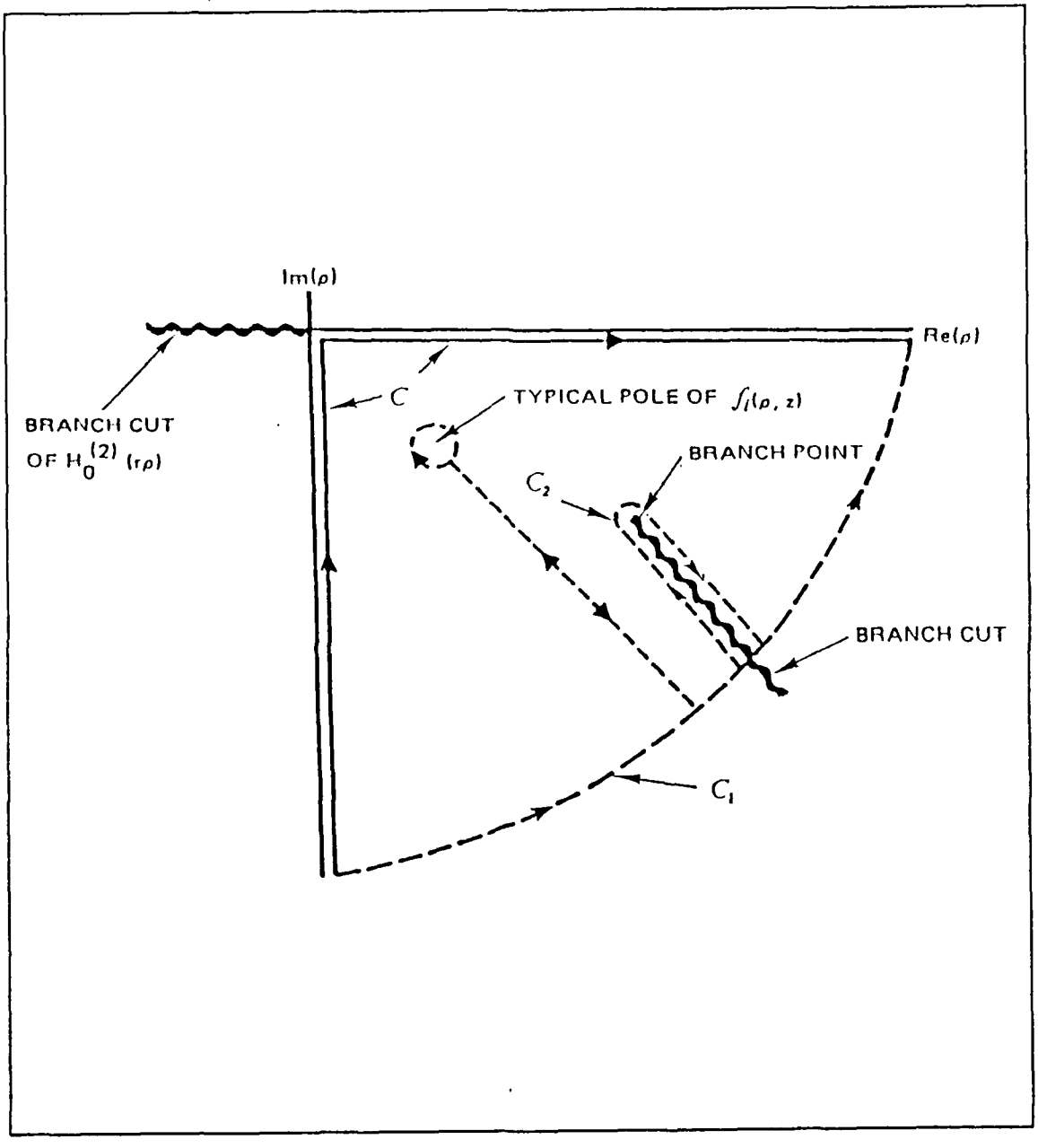

Figure 2. Contour of integration of Equation 11 [After Ref. 1]

The height gain function in the i^{th} tropospheric layer, denoted as $f_i(\rho, z)$, satisfies the following differential equation:

$$\left\{ \frac{\partial^2}{\partial z^2} + k^2 \left[m_i^2(z) - \frac{\rho^2}{k^2} \right] \right\} f_i(\rho, z) = -2\pi\delta(z - z_T) \quad . \tag{12}$$

In the ground, the height gain function, $f_g(\rho, z)$, is given by the solution of the following equation:

$$\left\{ \frac{\partial^2}{\partial z^2} + k^2 \left[n_g^2 - \frac{\rho^2}{k^2} \right] \right\} f_g(\rho, z) = 0 \quad , \tag{13}$$

where n_g is the complex index of refraction of the ground and is related to the relative permitivity, ε_g, and conductivity, σ_g, of the ground as

$$n_g^2 = \varepsilon_g - j\frac{\sigma_g}{\varepsilon_0 \omega} \quad . \tag{14}$$

The height gain function, $f_g(\rho, z)$, must represent an outgoing exponentially decaying wave as $z \to -\infty$, i.e.,

$$f_g(\rho, z) = A_g e^{j\gamma z} \quad , \tag{15}$$

where

$$\gamma = k\sqrt{n_g^2 - \beta^2} \tag{16}$$

and

$$\beta = \frac{\rho}{k} \quad . \tag{17}$$

For the wave to attenuate into the ground, the branch of the square root in Equation 16 should be chosen such that

$$Im(\gamma) < 0 \quad . \tag{18}$$

If the ground is not dissipative, the branch point and the integration contour satisfying Equation 18 is shown in Figure 3.

Continuity of the tangential components of $\vec{E}$ and $\vec{H}$ at each layer boundary requires that

$$f_g(\rho, 0) = f_1(\rho, 0) \quad , \tag{19}$$

$$\frac{\partial}{\partial z}\{f_g(\rho, 0)\} = \frac{\partial}{\partial z}\{f_1(\rho, 0)\} \quad , \tag{20}$$

$$f_i(\rho, z_{i+1}) = f_{i+1}(\rho, z_{i+1}) \quad ; \quad i = 1 \text{ to } I-1 \tag{21}$$

and

$$\frac{\partial}{\partial z}\{f_i(\rho, z_{i+1})\} = \frac{\partial}{\partial z}\{f_{i+1}(\rho, z_{i+1}) \quad ; \quad i = 1 \text{ to } I-1 \quad . \tag{22}$$

Define

$$q_i = \left[\frac{k}{\alpha_i}\right]^{2/3}\left[m^2(z_i) + \alpha_i(z - z_i) - \beta^2\right] \tag{23}$$

and with a change of variable, the solution to Equation 12 can be expressed as a linear combination of $k_1(q_i)$ and $k_2(q_i)$, satisfying

$$\left[\frac{\partial^2}{\partial q_i^2} + q_i\right] k_n(q_i) = 0 \qquad ; \quad n = 1, 2 \quad . \tag{24}$$

This is Stokes' differential equation. For i ≠ I

$$f_i(\rho, z) = B_i(\rho)\left[A_i(\rho)k_1(q_i) + k_2(q_i)\right] \quad , \tag{25}$$

where $k_1(q_i)$ and $k_2(q_i)$ are proportional to the Airy functions

$$k_1(q_i) \sim Ai(-q_i e^{j2\pi/3}) \tag{26}$$

and

$$k_2(q_i) \sim Ai(-q_i) \quad . \tag{27}$$

Note that the A_i's and B_i's are different from those in Reference 2 where the height gain function is expressed as $B_i(k_1 + A_i k_2)$. Equation 25 corresponds to that implemented in the program.

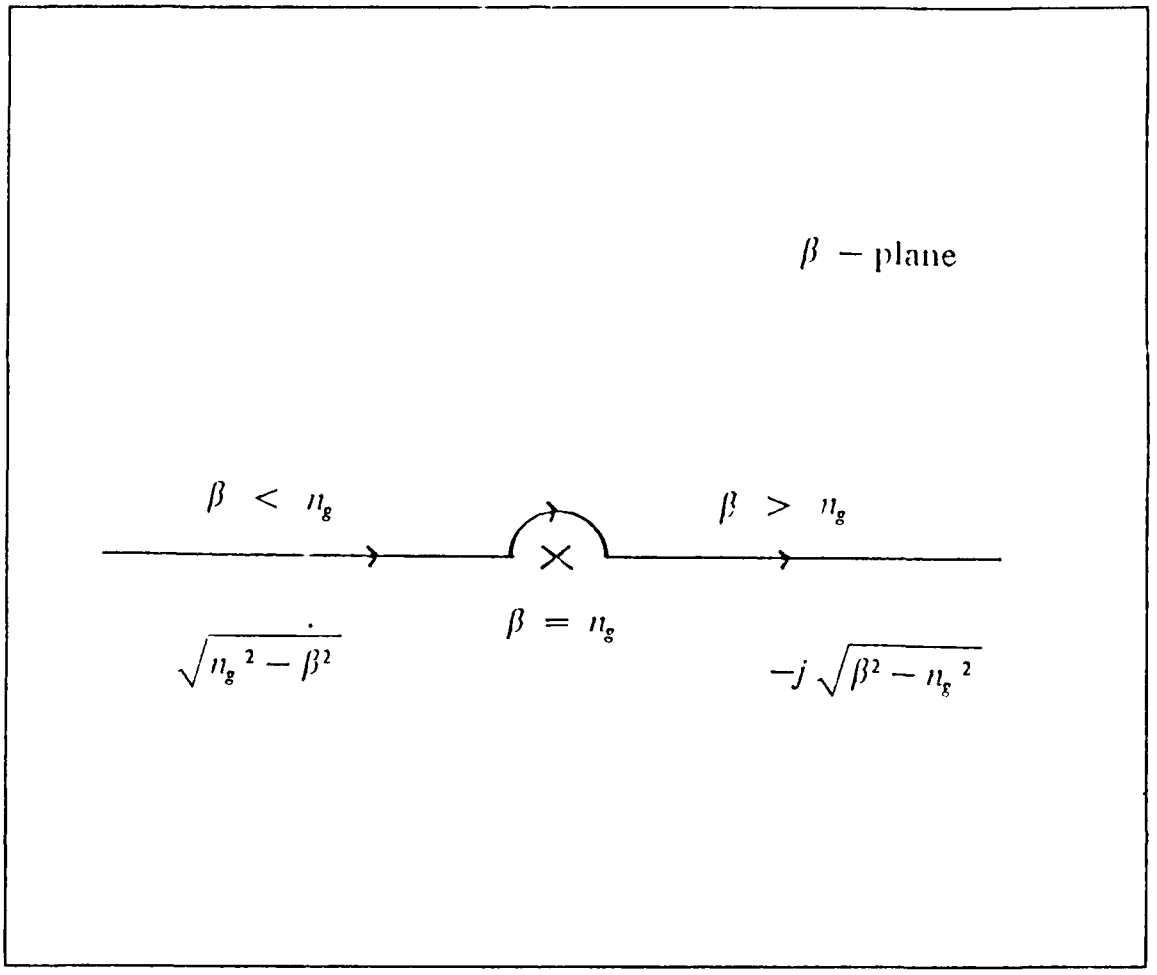

Figure 3. Branch of $\sqrt{n_g^2 - \beta^2}$

The constants of proportionality of Equations 26 and 27 are of no consequence as they affect only $B_i(\rho)$ and $A_i(\rho)$ of Equation 25 but not $f_i(\rho, z)$. The height gain functions, $f_i(\rho, z)$, used in the computations of the mode sum and path loss are normalized as in Equation 77. The solution of Stokes' equation is discussed i Chapter IV.

For the highest layer, i= I, the height gain function is given by

$$f_I(\rho, z) = B_I(\rho)\, h_2(q_I) \quad , \tag{28}$$

where $h_2(q_I)$ is the modified Hankel function of order one-third and is proprotional to the Airy function as

$$h_2(q_I) \sim Ai(-q_I\, e^{-j2\pi/3}) \quad . \tag{29}$$

As in Equations 26 and 27, the constant of proportionality of Equation 29 is also omitted in the program.

Equation 25 represents the solution of $f(\rho, z)$ for every layer except the one in which the source is located. In the layer where the source is located, the height gain function is given by

$$f_i(\rho, z) = B_i(\rho)\,[A_i(\rho)\,k_1(q_i) + k_2(q_i)] + f^{(s)}(\rho, q_i) \quad , \tag{30}$$

where $f^{(s)}(\rho, q)$ is the particular solution of the inhomogenous Equation 12. Therefore the complete solutions of $f_i(\rho, z)$ are given by

$$f_i(\rho, z) = B_i(\rho)\,[A_i(\rho)k_1(q_i) + k_2(q_i)] + f^{(s)}(\rho, q_i)\,\delta_{iM} \quad ; \; i = 1 \text{ to } I-1 \tag{31}$$

and

$$f_i(\rho, z) = B_i(\rho)h_2(q_i) + f^{(s)}(\rho, q_i)\,\delta_{iM} \quad ; \quad i = I \quad , \tag{32}$$

where

$$\delta_{iM} = \begin{cases} 1 & i = M \\ 0 & i \neq M \end{cases} \quad . \tag{33}$$

It is assumed that the source is located in the M^{th} layer.

Continuity of $f(\rho, z)$ and $\frac{\partial}{\partial z} f(\rho, z)$ at the ground level requires that

$$A_g = B_1[A_1 k_1(q_{1,1}) + k_2(q_{1,1})] + f^{(s)}(\rho, q_{1,1})\,\delta_{1M} \tag{34}$$

and

$$j\gamma_1 A_g = B_1[A_1 k'_1(q_{1,1}) + k'_2(q_{1,1})]\left[\frac{k}{\alpha_1}\right]^{2/3}\alpha_1 + \frac{\partial}{\partial z}[f^{(s)}(\rho, q_{1,1})]\,\delta_{1M} \quad . \tag{35}$$

From Equations 34 and 35,

$$\left\{\left(\frac{k}{\alpha_1}\right)^{2/3}\alpha_1 k'_1(q_{1,1}) - j\gamma_1 k_1(q_{1,1})\right\}B_1 A_1 + \left\{\left(\frac{k}{\alpha_1}\right)^{2/3}\alpha_1 k'_2(q_{1,1}) - j\gamma_1 k_2(q_{1,1})\right\}B_1 = j\gamma_1 f^{(s)}(\rho, q_{1,1})\,\delta_{1M} - \frac{\partial}{\partial z}[f^{(s)}(\rho, q_{1,1})]\,\delta_{1M} \quad . \tag{36}$$

Similiarly, at layer boundaries, i = 1 to I-2,

$$
\begin{aligned}
B_i\,[A_i\,k_1(q_{i,i+1}) + k_2(q_{i,i+1})] \;+\; & f^{(s)}(\rho, q_{i,i+1})\,\delta_{iM} \\
&= B_{i+1}[A_{i+1}\,k_1(q_{i+1,i+1}) + k_2(q_{i+1,i+1})] \\
&\quad + f^{(s)}(\rho, q_{i+1,i+1})\,\delta_{i+1,M}
\end{aligned}
\tag{37}
$$

and

$$
\begin{aligned}
B_i\,[A_i\,k'_1\,(q_{i,i+1}) + k'_2\,(q_{i,i+1})] & \left[\frac{k}{\alpha_i}\right]^{2/3}\alpha_i \\
&+ \frac{\partial}{\partial z}\,[f^{(s)}(\rho, q_{i,i+1})]\,\delta_{iM} \\
&= B_{i+1}\,[A_{i+1}\,k'_1(q_{i+1,i+1}) + k'_2(q_{i+1,i+1})]\left[\frac{k}{\alpha_{i+1}}\right]^{2/3}\alpha_{i+1} \\
&+ \frac{\partial}{\partial z}\,[f^{(s)}\,(\rho, q_{i+1,\,i+1})]\,\delta_{i+1,M}\quad .
\end{aligned}
\tag{38}
$$

From Equation 37,

$$
\begin{aligned}
k_1(q_{i,i+1})\,B_i A_i \;+\; & k_2(q_{i,i+1})B_i \\
&- k_1(q_{i+1,i+1})B_{i+1}\,A_{i+1} - k_2(q_{i+1,\,i+1})B_{i+1} \\
&= f^{(s)}\,(\rho, q_{i+1,\,i+1})\,\delta_{i+1,M} - f^{(s)}(\rho, q_{i,\,i+1})\,\delta_{iM}\quad .
\end{aligned}
\tag{39}
$$

From Equation 38,

$$
\begin{aligned}
k'_1(q_{i,\,i+1})\left(\frac{k}{\alpha_i}\right)^{2/3}\alpha_i\,B_i\,A_i \;+\; & k'_2(q_{i,\,i+1})\left(\frac{k}{\alpha_i}\right)^{2/3}\alpha_i\,B_i \\
&- k'_1(q_{i+1,\,i+1})\left(\frac{k}{\alpha_{i+1}}\right)^{2/3}\alpha_{i+1}\,B_{i+1}\,A_{i+1} \\
&- k_2(q_{i+1,\,i+1})\left(\frac{k}{\alpha_{i+1}}\right)^{2/3}\alpha_{i+1}\,B_{i+1} \\
&= \frac{\partial}{\partial z}\,[f^{(s)}(\rho, q_{i+1,\,i+1})]\,\delta_{i+1,M} \\
&- \frac{\partial}{\partial z}\,[f^{(s)}\,(\rho, q_{i,\,i+1})]\,\delta_{iM}\quad .
\end{aligned}
\tag{40}
$$

For i = I-1,

$$B_{I-1}\,[A_{I-1}k_1(q_{I-1,I}) + k_2(q_{I-1,I})] + f^{(s)}(\rho, q_{I-1,I})\delta_{I-1,M} = B_I\,h_2\,(q_{I,I}) + f^{(s)}(\rho, q_{I,I})\delta_{IM} \tag{41}$$

and

$$B_{I-1}\,[A_{I-1}k'_1(q_{I-1,I}) + k'_2(q_{I-1,I})]\left(\frac{k}{\alpha_{I-1}}\right)^{2/3}\alpha_{I-1} + \frac{\partial}{\partial z}[f^{(s)}(\rho, q_{I-1,I})]\delta_{I-1,M} = B_I\,h'_2(q_{I,I})\left(\frac{k}{\alpha_I}\right)^{2/3}\alpha_I + \frac{\partial}{\partial z}[f^{(s)}(\rho, q_{I,I})]\delta_{I,M}\ . \tag{42}$$

From Equation 41,

$$k_1(q_{I-1,I})\,B_{I-1}A_{I-1} + k_2(q_{I-1,I})\,B_{I-1} - h_2(q_{I,I})B_I = f^{(s)}(\rho, q_{I,I})\delta_{I,M} - f^{(s)}(\rho, q_{I-1,I})\delta_{I-1,M}\ . \tag{43}$$

From Equation 42,

$$k'_1(q_{I-1,I})\left(\frac{k}{\alpha_{I-1}}\right)^{2/3}\alpha_{I-1}\,B_{I-1}\,A_{I-1} + k'_2(q_{I-1,I})\left(\frac{k}{\alpha_{I-1}}\right)^{2/3}\alpha_{I-1}\,B_{I-1} - h'_2(q_{I,I})\left(\frac{k}{\alpha_I}\right)^{2/3}\alpha_I\,B_I = \frac{\partial}{\partial z}[f^{(s)}(\rho, q_{I,I})]\delta_{I,M} - \frac{\partial}{\partial z}[f^{(s)}(\rho, q_{I-1,I})]\delta_{I-1,M}\ . \tag{44}$$

In the above equations, $q_{i,k}$ is defined as

$$q_{i,k} \;=\; q_i\,(z = z_k)\ . \tag{45}$$

Equations 36, 39, 40, 43 and 44 can be written in matrix notation as:

$$\underset{\sim}{\Delta}\ \underset{\sim}{\xi} \;=\; \underset{\sim}{\psi}\ , \tag{46}$$

where

$\Delta =$

$$
\begin{bmatrix}
\Delta_{1,1} & \Delta_{1,2} & 0 & . & . & . & . & . & . & . & . & . & . & 0 \\
\Delta_{2,1} & \Delta_{2,2} & \Delta_{2,3} & \Delta_{2,4} & 0 & . & . & . & . & . & . & . & . & 0 \\
\Delta_{3,1} & \Delta_{3,2} & \Delta_{3,3} & \Delta_{3,4} & 0 & . & . & . & . & . & . & . & . & 0 \\
0 & . & \Delta_{4,3} & \Delta_{4,4} & \Delta_{4,5} & \Delta_{4,6} & 0 & . & & & . & . & . & 0 \\
. & . & . & . & & & & & & & . & . & . & . \\
. & . & . & . & & & & & & & . & . & . & . \\
. & . & . & . & & & & & & & . & . & . & . \\
. & . & . & . & & & & & & & . & . & . & . \\
 & & & & & & & & & & & & & . \\
 & & & & & & & & & & & & & . \\
 & & & & & & & & & & & & & . \\
 & & & & & & & . & 0 & $\Delta_{21-4,21-5}$ & $\Delta_{21-4,21-4}$ & $\Delta_{21-4,21-3}$ & $\Delta_{21-4,21-2}$ & 0 \\
 & & & & & & & . & 0 & $\Delta_{21-3,21-5}$ & $\Delta_{21-3,21-4}$ & $\Delta_{21-3,21-3}$ & $\Delta_{21-3,21-2}$ & 0 \\
 & & & & & & & . & . & . & 0 & $\Delta_{21-2,21-3}$ & $\Delta_{21-2,21-2}$ & $\Delta_{21-2,21-1}$ \\
0 & . & . & . & . & . & . & . & . & . & 0 & $\Delta_{21-1,21-3}$ & $\Delta_{21-1,21-2}$ & $\Delta_{21-1,21-1}$
\end{bmatrix}
\quad , \tag{47}
$$

$$\underset{\sim}{\xi} = \begin{bmatrix} B_1 A_1 \\ B_1 \\ B_2 A_2 \\ B_2 \\ \vdots \\ \\ \vdots \\ B_{I-1} A_{I-1} \\ B_{I-1} \\ B_I \end{bmatrix} \tag{48}$$

and

$$\underset{\sim}{\psi} = \begin{bmatrix} \psi_1 \\ \psi_2 \\ \vdots \\ \\ \psi_I \end{bmatrix} . \tag{49}$$

The elements of the matrix, $\underset{\sim}{\Delta}$, are

$$\Delta_{1,1} = \left(\frac{k}{\alpha_1} \right)^{2/3} \alpha_1 k'_1(q_{1,1}) - j\gamma k_1(q_{1,1}) \quad , \tag{50}$$

$$\Delta_{1,2} = \left(\frac{k}{\alpha_1} \right)^{2/3} \alpha_1 k'_2(q_{1,1}) - j\gamma k_2(q_{1,1}) \quad , \tag{51}$$

$$\Delta_{2,1} = k_1(q_{1,2}) \quad , \tag{52}$$

$$\Delta_{2,2} = k_2(q_{1,2}) \quad , \tag{53}$$

$$\Delta_{2,3} = -k_1(q_{2,2}) \quad . \tag{54}$$

$$\Delta_{2,2} = -k_2(q_{2,2}) \quad , \tag{55}$$

$$\Delta_{3,1} = k'_1(q_{1,2})\left(\frac{k}{\alpha_1}\right)^{2/3}\alpha_1 \quad , \tag{56}$$

$$\Delta_{3,2} = k'_2(q_{1,2})\left(\frac{k}{\alpha_1}\right)^{2/3}\alpha_1 \quad , \tag{57}$$

$$\Delta_{3,3} = -k'_1(q_{2,2})\left(\frac{k}{\alpha_2}\right)^{2/3}\alpha_2 \quad , \tag{58}$$

$$\Delta_{3,4} = k'_2(q_{2,2})\left(\frac{k}{\alpha_2}\right)^{2/3}\alpha_2 \quad , \tag{59}$$

$$\vdots$$

$$\vdots$$

$$\Delta_{2I-2,2I-3} = k_1(q_{I-1,I}) \quad , \tag{60}$$

$$\Delta_{2I-2,2I-2} = k_2(q_{I-1,I}) \quad , \tag{61}$$

$$\Delta_{2I-2,2I-1} = -h_2(q_{I,I}) \quad , \tag{62}$$

$$\Delta_{2I-1,2I-3} = k'_1(q_{I-1,I})\left(\frac{k}{\alpha_{I-1}}\right)^{2/3}\alpha_{I-1} \quad , \tag{63}$$

$$\Delta_{2I-1,2I-2} = k'_2(q_{I-1,I})\left(\frac{k}{\alpha_{I-1}}\right)^{2/3}\alpha_{I-1} \tag{64}$$

and

$$\Delta_{2I-1,2I-1} = -h'_2(q_{I,I})\left(\frac{k}{\alpha_I}\right)^{2/3}\alpha_I \quad . \tag{65}$$

The elements of the column vector, $\underset{\sim}{\psi}$, are

$$\psi_1 = j\chi f^{(s)}(\rho, q_{1,1})\delta_{1M} - \frac{\hat{c}}{\hat{c}z}[f^{(s)}(\rho, q_{1,1})]\delta_{1M} \quad , \tag{66}$$

$$\psi_2 = f^{(s)}(\rho, q_{2,2})\delta_{2M} - f^{(s)}(\rho, q_{1,2})\delta_{1M} \quad . \tag{67}$$

$$\psi_3 = \frac{\hat{c}}{\hat{c}z}[f^{(s)}(\rho, q_{2,2})]\delta_{2M} - \frac{\hat{c}}{\hat{c}z}[f^{(s)}(\rho, q_{1,2})]\delta_{1M} \quad . \tag{68}$$

$$\vdots$$

$$\vdots$$

$$\psi_{I-1} = f^{(s)}(\rho, q_{I,I})\delta_{IM} - f^{(s)}(\rho, q_{I-1,I})\delta_{I-1,M} \tag{69}$$

and

$$\psi_I = \frac{\hat{c}}{\hat{c}z}[f^{(s)}(\rho, q_{I,I})]\delta_{IM} - \frac{\hat{c}}{\hat{c}z}[f^{(s)}(\rho, q_{I-1,I})]\delta_{I-1,M} \quad . \tag{70}$$

To determine the modes that propagate in the tropospheric ducts, the roots of

$$\| \underset{\sim}{\Delta} \| = 0 \tag{71}$$

have to be located. This is discussed in Chapter III. The symbol, $\| \underset{\sim}{\Delta} \|$, denotes the determinant of $\underset{\sim}{\Delta}$.

From Equation 11, the solution of Equation 8 in the i^{th} layer is

$$\Pi(r, z) = \frac{1}{2}\int_C \rho d\rho H_0^{(2)}(r\rho) f_i(\rho, z) \quad . \tag{72}$$

From the theory of residues, Equation 72 can be expressed as

$$\Pi(r, z) = -\frac{2\pi j}{2}\sum_{m} b_i(m) + \frac{1}{2}\int_{C_1} \rho d\rho H_0^{(2)}(r\rho) f_i(\rho, z) + \frac{1}{2}\int_{C_2} \rho d\rho H_0^{(2)}(r\rho) f_i(\rho, z) \quad , \tag{73}$$

where b_i (m) are the residues of $\rho H_0^{(2)}(r\rho) f_i(\rho, z)$ evaluated at the poles of $f_i(\rho, z)$ in the fourth quadrant. The contour C_1 is the quarter-circle of infinite radius and C_2 is the contour enclosing the branch cut of the radical of Equation 16. Since $H_0^{(2)}(r\rho)$ decays exponentially in the lower half complex ρ-plane,

$$\int_{C_1} \rho d\rho H_0^{(2)}(r\rho) f_i(\rho, z) = 0 \quad . \tag{74}$$

For small height, z, the integral over contour C_2 represents the contribution by the surface wave to the total field. Beyond the horizon, this field is small compared to the total field and can be neglected. Therefore Equation 73 becomes

$$\Pi(r, z) = -\pi j \sum_{m} b_i(m) \quad . \tag{75}$$

where b_i (m) is given by

$$b_i(m) = H_0^{(2)}(r\rho_m)\, g_m(z)\, g_m(z_T) \tag{76}$$

and g_m (z) is the normalized height gain function given by [Ref. 2]

$$g_m(z) = \frac{f_m[q(z)]}{\sqrt{\int_0^{\infty} f_m{}^2[q(z)]dz + \frac{f_m{}^2[q(0)]}{2\rho_m}\left(j\frac{d\gamma}{d\rho}\right)_{\rho=\rho_m}}} \quad , \tag{77}$$

where $q(z) = q(z)$ for $z_i \le z < z_{i-1}$.

According to the program source code, the integral, $II = \int_0^{\infty} f_m{}^2[q(z)]dz$, is evaluated by considering that $f_m[q(z)]$ is a solution of Stokes's equation,

$$\frac{d^2 f_m}{dq^2} + q f_m = 0 \quad . \tag{78}$$

This leads to

$$\frac{d}{dq}\left[q f_m^{\,2} + \left(\frac{df_m}{dq}\right)^2\right] = f_m^{\,2} + 2q f_m \frac{df_m}{dq} + 2\frac{df_m}{dq}\cdot\frac{d^2 f_m}{dq^2}$$

$$= f_m^{\,2} + 2\frac{df_m}{dq}\left[\frac{d^2 f_m}{dq^2} + q f_m\right] \tag{79}$$

$$= f_m^{\,2} \ .$$

Note that Equations 78 and 79 imply that the derivative of f_m is continous at z_T. That is, $f_m(q)$ does not include the contribution from the last term of Equations 31 and 32. The integral of $f_m^{\,2}[q(z)]$ in the i^{th} layer is given by

$$\int_{z_i}^{z_{i-1}} f_m^{\,2}[q(z)]\,dz = \frac{1}{q'_i}\int_{q_{i,i}}^{q_{i,i-1}} f_m^{\,2}(q_i)\,dq_i$$

$$= \frac{1}{q'_i}\left\{q f_m^{\,2}(q_i) + \left[\frac{df_m(q_i)}{dq_i}\right]^2\right\}_{q_{i,i}}^{q_{i,i-1}} \ , \tag{80}$$

where

$$q'_i = \frac{dq_i}{dz} \ . \tag{81}$$

From Equation (80), it can be seen that the contribution of ΔI_i to II at $z = z_i$ $(i \neq 1)$ is given by

$$\Delta I_i = \frac{1}{q'_i}\left\{q_i f_m^{\,2}(q_i) + \left[\frac{df_m(q_i)}{dq_i}\right]^2\right\}_{q_{i,i}}^{q_{i-1,i}}$$

$$= \left[-\frac{q_{i,i}}{q'_i} + \frac{q_{i-1,i}}{q'_{i-1}}\right] f_m^{\,2}(q_{i,i}) \tag{82}$$

$$- \frac{1}{q'_i}\left\{\frac{d}{dq_i}[f_m(q_{i,i})]\right\}^2 + \frac{1}{q'_{i-1}}\left\{\frac{d}{dq_{i-1}}[f_m(q_{i-1,i})]\right\}^2 \ .$$

By making use of the fact that $\frac{df_m}{dz}$ is continous at the layer boundaries,

$$\frac{d}{dz}[f_m(q_{i-1,i})] = \frac{d}{dz}[f_m(q_{i,i})] \ . \tag{83}$$

which implies

$$q_{i-1}' \frac{d}{dq_{i-1}} [f_m(q_{i-1,i})] = q'_i \frac{d}{dq_i} [f_m(q_{i,i})] \tag{84}$$

and

$$\left\{ \frac{d}{dq_{i-1}} [f_m(q_{i-1,i})] \right\}^2 = \left(\frac{q'_i}{q_{i-1}'} \right)^2 \left\{ \frac{d}{dq_i} [f_m(q_{i,i})] \right\}^2 . \tag{85}$$

Substituting Equation 85 into Equation 82, ΔI_i becomes

$$\begin{aligned} \Delta I_i = & \left[-\frac{q_{i,i}}{q'_i} + \frac{q_{i-1,i}}{q'_{i-1}} \right] f_m{}^2(q_{i,i}) \\ & + \left[-\frac{1}{q'_i} + \frac{(q'_i)^2}{(q_{i-1})^3} \right] \left\{ \frac{d}{dq_i} [f_m(q_{i,i})] \right\}^2 . \end{aligned} \tag{86}$$

For i = 1,

$$\Delta I_1 = -\frac{1}{q'_i} q_{1,1} f_m{}^2(q_{1,1}) - \frac{1}{q'_1} \left\{ \frac{\partial}{\partial q_1} [f_m(q_{1,1})] \right\}^2 . \tag{87}$$

The integral, II, is

$$II = \sum_{i=1}^{I} \Delta I_i . \tag{88}$$

The second term of the denominator of Equation 77 can be written as

$$\begin{aligned} \frac{f_m{}^2[q(0)]}{2\rho_m} j \left(\frac{dr}{d\rho} \right)_{\rho=\rho_m} &= \frac{f_m{}^2[q(0)]}{2\rho_m} j \left(\frac{dr}{dq_1} \cdot \frac{dq_1}{d\rho} \right)_{\rho=\rho_m} \\ &= j \frac{f_m{}^2[q(0)]}{2\rho_m} \frac{dr}{dq_1} \left(\frac{k}{\alpha_1} \right)^{2/3} \frac{2\rho_m}{k^2} \\ &= j \frac{f_m{}^2[q(0)]}{k^2} \left(\frac{k}{\alpha_1} \right)^{2/3} \frac{dr}{dq_1} . \end{aligned} \tag{89}$$

For cases of interest, $|\rho_m r| \gg 1$. The Hankel function in Equation 76 can be replaced by its asymptotic approximation:

$$H_0^{(2)}(\rho_m r) \sim \left(\frac{2}{\pi\rho_m r}\right)^{1/2} \exp\left(-j\rho_m r + j\frac{\pi}{4}\right) \quad . \tag{90}$$

Therefore Equation 75 becomes

$$\begin{aligned}\Pi(r, z) &= -\pi j \sum_m \left(\frac{2}{\pi\rho_m r}\right)^{1/2} \exp\left(-j\rho_m r + j\frac{\pi}{4}\right) g_m(z)\, g_m(z_T) \\ &= \pi e^{-j\pi/2}\left(\frac{2}{\pi r}\right)^{1/2} e^{j\pi/4} \sum_m \rho_m^{-1/2}\, g_m(z)\, g_m(z_T)\, e^{-j\rho_m r} \\ &= \left(\frac{2\pi}{r}\right)^{1/2} e^{-j\pi/4} \sum_m \rho_m^{-1/2}\, g_m(z)\, g_m(z_T)\, e^{-j\rho_m r} \quad .\end{aligned} \tag{91}$$

To allow for spherical spreading, the $r^{-1/2}$ term in Equation 91 can be replaced by $[a \sin(\frac{r}{a})]^{-1/2}$, a being the earth's radius. Equation 91 becomes

$$\Pi(r, z) = \left[\frac{2\pi}{a \sin(\frac{r}{a})}\right]^{1/2} e^{-j\pi/4} \sum_m \rho_m^{-1/2}\, g_m(z)\, g_m(z_T) e^{-j\rho_m r} \quad . \tag{92}$$

In the cylindrical coordinate system, (r, ϕ, z), the transverse electric field component, E_ϕ, is given by

$$E_\phi = -\omega\mu_0 \frac{\partial\Pi}{\partial r} \quad . \tag{93}$$

Differentiating Equation 92 with respect to r gives

$$\begin{aligned}\frac{\partial\Pi}{\partial r} = &\left\{-\left(\frac{2\pi}{a}\right)^{1/2}\left(\frac{\cos(\frac{r}{a})}{2a}\right)\frac{1}{\sqrt{\sin^3(\frac{r}{a})}} - j\left[\frac{2\pi}{a\sin(\frac{r}{a})}\right]^{1/2}\rho_m\right\} \\ &\times e^{-j\pi/4}\sum_m \rho_m^{-1/2}\, g_m(z)\, g_m(z_T)\, e^{-j\rho_m r} \quad .\end{aligned} \tag{94}$$

Neglecting higher order terms of $\frac{1}{r}$, Equation 94 becomes

$$\frac{\partial \Pi}{\partial r} = -j\left[\frac{2\pi}{a\sin(\frac{r}{a})}\right]^{1/2} e^{-j\pi/4} \sum_m \rho_m^{1/2}\, g_m(z)\, g_m(z_T)\, e^{-j\rho_m r} \quad . \tag{95}$$

The free-space solution to Equation 8 is given by

$$\Pi_{FS} = \frac{e^{-jk\sqrt{r^2+z^2}}}{\sqrt{r^2+z^2}} \simeq \frac{e^{-jkr}}{r} \quad ; \; r \gg z \quad . \tag{96}$$

Thus,

$$\frac{\partial \Pi_{FS}}{\partial r} = \frac{jk}{r} e^{-jkr} - \frac{e^{-jkr}}{r^2} \tag{97}$$

and similarly, the higher order term of $\frac{1}{r}$ in Equation 97 is neglected, giving

$$\frac{\partial \Pi_{FS}}{\partial r} \simeq \frac{jk}{r} e^{-jkr} \quad . \tag{98}$$

Normalizing the field to the free space broadside field, the mode sum becomes

$$\left|\frac{E_\phi}{E_{\phi FS}}\right| = \left[\frac{2\pi r^2}{k^2 a\sin(\frac{r}{a})}\right]^{1/2} \left|\sum_m \rho_m^{1/2}\, g_m(z)\, g_m(z_T)\, e^{-j\rho_m r}\right| \quad . \tag{99}$$

The coherent mode sum in decibels is given by

$$\begin{aligned} ECMS &= 10\,\log\left|\frac{E_\phi}{E_{\phi FS}}\right|^2 \\ &= 10\,\log\left\{\frac{2\pi r^2}{k^2 a\sin(\frac{r}{a})}\left|\sum_m \rho_m^{1/2}\, g_m(z)\, g_m(z_T)\, e^{-j\rho_m r}\right|^2\right\} \quad . \end{aligned} \tag{100}$$

The power sum or incoherent mode sum (EIMS) signal can also be calculated if the phase of each term is ignored:

$$EIMS = 10\,\log\left\{\frac{2\pi r^2}{k^2 a\sin(\frac{r}{a})}\sum_m \left|\rho_m^{1/2}\, g_m(z)\, g_m(z_T)\, e^{-j\rho_m r}\right|^2\right\} \quad . \tag{101}$$

The path lossses are

$$\text{Coherent path loss} = 32.45 + 20 \log r + 20 \log f - \text{ECMS} \tag{102}$$

and

$$\text{Incoherent path loss} = 32.45 + 20 \log r + 20 \log f - \text{EIMS} \ , \tag{103}$$

where r is the range in kilometers and f is the frequency in MHz.

B. VERTICALLY POLARIZED WAVE PROPAGATION

A vertically polarized wave may be treated as due to a radiating electric dipole oriented in the z direction and located at $r = 0$ and $z = z_T$.

The electric field and magnetic field can be approximated by [Ref. 1]

$$\vec{H} = j\varepsilon_0 \omega \vec{\nabla} \times \vec{\Pi} \tag{104}$$

and

$$\vec{E} = \vec{\nabla} \times \vec{\nabla} \times \vec{\Pi} \ , \tag{105}$$

where $\vec{\Pi}$ is the electric Hertz vector.

Calculation of the electric Hertz vector is identical to that of the magnetic Hertz vector except for the following modifications:

1. The height gain function satisfies the following differential equation:

$$\left\{ \frac{\partial^2}{\partial z^2} + k^2 \left[m_i^{\ 2}(z) - \frac{\rho^2}{k^2} \right] \right\} f_i(\rho, z) = -\frac{2z}{\varepsilon_0} \delta(z - z_T) \ . \tag{106}$$

2. Continuity condition at i = 1 becomes

$$n_s^2 f_1(\rho, 0) = n_1^2(0) f_1(\rho, 0) \ . \tag{107}$$

This leads to

$$\Delta_{1,1} = \left(\frac{k}{\alpha_1} \right)^{2/3} \alpha_1 k'_1(q_{1,1}) - jz \frac{n_1^2(0)}{n_s^2} k_1(q_{1,1}) \ . \tag{108}$$

$$\Delta_{1,2} = \left(\frac{k}{\gamma_1}\right)^{2/3} \gamma_1 k'_2(q_{1,1}) - j\gamma \frac{n_1^2(0)}{n_2^2} k_2(q_{1,1}) \tag{109}$$

and

$$\psi_1 = j\gamma \frac{n_1^2(0)}{n_2^2} f_1^{(\rho)}(\rho, q_{1,1})\delta_{1M} - \frac{\partial}{\partial z}[f_1^{(\rho)}(\rho, q_{1,1})]\delta_{1M} \quad . \tag{110}$$

The transverse magnetic field component, H_z, is given by

$$H_z = -j\omega\varepsilon_0 \frac{\partial \Pi}{\partial r} \quad . \tag{111}$$

From Equations 94 to 98, it can be seen that

$$\begin{aligned} \left| \frac{H_z}{H_{zFS}} \right| &= \left| \frac{E_z}{E_{zFS}} \right| \\ &= \left[\frac{2\pi r^2}{k^2 a \sin\left(\frac{r}{a}\right)} \right]^{1/2} \left| \sum_m \rho_m^{1/2} g_m(z) g_m(z_T) e^{-j\gamma_m r} \right| \quad . \end{aligned} \tag{112}$$

It follows from Equation 112 that ECMS, EIMS, coherent path loss and incoherent path loss are given by Equations 100, 101, 102 and 103 respectively.

C. DETERMINATION OF THE HEIGHT GAIN FUNCTION

The height gain function, $f_i(\rho, z)$, is given by

$$f_i(\rho, z) = B_i [A_i k_1(q_i) + k_2(q_i)] \quad ; \; i = 1 \text{ to } I-1 \tag{113}$$

or

$$f_i(\rho, z) = B_i h_2(q_i) \quad ; \; i = I \quad . \tag{114}$$

The coefficients, A_i and B_i, are functions of ρ as in Equation 25.

Determination of the values of A_i and B_i is dependent on the evaluation of the integral (or summation) of Equation 88. It was found that if the attenuation rate of a particular mode is small ($\leq$ 0.1 dB km), the integration Equation 88 is carried out from the top layer to the first layer with the height gain function at the top layer set to a certain finite value. This will prevent the integral from blowing up.

On the other hand, if the rate of attenuation is large (> 0.1 dB km), the integration is performed from the first layer to the top layer with the height gain function at the first layer set to a certain finite value. This will ensure that the value of integral will not become too small.

Therefore, for attenuation rates greater than 0.1 dB km, A_i's and B_i's are determined successively starting from A_1 and B_1 up to A_I and B_I. At i = 1 and z = 0,

$$f_g(\rho, z=0) = f_1(\rho, z=0) \tag{115}$$

and

$$\frac{\partial}{\partial z}[f_g(\rho, z)]_{z=0} = \frac{\partial}{\partial z}[f_1(\rho, z)]_{z=0} \quad . \tag{116}$$

Thus,

$$A_g = B_1 [A_1 k_1(q_{1,1}) + k_2(q_{1,1})] \tag{117}$$

and

$$jr A_g = B_1 [A_1 k'_1(q_{1,1}) + k'_2(q_{1,1})] \left(\frac{k}{\alpha_1}\right)^{2/3} \alpha_1 \quad . \tag{118}$$

Dividing Equation 118 by Equation 117 gives

$$\begin{aligned} A_1 &= \frac{\left(\frac{k}{\alpha_1}\right)^{2/3} \alpha_1 k'_2(q_{1,1}) - jr k_2(q_{1,1})}{jr k_1(q_{1,1}) - \left(\frac{k}{\alpha_1}\right)^{2/3} \alpha_1 k'_1(q_{1,1})} \\ &= \frac{q'_1 k'_2(q_{1,1}) - jr k_2(q_{1,1})}{jr k_1(q_{1,1}) - q'_1 k'_1(q_{1,1})} \quad , \end{aligned} \tag{119}$$

where

$$q'_1 = \frac{dq_1}{dz} = \left(\frac{k}{\alpha_1}\right)^{2/3} \alpha_1 \quad . \tag{120}$$

In the program, $f_1(\rho, z_1)$ is set to 1. This gives

$$B_1 = \frac{1}{A_1(\rho) k_1(q_{1,1}) + k_2(q_{1,1})} \quad . \tag{121}$$

For i = 2 to I-1, A_i's and B_i's are determined by matching conditions at every layer boundary. At layer boundary $z = z_i$,

$$f_i(\rho, z_i) = f_{i-1}(\rho, z_i) \tag{122}$$

and

$$\frac{\partial}{\partial z}[f_i(\rho, z_i)] = \frac{\partial}{\partial z}[f_{i-1}(\rho, z_i)] \quad . \tag{123}$$

From Equation 122,

$$\begin{aligned} B_i [A_i k_1(q_{i,j}) + k_2(q_{i,j})] \\ = B_{i-1}[A_{i-1} k_1(q_{i-1,j}) + k_2(q_{i-1,j})] \quad . \end{aligned} \tag{124}$$

Thus,

$$B_i = \frac{B_{i-1}[A_{i-1} k_1(q_{i-1,j}) + k_2(q_{i-1,j})]}{A_i k_1(q_{i,j}) + k_2(q_{i,j})} \quad . \tag{125}$$

The coefficient, A_i, is determined from Equation 123 as follows:

$$\begin{aligned} B_i [A_i k'_1(q_{i,j}) + k'_2(q_{i,j})] q'_i \\ = B_{i-1}[A_{i-1} k'_1(q_{i-1,j}) + k'_2(q_{i-1,j})] q'_{i-1} \quad . \end{aligned} \tag{126}$$

Substituting Equation 125 into Equation 126 gives

$$\begin{aligned} \frac{A_{i-1} k_1(q_{i-1,j}) + k_2(q_{i-1,j})}{A_i k_1(q_{i,j}) + k_2(q_{i,j})} [A_i k'_1(q_{i,j}) + k'_2(q_{i,j})] q'_i \\ = [A_{i-1} k'_1(q_{i-1,j}) + k'_2(q_{i-1,j})] q'_{i-1} \quad . \end{aligned} \tag{127}$$

Thus,

$$A_i \equiv \frac{n A_i}{d A_i} \quad , \tag{128}$$

where

$$\begin{aligned} nA_i = {} & q'_i\, k'_2(q_{i,i})[A_{i-1}\, k_1(q_{i-1,i}) + k_2(q_{i-1,i})] \\ & - q'_{i-1}\, k_2(q_{i,i})[A_{i-1}\, k'_1(q_{i-1,i}) + k'_2(q_{i-1,i})] \end{aligned} \tag{129}$$

and

$$\begin{aligned} dA_i = {} & q'_{i-1}\, k_1(q_{i,i})[A_{i-1}\, k'_1(q_{i-1,i}) + k'_2(q_{i-1,i})] \\ & - q'_i\, k'_1(q_{i,i})[A_{i-1}\, k_1(q_{i-1,i}) + k_2(q_{i-1,i})] \quad . \end{aligned} \tag{130}$$

For i = I and at the layer boundary, z = z_I ,

$$f_I(\rho, z_I) = f_{I-1}(\rho, z_I) \quad . \tag{131}$$

This gives

$$B_I = \frac{B_{I-1}[A_{I-1}\, k_1(q_{I-1,I}) + k_2(q_{I-1,I})]}{h_2(q_{I,I})} \quad . \tag{132}$$

For attenuation rates less than or equal to 0.1 dB km, A_i's and B_i's are determined successively starting from A_I and B_I down to A_1 and B_1 .

The height gain function at the top layer is given by

$$f_I(\rho, z_I) = h_2(q_I) \quad . \tag{133}$$

where the coefficient, B_I, is set to one. Matching the boundary condition at $z = z_I$ gives

$$B_{I-1} = \frac{h_2(q_{I,I})}{A_{I-1}\, k_1(q_{I-1,I}) + k_2(q_{I-1,I})} \tag{134}$$

and

$$A_{I-1} = \frac{nA_{I-1}}{dA_{I-1}} \quad , \tag{135}$$

where

$$n.A_{I-1} = q'_I h'_2(q_{I,I}) k_2(q_{I-1,I}) - q'_{I-1} h_2(q_{I,I}) k'_2(q_{I-1,I}) \tag{136}$$

and

$$d.A_{I-1} = q'_{I-1} h_2(q_{I,I}) k'_1(q_{I-1,I}) - q'_I h'_2(q_{I,I}) k_1(q_{I-1,I}) \quad . \tag{137}$$

Similarly, the coefficients, A_i and B_i, are obtained by matching boundary conditions at $z = z_i$ for i= I-2 to 1.

Thus,

$$B_i = B_{i+1} \frac{A_{i+1} k_1(q_{i+1,i+1}) + k_2(q_{i+1,i+1})}{A_i k_1(q_{i,i+1}) + k_2(q_{i,i+1})} \tag{138}$$

and

$$A_i = \frac{n.A_i}{d.A_i} \quad . \tag{139}$$

where

$$n.A_i = q'_{i+1} k_2(q_{i,i+1}) [A_{i+1} k'_1(q_{i+1,i+1}) + k'_2(q_{i+1,i+1})] - q'_i k'_2(q_{i,i+1}) [A_{i+1} k_1(q_{i+1,i+1}) + k_2(q_{i+1,i+1})] \tag{140}$$

and

$$d.A_i = q'_i k'_1(q_{i,i+1}) [A_{i+1} k_1(q_{i+1,i+1}) + k_2(q_{i+1,i+1})] - q'_{i+1} k_1(q_{i,i+1}) [A_{i+1} k'_1(q_{i+1,i+1}) + k_2(q_{i+1,i+1})] \quad . \tag{141}$$

D. TEST FOR EVANESCENCE

The functions, $k_1(q)$ and $k_2(q)$, in Equation 26 and 27 can also be expressed in terms of the modified Hankel functions of order one third as follows (see Appendix A):

$$
\begin{aligned}
k_1(q) &= -j\,2(12)^{1/6}\,Ai\left(-q\,e^{j2\pi/3}\right) \\
&= \left(\frac{2}{3}q^{3/2}\right)^{1/3} H_{1/3}^{(1)}\left(\frac{2}{3}q^{3/2}\right) \\
&= h_1(q)
\end{aligned}
\tag{142}
$$

and

$$
\begin{aligned}
k_2(q) &= 2(12)^{1/6}\,e^{j\pi/6}\,Ai(-q) \\
&= h_2(q) - e^{j4\pi/3}\,h_1(q) \quad ,
\end{aligned}
\tag{143}
$$

where

$$
h_1(q) \equiv \left(\frac{2}{3}q^{3/2}\right)^{1/3} H_{1/3}^{(1)}\left(\frac{2}{3}q^{3/2}\right) \tag{144}
$$

and

$$
\begin{aligned}
h_2(q) &= j\,2(12)^{1/6}\,Ai\left(-qe^{-j2\pi/3}\right) \\
&\equiv \left(\frac{2}{3}q^{3/2}\right)^{1/3} H_{1/3}^{(2)}\left(\frac{2}{3}q^{3/2}\right) \quad .
\end{aligned}
\tag{145}
$$

For large $|q|$, $k_1(q)$ and $k_2(q)$ can be approximated by the asymptotic expansion of the Hankel function [Ref. 4 and Appendix A]. That is,

$$
\begin{aligned}
k_1(q) &\sim (12)^{1/6}\,\pi^{-1/2}\,q^{-1/4}\exp\left[j\left(\frac{2}{3}q^{3/2} - \frac{5\pi}{12}\right)\right] \quad ; \\
&-\frac{2\pi}{3} < \arg(q) < \frac{4\pi}{3}
\end{aligned}
\tag{146}
$$

and

$$
\begin{aligned}
k_2(q) &\sim (12)^{1/6}\,\pi^{-1/2}\,q^{-1/4}\exp\left[-j\left(\frac{2}{3}q^{3/2} - \frac{5\pi}{12}\right)\right] \quad ; \\
&0 < \arg(q) < 2\pi \quad .
\end{aligned}
\tag{147}
$$

From Equations 146 and 147, it can be deduced that for large $|q|$ and in the region

$$\frac{2\pi}{3} \;<\; \arg(q) \;<\; \frac{4\pi}{3}, \tag{148}$$

$k_1(q)$ will be exponentially large and $k_2(q)$ exponentially small. When this occurs, $h_1(q)$ and $h_2(q)$ become linearly dependent numerically, i.e., from Equation 143,

$$h_2(q) \;\simeq\; e^{j4\pi/3} h_1(q) \quad . \tag{149}$$

This implies that $k_1(q)$ and $k_2(q)$ are also linearly dependent numerically. Under this condition, the matrix of the modal function will become singular (in a numerical sense) for all values of q. Pappert and Goodhart defined the fields as evanescent when Equation 149 holds [Ref. 5 and 6].

When evanescence occurs, the height gain function is represented by an exponentially decaying field, i.e.,

$$f_i(\rho, z) \;=\; B_i\, k_2(q_i) \quad . \tag{150}$$

It is necessary to incorporate test conditions in the program to check if the rf field has become evanescent. This is achieved by tracking the real part of the exponent of $k_1(q)$ in Equation 146.

Since evanescence may only occur in the region specified by Equation 148, it can be deduced by simple transformation of Equation 148 that

$$\frac{3\pi}{2} \;<\; \arg\left[\frac{2}{3} j\, q^{2/3}\right] \;<\; \frac{5\pi}{2} \quad . \tag{151}$$

This shows that one needs only to test for evanscence when the real part of the exponent of $k_1(q)$ is positive. That is,

$$Re\left[\frac{2}{3} j\, q^{2/3}\right] \;\geq\; 0 \quad . \tag{152}$$

As the coefficients of the height gain function are dependent on how the integral of Equation 88 is evaluated, it follows that different test conditions exist for upward and downward integration. For upward integration, conditions for non-evanscence in the i^{th} layer are

$$Re\left[\frac{2}{3}j\,(q_{i,i+1})^{3/2}\right] - Re\left[\frac{2}{3}j\,(q_{i,i})^{3/2}\right] \;<\; 7$$

$$\text{for } Re\left[\frac{2}{3}j\,(q_{i,i+1})^{3/2}\right] \;\geq\; 0 \qquad (153)$$

$$\text{and } Re\left[\frac{2}{3}j\,(q_{i,i})^{3/2}\right] \;\geq\; 0$$

or

$$Re\left[\frac{2}{3}j\,(q_{i,i+1})^{3/2}\right] \;<\; 7 \qquad \text{for } Re\left[\frac{2}{3}j\,(q_{i,i})^{3/2}\right] \;<\; 0 \qquad (154)$$

$$\text{and } Re\left[\frac{2}{3}j(q_{i,i+1})^{3/2}\right] \;\geq\; 0$$

or

$$Re\left[\frac{dq_i}{dz}\right] \;>\; 0 \qquad (155)$$

or

$$z_{i+1} \;<\; 45\,m \;. \qquad (156)$$

In principle, the right side of Equation 153 should be as large as possible. However, a large quantity will lead to severe cancellation error when extracting $k_2(q)$ (which is a small number) from a linear combination of two large numbers, $h_1(q)$ and $h_2(q)$.

Equation 154 is obtained from Equation 153 by setting $Re[\frac{2}{3}j(q_{i,i})^{3/2}]$ to zero when its value is negative. This is true because when the real part of the exponent of $k_1(q)$ is negative, the condition of evanscence will not occur.

With regards the condition in Equation 155, it can be shown that when $\frac{dq_i}{dz}$ is small (which is usually the case) and Equation 155 is true, then

$$Re\,(\alpha_i) \;>\; 0 \;. \qquad (157)$$

This implies

$$m^2\,(z_{i+1}) \;>\; m^2\,(z_i) \;, \qquad (158)$$

which leads to

$$Re[q_{i,j+1}] \;>\; Re[q_{i,j}] \tag{159}$$

or

$$Re\left[\frac{2}{3} j\,(q_{i,j+1})^{3/2}\right] \;<\; Re\left[\frac{2}{3} j\,(q_{i,j})^{3/2}\right] \tag{160}$$

or

$$Re\left[\frac{2}{3} j\,(q_{i,j+1})^{3/2}\right] - Re\left[\frac{2}{3} j\,(q_{i,j})^{3/2}\right] \;<\; 0 \quad . \tag{161}$$

By comparing Equation 161 with Equation 153, it is clear that Equation 161 is a condition for non-evanescence.

Finally, the condition in Equation 156 was based on the fact that at lower altitude, the magnitude of q is small enough such that $h_1(q)$ and $h_2(q)$ are well behaved in the region stated in Equation 148.

By the same argument, conditions for non-evanescence in the i^{th} layer for downward integration are as follows:

$$Re\left[\frac{2}{3} j\,(q_{i-1,j-1})^{3/2}\right] - Re\left[\frac{2}{3} j\,(q_{i-1,j})^{3/2}\right] \;<\; 7$$
$$\text{for } Re\left[\frac{2}{3} j\,(q_{i-1,j-1})^{3/2}\right] \;\geq\; 0 \tag{162}$$
$$\text{and } Re\left[\frac{2}{3} j\,(q_{i-1,j})^{3/2}\right] \;\geq\; 0$$

or

$$Re\left[\frac{2}{3} j\,(q_{i-1,j-1})^{3/2}\right] \;<\; 7 \qquad \text{for } Re\left[\frac{2}{3} j\,(q_{i-1,j})^{3/2}\right] \;<\; 0$$
$$\text{and } Re\left[\frac{2}{3} j(q_{i-1,j-1})^{3/2} \;\geq\; 0\right. \tag{163}$$

or

$$Re\left[\frac{dq_{i-1}}{dz}\right] \;<\; 0 \tag{164}$$

or

$$z_i \quad < \quad 45\,m \quad . \tag{165}$$

E. EVALUATION OF THE MODAL FUNCTION

When evaluating the relative field strength of the electromagnetic waves using Equations 100 and 101, the eigenvalues, $\rho = \rho_n$, for which

$$\| \underset{\sim}{\Delta} \| \quad = \quad 0 \tag{166}$$

are required. The determinant, $\| \underset{\sim}{\Delta} \|$, is known as the modal function. Each eigenvalue represents a different electromagnetic mode that propagates in the multilayer tropospheric waveguide environment.

The roots of Equation 166 are found by the Shellman-Morfitt complex root-finding routine to be discussed in Chapter III. Instead of searching for solutions of Equation 166 in the ρ-space, it is more convenient to conduct the search in the $q_{1,1}$-plane. The variable, ρ, is related to $q_{1,1}$ by

$$q_{1,1} = \left(\frac{k}{\alpha_1} \right)^{2/3} \left[m^2 (z_1) - \left(\frac{\rho_n}{k} \right)^2 \right] \quad . \tag{167}$$

In searching for the roots of the modal function, the determinant must be evaluated many times. Therefore an efficient method for accomplishing this is required. In particular, the Laplace's expansion is used to obtain the determinant. The Laplace's expansion is based on the following theorem [Ref. 7].

> Theorem: Laplace's Theorem states that if one selects any r rows of a determinant, $| A |$, forms all possible r-rowed minors from these r rows, multiplies each of these minors by its co-factor and then adds the results, one obtains $| A |$.

The method also takes advantage of the presence of zero elements in the determinant to reduce numerical computations.

The understanding of this technique can be best achieved with an example. Consider a trilinear refractivity profile with the following modal function:

$$\| \underset{\sim}{\Delta} \|_3 = \begin{vmatrix} a_{11} & a_{12} & 0 & 0 & 0 \\ a_{21} & a_{22} & a_{23} & a_{24} & 0 \\ a_{31} & a_{32} & a_{33} & a_{34} & 0 \\ 0 & 0 & a_{43} & a_{44} & a_{45} \\ 0 & 0 & a_{53} & a_{54} & a_{55} \end{vmatrix} . \quad (168)$$

Let the last two rows be the r rows from which minors are to be formed. Then applying Laplace's Theorem, the modal function is given by

$$\| \underset{\sim}{\Delta} \|_3 = \begin{vmatrix} a_{11} & a_{12} & 0 \\ a_{21} & a_{22} & a_{23} \\ a_{31} & a_{32} & a_{33} \end{vmatrix} . \begin{vmatrix} a_{44} & a_{45} \\ a_{54} & a_{55} \end{vmatrix} - \begin{vmatrix} a_{11} & a_{12} & 0 \\ a_{21} & a_{22} & a_{24} \\ a_{31} & a_{32} & a_{34} \end{vmatrix} . \begin{vmatrix} a_{43} & a_{45} \\ a_{53} & a_{55} \end{vmatrix} , \quad (169)$$

If a four-layer piecewise linear refractivity profile is used, the modal function will be

$$\| \underset{\sim}{\Delta} \|_4 = \begin{vmatrix} a_{11} & a_{12} & 0 & 0 & 0 & 0 & 0 \\ a_{21} & a_{22} & a_{23} & a_{24} & 0 & 0 & 0 \\ a_{31} & a_{32} & a_{33} & a_{34} & 0 & 0 & 0 \\ 0 & 0 & a_{43} & a_{44} & a_{45} & a_{46} & 0 \\ 0 & 0 & a_{53} & a_{54} & a_{55} & a_{56} & 0 \\ 0 & 0 & 0 & 0 & a_{65} & a_{66} & a_{67} \\ 0 & 0 & 0 & 0 & a_{75} & a_{76} & a_{77} \end{vmatrix} . \quad (170)$$

Notice that Equation 170 is built from Equation 168 by adding eight non-zero entries, namely, a_{56}, a_{65}, a_{66}, a_{67}, a_{76}, a_{75}, a_{74} and a_{77}. Therefore, the results from Equation 168 can be used to compute Equation 170, i.e.,

$$\| \underset{\sim}{\Delta} \|_4 = \| \underset{\sim}{\Delta} \|_3 . \begin{vmatrix} a_{66} & a_{67} \\ a_{76} & a_{77} \end{vmatrix} - \begin{vmatrix} a_{11} & a_{12} & 0 & 0 & 0 \\ a_{21} & a_{22} & a_{23} & a_{24} & 0 \\ a_{31} & a_{32} & a_{33} & a_{34} & 0 \\ 0 & 0 & a_{43} & a_{44} & a_{46} \\ 0 & 0 & a_{53} & a_{54} & a_{56} \end{vmatrix} . \begin{vmatrix} a_{65} & a_{67} \\ a_{75} & a_{77} \end{vmatrix} . \quad (171)$$

In Equation 171, the determinant of the 5 × 5 matrix is also evaluated using the Laplace's expansion.

Without loss of generality, the evaluation of modal functions of multilayer piecewise linear refractivity profile is performed by systematically increasing the number of rows and columns of $\underset{\sim}{\Delta}$ and applying the Laplace's expansion.

The derivative of the modal function, $\| \underset{\sim}{\Delta} \|$, with respect to q_{ij} is also required by the Shellman-Morfitt root finding routine. This is accomplished by expanding $\| \underset{\sim}{\Delta} \|$ using the Laplace's expansion and performing differentiation using the chain-rule.

F. EFFECTS OF SURFACE ROUGHNESS

The materials in this section are adapted from Chapter III of XWVG [Ref. 1]. It is included in this document for completeness.

Surface roughness could have significant effect on the signal levels at large ranges, especially when the frequencies of the rf waves are above several gigahertz.

The effects of surface roughness is modelled by Baumgartner in XWVG [Ref. 1] as a lossy infinitesimally thin bottom layer of constant modified refractivity shown in Figure 4.

In the bottom layer, $0 \leq z \leq z_p$, the height gain function, $f_0(\rho, z)$, can be written as

$$f_0(\rho, z) = A_0 \left[e^{j\mu z} + Re^{-j\mu z} \right] \quad , \tag{172}$$

where

$$\mu = k_\backslash \sqrt{n_1^2(0) - \beta^2} \quad , \tag{173}$$

$$\beta^2 = \frac{\rho^2}{k^2} \tag{174}$$

and R is the plane wave reflection coefficient.

By matching boundary conditions at each layer boundary as was done in Section A, it can be seen that all previous results still hold if the following substitution is made:

$$\gamma \quad \rightarrow \quad \gamma_s = \mu \frac{1 - R}{1 + R} \quad . \tag{175}$$

In general, the bump heights of the rough surface are assumed to be Gaussian distributed. In this case, the reflection coefficient, R, can be represented as the product of the smooth surface plane wave reflection coefficient and a surface roughness factor [Ref. 8]. For horizontal polarization, the reflection coefficient, R, is given by

$$R = \begin{cases} R_H \exp\left[-2k^2\delta^2 \left(\frac{\alpha_1}{k} \right)^{2/3} q_{1,1} \right] & ; \quad Re(q_{1,1}) \geq 0 \\ R_H & ; \quad Re(q_{1,1}) < 0 \end{cases} \quad , \tag{176}$$

where δ is the root mean square surface bump heights and R_H is the Fresnel reflection coefficient for a horizontally polarized wave given by

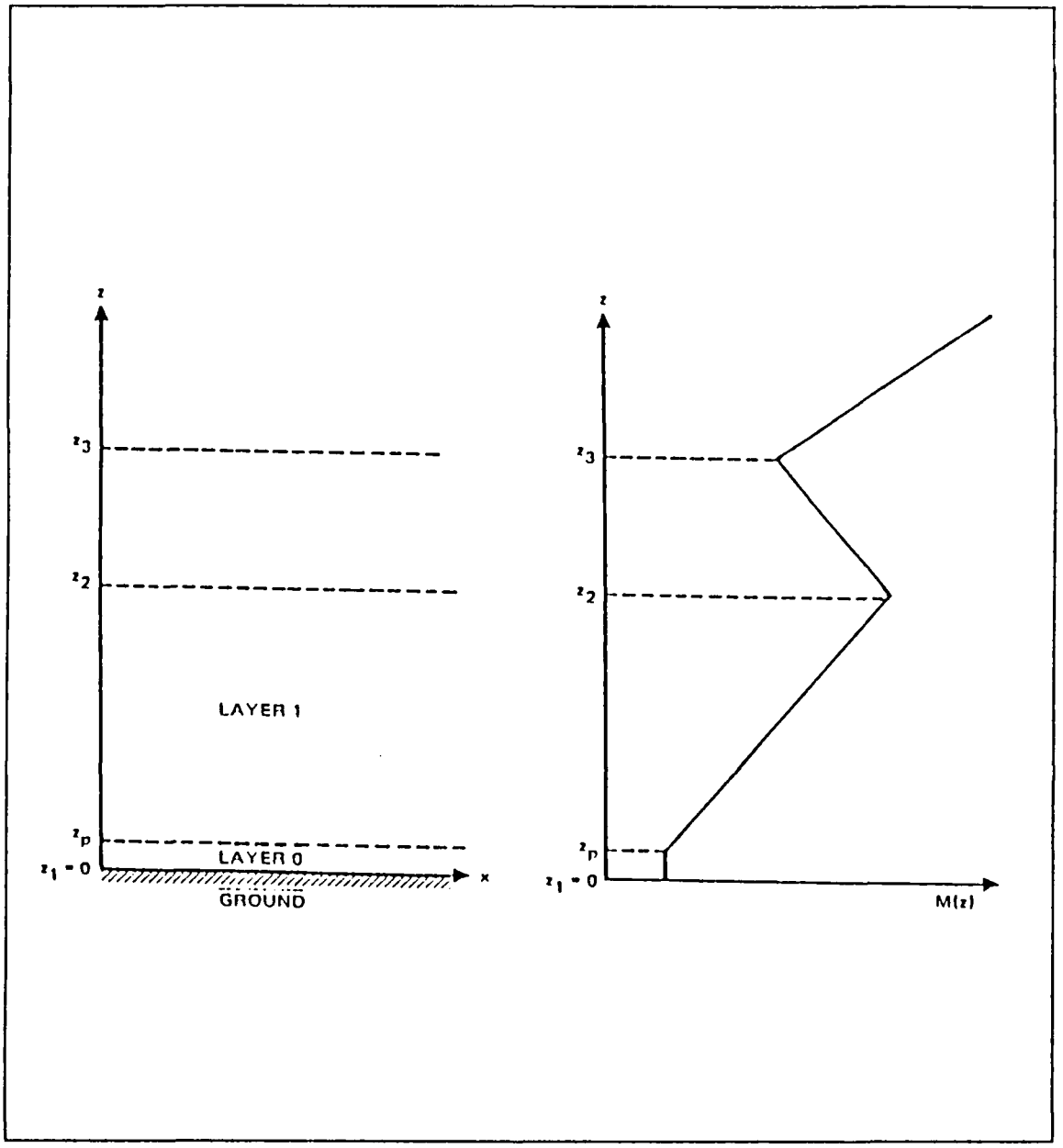

Figure 4. Effects of surface roughness modelled as layer 0 [From Ref. 1]

$$R_H = \frac{\left[n_1^2(0) - \beta^2\right]^{1/2} - \left[n_g^2 - \beta^2\right]^{1/2}}{\left[n_1^2(0) - \beta^2\right]^{1/2} + \left[n_g^2 - \beta^2\right]^{1/2}} \quad . \tag{177}$$

For vertical polarization, R is given by

$$R = \begin{cases} R_v \exp\left[-2k^2\delta^2 \left(\frac{\alpha_1}{k} \right)^{2/3} q_{1,1} \right] & : \quad Re(q_{1,1}) \geq 0 \\ R_v & : \quad Re(q_{1,1}) < 0 \end{cases} , \qquad (178)$$

where R_v is the Fresnel reflection coefficient for a vertically polarized wave given by

$$R_v = \frac{n_g^2 \left[n_1^2(0) - \beta^2 \right]^{1/2} - n_1^2(0) \left[n_g^2 - \beta^2 \right]^{1/2}}{n_g^2 \left[n_1^2(0) - \beta^2 \right]^{1/2} + n_1^2(0) \left[n_g^2 - \beta^2 \right]^{1/2}} . \qquad (179)$$

For horizontal polarization, γ_s can be expressed as follows [Ref. 1]:

$$\gamma_{SH} = k \frac{a(q_{1,1})}{b(q_{1,1})} , \qquad (180)$$

where

$$a(q_{1,1}) = \left(\frac{\alpha_1}{k} \right)^{1/3} (q_{1,1})^{1/2} \tanh\left(\frac{\phi}{2} \right) + \left[T + \left(\frac{\alpha_1}{k} \right)^{2/3} q_{1,1} \right]^{1/2} , \qquad (181)$$

$$b(q_{1,1}) = 1 + \left(\frac{k}{\alpha_1} \right)^{1/3} (q_{1,1})^{-1/2} \tanh\left(\frac{\phi}{2} \right) \left[T + \left(\frac{\alpha_1}{k} \right)^{2/3} q_{1,1} \right]^{1/2} , \qquad (182)$$

$$T = n_g^2 - n^2(0) \qquad (183)$$

and

$$\phi = 2k^2\delta^2 \left(\frac{\alpha_1}{k} \right)^{2/3} q_{1,1} . \qquad (184)$$

For small values of $| q_{1,1} |$, $a(q_{1,1})$ and $b(q_{1,1})$ can be expanded in series as

$$a(q_{1,1}) = \left(\frac{\alpha_1}{k}\right)^{1/3} q_{1,1}^{1/2} \left\{ k^2\delta^2 \left(\frac{\alpha_1}{k}\right)^{2/3} q_{1,1} \right.$$
$$\left. - \frac{1}{3} k^6\delta^6 \left(\frac{\alpha_1}{k}\right)^2 q_{1,1}^3 + \frac{2}{15} k^{10}\delta^{10} \left(\frac{\alpha_1}{k}\right)^{10/3} q_{1,1}^5 - \ldots\ldots \right\}$$
$$+ T^{1/2} \left\{ 1 + \frac{1}{2T} \left(\frac{\alpha_1}{k}\right)^{2/3} q_{1,1} - \frac{1}{8T^2} \left(\frac{\alpha_1}{k}\right)^{4/3} q_{1,1}^2 \right. \qquad (185)$$
$$+ \frac{1}{16T^3} \left(\frac{\alpha_1}{k}\right)^2 q_{1,1}^3 - \frac{2}{128T^4} \left(\frac{\alpha_1}{k}\right)^{8/3} q_{1,1}^4$$
$$\left. + \frac{7}{256T^5} \left(\frac{\alpha_1}{k}\right)^{10/3} q_{1,1}^5 - \ldots\ldots \right\}$$

and

$$b(q_{1,1}) = 1 + T^{1/2} q_{1,1}^{1/2} \left\{ k^2\delta^2 \left(\frac{\alpha_1}{k}\right)^{1/3} + \frac{1}{2T} k^2\delta^2 \left(\frac{\alpha_1}{k}\right) q_{1,1} \right.$$
$$- \left[\frac{1}{3} k^6\delta^6 + \frac{1}{8T^2} k^2\delta^2 \right] \left(\frac{\alpha_1}{k}\right)^{5/3} q_{1,1}^2$$
$$+ \left[-\frac{1}{6T} k^6\delta^6 + \frac{1}{16T^3} k^2\delta^2 \right] \left(\frac{\alpha_1}{k}\right)^{7/3} q_{1,1}^3 \qquad (186)$$
$$+ \left[\frac{2}{15} k^{10}\delta^{10} + \frac{1}{24T^2} k^6\delta^6 - \frac{5}{128T^4} k^2\delta^2 \right] \left(\frac{\alpha_1}{k}\right)^3 q_{1,1}^4$$
$$\left. + \left[\frac{1}{15T} k^{10}\delta^{10} - \frac{1}{48T^3} k^6\delta^6 + \frac{7}{256T^5} k^2\delta^2 \right] \left(\frac{\alpha_1}{k}\right)^{11/3} q_{1,1}^5 + \ldots \right\} .$$

The derivative of γ_{SH} with respect to $q_{1,1}$ can be obtained by differentiating Equation 180, i.e .

$$\frac{\partial \gamma_{SH}}{\partial q_{1,1}} = \frac{k}{b^2(q_{1,1})} \left[b(q_{1,1}) \frac{\partial a}{\partial q_{1,1}} - a(q_{1,1}) \frac{\partial b}{\partial q_{1,1}} \right] . \qquad (187)$$

Similarly, $\frac{\partial a}{\partial q_{1,1}}$ and $\frac{\partial b}{\partial q_{1,1}}$ are obtained from Equation 181 and 182 respectively:

$$\frac{\partial a}{\partial q_{1,1}} = \frac{1}{2} q_{1,1}^{-1/2} \left(\frac{\alpha_1}{k} \right)^{1/3} \tanh\left(\frac{\phi}{2} \right) + q_{1,1}^{1/2} \left(\frac{\alpha_1}{k} \right) k^2 \delta^2 \operatorname{sech}^2\left(\frac{\phi}{2} \right) + \frac{1}{2} \left(\frac{\alpha_1}{k} \right)^{2/3} \left[T + \left(\frac{\alpha_1}{k} \right)^{2/3} q_{1,1} \right]^{-1/2} \tag{188}$$

and

$$\frac{\partial b}{\partial q_{1,1}} = -\frac{1}{2} \left(\frac{k}{\alpha_1} \right)^{1/3} q_{1,1}^{3/2} \tanh\left(\frac{\phi}{2} \right) \left[T + \left(\frac{\alpha_1}{k} \right)^{2/3} q_{1,1} \right]^{1/2} + \frac{1}{2} q_{1,1}^{-1/2} \left(\frac{\alpha_1}{k} \right)^{1/3} \tanh\left(\frac{\phi}{2} \right) \left[T + \left(\frac{\alpha_1}{k} \right)^{2/3} q_{1,1} \right]^{-1/2} + q_{1,1}^{-1/2} k^2 \delta^2 \left(\frac{\alpha_1}{k} \right)^{1/3} \operatorname{sech}^2\left(\frac{\phi}{2} \right) \left[T + \left(\frac{\alpha_1}{k} \right)^{2/3} q_{1,1} \right]^{1/2} . \tag{189}$$

For small values of $| q_{1,1} |$, $\frac{\partial a}{\partial q_{1,1}}$ and $\frac{\partial b}{\partial q_{1,1}}$ can be expanded into series as

$$\frac{\partial a}{\partial q_{1,1}} = \left(\frac{\alpha_1}{k} \right)^{1/3} q_{1,1}^{1/2} \left\{ \frac{3}{2} k^2 \delta^2 \left(\frac{\alpha_1}{k} \right)^{2/3} - \frac{7}{6} k^6 \delta^6 \left(\frac{\alpha_1}{k} \right)^2 q_{1,1}^{2} + \frac{11}{15} k^{10} \delta^{10} \left(\frac{\alpha_1}{k} \right)^{10/3} q_{1,1}^{4} - \ldots\ldots \right\} + T^{1/2} \left\{ \frac{1}{2T} \left(\frac{\alpha_1}{k} \right)^{2/3} - \frac{1}{4T^2} \left(\frac{\alpha_1}{k} \right)^{4/3} q_{1,1} + \frac{3}{16T^3} \left(\frac{\alpha_1}{k} \right)^2 q_{1,1}^{2} - \frac{5}{32T^4} \left(\frac{\alpha_1}{k} \right)^{8/3} q_{1,1}^{3} + \frac{35}{256T^5} \left(\frac{\alpha_1}{k} \right)^{10/3} q_{1,1}^{4} - \ldots\ldots \right\} \tag{190}$$

and

$$\frac{\partial b}{\partial q_{1,1}} = T^{1/2} q_{1,1}^{-1/2} \left\{ \frac{1}{2} k^2\delta^2 \left(\frac{\alpha_1}{k} \right)^{1/3} + \frac{3}{4T} k^2\delta^2 \left(\frac{\alpha_1}{k} \right) q_{1,1} \right.$$
$$- \frac{5}{2} \left[\frac{1}{3} k^6\delta^6 + \frac{1}{8T^2} k^2\delta^2 \right] \left(\frac{\alpha_1}{k} \right)^{5/3} q_{1,1}^{\ 2}$$
$$+ \frac{7}{2} \left[-\frac{1}{6T} k^6\delta^6 + \frac{1}{16T^3} k^2\delta^2 \right] \left(\frac{\alpha_1}{k} \right)^{7/3} q_{1,1}^{\ 3} \qquad (191)$$
$$+ \frac{9}{2} \left[\frac{2}{15} k^{10}\delta^{10} + \frac{1}{24T^2} k^6\delta^6 - \frac{5}{128T^4} k^2\delta^2 \right] \left(\frac{\alpha_1}{k} \right)^3 q_{1,1}^{\ 4}$$
$$\left. + \frac{11}{2} \left[\frac{1}{15T} k^{10}\delta^{10} - \frac{1}{48T^3} k^6\delta^6 + \frac{7}{256T^5} k^2\delta^2 \right] \left(\frac{\alpha_1}{k} \right)^{11/3} q_{1,1}^{\ 5} + \ldots \right\} .$$

The corresponding results for vertical polarization are:

$$\gamma_{SV} = k \frac{\tilde{a}(q_{1,1})}{\tilde{b}(q_{1,1})} \qquad (192)$$

and

$$\frac{\partial \gamma_{SV}}{\partial q_{1,1}} = \frac{k}{\tilde{b}^2(q_{1,1})} \left[\tilde{b}(q_{1,1}) \frac{\partial \tilde{a}}{\partial q_{1,1}} - \tilde{a}(q_{1,1}) \frac{\partial \tilde{b}}{\partial q_{1,1}} \right] . \qquad (193)$$

where

$$\tilde{a}(q_{1,1}) = \left(\frac{\alpha_1}{k} \right)^{1/3} q_{1,1}^{\ 1/2} \tanh \left(\frac{\phi}{2} \right) + \frac{n_1^2(0)}{n_g^{\ 2}} \left[T + \left(\frac{\alpha_1}{k} \right)^{2/3} q_{1,1} \right]^{1/2} \qquad (194)$$

and

$$\tilde{b}(q_{1,1}) = 1 + \frac{n_1^2(0)}{n_g^2} q_{1,1}^{-1/2} \left(\frac{k}{\alpha_1} \right)^{1/3} \tanh \left(\frac{\phi}{2} \right) \left[T + \left(\frac{\alpha_1}{k} \right)^{2/3} q_{1,1} \right]^{1/2} . \qquad (195)$$

For small values of $|q_{1,1}|$, $\tilde{a}(q_{1,1})$ and $\tilde{b}(q_{1,1})$ becomes

$$\tilde{a}(q_{1,1}) = \left(\frac{\alpha_1}{k}\right)^{1/3} q_{1,1}^{1/2}\left\{k^2\delta^2\left(\frac{\alpha_1}{k}\right)^{2/3} q_{1,1} - \frac{1}{3}k^6\delta^6\left(\frac{\alpha_1}{k}\right)^2 q_{1,1}^3 + \frac{2}{15}k^{10}\delta^{10}\left(\frac{\alpha_1}{k}\right)^{10/3} q_{1,1}^5 - \cdots\cdots\right\}$$
$$+ \frac{n_1^2(0)}{n_g^2} T^{1/2}\left\{1 + \frac{1}{2T}\left(\frac{\alpha_1}{k}\right)^{2/3} q_{1,1} - \frac{1}{8T^2}\left(\frac{\alpha_1}{k}\right)^{4/3} q_{1,1}^2 + \frac{1}{16T^3}\left(\frac{\alpha_1}{k}\right)^2 q_{1,1}^3 - \frac{5}{128T^4}\left(\frac{\alpha_1}{k}\right)^{8/3} q_{1,1}^4 + \frac{7}{256T^5}\left(\frac{\alpha_1}{k}\right)^{10/3} q_{1,1}^5 - \cdots\cdots\right\} \quad (196)$$

and

$$\tilde{b}(q_{1,1}) = 1 + \frac{n_1^2(0)}{n_g^2} T^{1/2} q_{1,1}^{1/2}\left\{k^2\delta^2\left(\frac{\alpha_1}{k}\right)^{1/3} + \frac{1}{2T}k^2\delta^2\left(\frac{\alpha_1}{k}\right) q_{1,1} - \left[\frac{1}{3}k^6\delta^6 + \frac{1}{8T^2}k^2\delta^2\right]\left(\frac{\alpha_1}{k}\right)^{5/3} q_{1,1}^2 + \left[-\frac{1}{6T}k^6\delta^6 + \frac{1}{16T^3}k^2\delta^2\right]\left(\frac{\alpha_1}{k}\right)^{7/3} q_{1,1}^3 + \left[\frac{2}{15}k^{10}\delta^{10} + \frac{1}{24T^2}k^6\delta^6 - \frac{5}{128T^4}k^2\delta^2\right]\left(\frac{\alpha_1}{k}\right)^3 q_{1,1}^4 + \left[\frac{1}{15T}k^{10}\delta^{10} - \frac{1}{48T^3}k^6\delta^6 + \frac{7}{256T^5}k^2\delta^2\right]\left(\frac{\alpha_1}{k}\right)^{11/3} q_{1,1}^5 + \cdots\cdots\right\} . \quad (197)$$

The derivative of $\tilde{a}(q_{1,1})$ and $\tilde{b}(q_{1,1})$ are obtained from Equation 196 and 197 respectively:

$$\frac{\partial\tilde{a}}{\partial q_{1,1}} = \frac{1}{2} q_{1,1}^{-1/2}\left(\frac{\alpha_1}{k}\right)^{1/3} \tanh\left(\frac{\phi}{2}\right) + k^2\delta^2\frac{\alpha_1}{k} q_{1,1}^{1/2} \operatorname{sech}^2\left(\frac{\phi}{2}\right) + \frac{1}{2}\frac{n_1^2(0)}{n_g^2}\left(\frac{\alpha_1}{k}\right)^{2/3}\left[T + \left(\frac{\alpha_1}{k}\right)^{2/3} q_{1,1}\right]^{-1/2} \quad (198)$$

and

$$\frac{\partial \tilde{b}}{\partial q_{1,1}} = \frac{n_i^{\,2}(0)}{n_g^2}\left\{-\frac{1}{2}\,q_{1,1}^{\,-3/2}\left(\frac{k}{\alpha_1}\right)^{1/3}\tanh\left(\frac{\phi}{2}\right)\left[\mathrm{T}+\left(\frac{\alpha_1}{k}\right)^{2/3}q_{1,1}\right]^{1/2}\right.$$

$$+\frac{1}{2}\,q_{1,1}^{\,-1/2}\left(\frac{\alpha_1}{k}\right)^{1/3}\tanh\left(\frac{\phi}{2}\right)\left[\mathrm{T}+\left(\frac{\alpha_1}{k}\right)^{2/3}q_{1,1}\right]^{-1/2} \qquad (199)$$

$$\left.+k^2\,\delta^2\,q_{1,1}^{\,-1/2}\left(\frac{\alpha_1}{k}\right)^{1/3}\mathrm{sech}^2\left(\frac{\phi}{2}\right)\left[\mathrm{T}+\left(\frac{\alpha_1}{k}\right)^{2/3}q_{1,1}\right]^{1/2}\right\} \quad .$$

For small values of $|\,q_{1,1}\,|$, $\frac{\partial \tilde{a}}{\partial q_{1,1}}$ and $\frac{\partial \tilde{b}}{\partial q_{1,1}}$ becomes

$$\frac{\partial \tilde{q}}{\partial q_{1,1}} = \left(\frac{\alpha_1}{k}\right)^{1/3} q_{1,1}^{\,1/2}\left\{\frac{3}{2}\,k^2\delta^2\left(\frac{\alpha_1}{k}\right)^{2/3} - \frac{7}{6}\,k^6\delta^6\left(\frac{\alpha_1}{k}\right)^2 q_{1,1}^{\,2}\right.$$

$$\left.+\frac{11}{15}\,k^{10}\delta^{10}\left(\frac{\alpha_1}{k}\right)^{10/3} q_{1,1}^{\,4} - \cdots\cdots\right\}$$

$$+\frac{n_i^2(0)}{n_g^2}\,\mathrm{T}^{1/2}\left\{\frac{1}{2\mathrm{T}}\left(\frac{\alpha_1}{k}\right)^{2/3} - \frac{1}{4\mathrm{T}^2}\left(\frac{\alpha_1}{k}\right)^{4/3} q_{1,1}\right. \qquad (200)$$

$$+\frac{3}{16\mathrm{T}^3}\left(\frac{\alpha_1}{k}\right)^2 q_{1,1}^{\,2} - \frac{5}{32\mathrm{T}^4}\left(\frac{\alpha_1}{k}\right)^{8/3} q_{1,1}^{\,3}$$

$$\left.+\frac{35}{256\mathrm{T}^5}\left(\frac{\alpha_1}{k}\right)^{10/3} q_{1,1}^{\,4} - \cdots\cdots\right\}$$

and

$$\frac{\partial \tilde{b}}{\partial q_{1,1}} = \frac{n_1^2(0)}{n_g^2} T^{1/2} q_{1,1}^{-1/2} \left\{ \frac{1}{2} k^2\delta^2 (\frac{\alpha_1}{k})^{1/3} + \frac{3}{4T} k^2\delta^2 (\frac{\alpha_1}{k}) q_{1,1} - \frac{5}{2}\left[\frac{1}{3} k^6\delta^6 + \frac{1}{8T^2} k^2\delta^2 \right] (\frac{\alpha_1}{k})^{5/3} q_{1,1}^{2} + \frac{7}{2}\left[-\frac{1}{6} k^6\delta^6 + \frac{1}{16T^3} k^2\delta^2 \right] (\frac{\alpha_1}{k})^{7/3} q_{1,1}^{3} + \frac{9}{2}\left[\frac{2}{15} k^{10}\delta^{10} + \frac{1}{24T^2} k^6\delta^6 - \frac{5}{128T^4} k^2\delta^2 \right] (\frac{\alpha_1}{k})^{3} q_{1,1}^{4} + \frac{11}{2}\left[\frac{1}{15T} k^{10}\delta^{10} - \frac{1}{48T^3} k^6\delta^6 + \frac{7}{256T^5} k^2\delta^2 \right] (\frac{\alpha_1}{k})^{11/3} q_{1,1}^{5} + \cdots \right\} . \quad (201)$$

G. COMPLEX INDEX OF REFRACTION OF SEA WATER

The materials in this section are adapted from Chapter IV of XWVG [Ref. 1].

The complex index of refraction is one of the physical parameters required for evaluating the modal function and height gain functions. The complex index of refraction of sea water, n_g, is a function of frequency, temperature and salinity. It is related to the effective relative dielectric function, ε_{eff}, and the effective conductivity, σ_{eff}, through

$$n_g^2 = \varepsilon_{eff} - j\frac{\sigma_{eff}}{\omega\varepsilon_0} , \quad (202)$$

where ε_0 is the permittivity of free space and ω is the frequency at which n_g is evaluated. The effective relative dielectric function and the effective conductivity are related to the complex dielectric function, ε, and the ionic conductivity, σ, through

$$\varepsilon = \varepsilon' - j\varepsilon'', \quad (203)$$

$$\varepsilon_{eff} = \varepsilon' \quad (204)$$

and

$$\sigma_{eff} = \sigma + \omega\varepsilon_0\varepsilon'' . \quad (205)$$

In Equation 205, σ is assumed to be real. This is a good approximation for frequencies much less than 10^5 GHz [Ref. 1].

The theory of an ideal polar dielectric in an alternating electromagnetic field was first formulated by Debye [Ref. 9]. In the theory, the complex dielectric function is expressed as a function of a single relaxation time, τ, as follows:

$$\varepsilon = \varepsilon' - j\varepsilon'' \quad , \tag{206}$$

$$\varepsilon' = \frac{\varepsilon_s - \varepsilon_\infty}{1 + \omega^2 \tau^2} \quad , \tag{207}$$

and

$$\varepsilon'' = \frac{(\varepsilon_s - \varepsilon_\infty)\omega\tau}{1 + \omega^2 \tau^2} \quad , \tag{208}$$

where ε_∞ is the part of the dielectric function due to the atomic and dielectric polarization, ε_s is the static dielectric function and ω is the frequency of the electromagnetic wave. Equations 206 to 208 represent the fall in the value of the dielectric function from ε_s to ε_∞. This fall is accompanied by a single broad absorption band in the vicinity of the characteristic wavelength, λ_s, given by

$$\lambda_s = \frac{1}{\tau} \quad . \tag{209}$$

The characterisation of the variation with frequency of the complex dielectric function of water in terms of a single relaxation time is valid for frequencies up to 300 GHz [Ref. 1]. For higher frequencies, more than one relaxation time may be required.

In the model of Klein and Swift [Ref. 10], ε_∞ is assumed to be 4.9 for both pure water and seawater. With this assumption, the static dielectric function for pure water is given by

$$\varepsilon_{S,P} = 88.045 - 0.4147\, t_c - 6.295 \times 10^{-4}\, t_c^{\,2} + 1.075 \times 10^{-5}\, t_c^{\,3} \tag{210}$$

and the static dielectric function of seawater is given by

$$\varepsilon_{S,S} = \varepsilon_{S,a}\, a(S,\, t_c) \quad , \tag{211}$$

where

$$\varepsilon_{S,a} = 87.134 - 1.949 \times 10^{-1}\, t_c - 1.276 \times 10^{-2}\, t_c^{\,2} + 2.491 \times 10^{-4}\, t_c^{\,3} \qquad (212)$$

and

$$\begin{aligned} a(S,\ t_c) = {} & 1.000 + 1.613 \times 10^{-5}\, S\, t_c - 3.656 \times 10^{-3}\, S \\ & + 3.210 \times 10^{-5}\, S^2 - 4.232 \times 10^{-7}\, S^3 \ . \end{aligned} \qquad (213)$$

In the above equations, t_c is the temperature in degrees Celcius and S is the salinity in grams of salt per kilogram of seawater. The relaxation time of seawater is given by

$$\tau_S = \tau_p\, b(S,\ t_c) \ . \qquad (214)$$

where τ_p is the relaxation of pure water given by

$$\tau_p = 1.768 \times 10^{-11} - 6.086 \times 10^{-13}\, t_c + 1.104 \times 10^{-14}\, t_c^{\,2} - 8.111 \times 10^{-17}\, t_c^{\,3} \qquad (215)$$

and

$$\begin{aligned} b(S,\ t_c) = {} & 1.000 + 2.282 \times 10^{-5}\, S\, t_c - 7.638 \times 10^{-4}\, S \\ & - 7.760 \times 10^{-6}\, S^2 + 1.105 \times 10^{-8}\, S^3 \ . \end{aligned} \qquad (216)$$

The ionic conductivity of seawater in siemens per meter is given by

$$\sigma(t_c,\ S) = \sigma(25,\ S)\, \exp(-\Delta\varphi) \ . \qquad (217)$$

where

$$\Delta = 25 - t_c \ , \qquad (218)$$

$$\begin{aligned} \varphi = {} & 2.033 \times 10^{-2} + 1.266 \times 10^{-4}\, \Delta + 2.464 \times 10^{-6}\, \Delta^2 \\ & - S[1.849 \times 10^{-5} - 2.551 \times 10^{-7}\, \Delta + 2.551 \times 10^{-8}\, \Delta^2] \end{aligned} \qquad (219)$$

and

$$\begin{aligned} \sigma(25,\ S) = {} & S\,[0.182521 - 1.46192 \times 10^{-3}\, S + 2.09324 \\ & \times 10^{-5}\, S^2 - 1.28205 \times 10^{-7}\, S^3\,] \ . \end{aligned} \qquad (220)$$

H. ATMOSPHERIC ABSORPTION

The materials in this section are adapted from References 11, 12 and 13.

The gas molecules in the air absorb energy from electromagnetic waves. The absorption is due to the quantum mechanical resonances of the gas molecules. These resonances at specific frequencies then broaden into bands as a result of collisons of the gas particles. In the lower atmosphere, the density of gas particles is higher. This means that collisons are more frequent and the absorption bands are broader.

In the troposphere (height < 10 km), only the lines bands of oxygen and water vapour are important. The principal resonance of oxygen is at 60 GHz and that of water vapour is at 22.2 GHz. The extent of absorption by oxygen molecules is dependent on the pressure, p, and temperature, t. In the case of water vapour, absorption is also dependent on the water vapour density, ρ. For specific values of p, t, and ρ, the absorption coefficient, g_{ab}, is computed as [Ref. 11]

$$g_{ab} = 0.1820 f N_f \qquad dB/km \quad , \tag{221}$$

where f is the frequency and N_f is the absorption spectrum. The absorption spectrum, N_f, is related to the line spectra of absorption, SF, the continuum spectra, N_c, and the liquid water extinction, N_w, by the following expressions [Ref. 11]:

$$N_f = \sum_i SF + N_w + N_c \qquad ppm \quad . \tag{222}$$

The summation of SF is done over 44 spectral lines of oxygen and 29 spectral lines of water vapour, [Ref. 11], i.e.,

$$\begin{aligned} \sum_i SF = & \sum_{i=1}^{44} a_1(i)\, p\theta^3 \exp\left[a_2(i)(1-\theta)\right] F \\ & + \sum_{i=1}^{29} b_1(i)\, c\, \theta^{3.5} \exp\left[b_2(i)(1-\theta)\right] F \quad , \end{aligned} \tag{223}$$

where $a_1(i)$, $a_2(i)$, $b_1(i)$ and $b_2(i)$ are spectroscopic coefficients derived from experiments and spectroscopic parameter compilations. Values of $a_1(i)$, $a_2(i)$, $b_1(i)$ and $b_2(i)$ are listed in Table 1.

The dry air pressure, p, at a height of z above the earth's surface is given by [Ref. 12]

$$p = 101.325\left[1 - \frac{0.0065z}{288}\right]^{5.256} \quad kPa \quad . \tag{224}$$

The relative inverse temperature, θ, is related to the temperature, t_k, in °K by

$$\theta = \frac{300}{t_k} \quad . \tag{225}$$

The water vapour partial pressure, e_w, in kPa is related to the saturation water vapour pressure, e_s, and relative humidity, rh, by the following equations:

$$e_w = e_s(rh) \times 10^{-2} \quad , \tag{226}$$

$$e_s = 0.6105 \exp\left[25.22\left(\frac{t_c}{t_k}\right) - 5.31 \log\left(\frac{t_k}{273.15}\right)\right] \quad kPa \tag{227}$$

and

$$t_c = t_k - 273.15\,°C \quad . \tag{228}$$

In Equation 223, F is the shape factor of the broadened resonance lines given by [Ref. 11]

$$F = \left(\frac{f}{v_0}\right)\left[\frac{g - (v_0 - f)\hat{c}}{(v_0 - f)^2 + g^2} + \frac{g - (v_0 + f)\hat{c}}{(v_0 + f)^2 + g^2}\right] \tag{229}$$

for oxygen line 1 to line 38 and

$$F = \left(\frac{f}{v_0}\right)\left[\frac{g}{(v_0 - f)^2 + g^2} + \frac{g}{(v_0 + f)^2 + g^2}\right] \tag{230}$$

for oxygen line 39 to 44 and the water vapour lines.

In Equation 229 and 230, v_0 is the molecular line centre frequency, g is the width and $\hat{c}$ is the overlap interference.

For oxygen in air,

$$g = a_3 (p + 1.3\, e)\, \theta^{0.9} \quad , \tag{231}$$

$$\hat{c} = a_4\, p\, \theta^{a_5} \tag{232}$$

and for water vapour in air,

$$g = b_3 (4.8\, e + p)\, \theta^{0.6} \quad . \tag{233}$$

The line data a_3, a_4 and b_3 are listed in Table 1.

The continuum spectrum, N_c, is given by

$$N_c \simeq 1.9 fep\theta^{3.1} \times 10^{-6} + 6.25 fp\theta^2 \times 10^{-4} \left[\frac{g_0}{f^2 + g_0^2} + 2.1 p\theta^{0.5} \times 10^{-7} \right] \quad ppm \tag{234}$$

and

$$g_0 = 0.012(p + 1.3\, e)\, \theta^{0.9} \quad . \tag{235}$$

The liquid water extinction, N_w, is evaluated from the following expressions:

$$N_w = \frac{4.49\, \varepsilon''}{(\varepsilon' + 2)^2 + (\varepsilon'')^2} \quad ppm \text{ for } f \leq 300 \text{ GHz} \tag{236}$$

and

$$N_w \simeq 0.55\, wf^{-0.1}\, \theta^{-6} \quad ppm \text{ for } f > 300 \text{ GHz} \quad , \tag{237}$$

where w is the liquid water concentration in grams per cubic meter. The real and imaginary part of the dielectric function of water, ε' and ε'', are given by Equations 207 and 208 respectively. It is assumed that ε_s and τ given in Equations 207 and 208 are given by Equations 210 and 215 respectively.

The absorptivity of tropospheric gases, η, is related to the atmospheric absorption, g_{ab}, in dB km, by the following expression [Ref. 13]:

$$g_{ab} = \frac{2\pi}{\lambda} 10^6\, \eta \log_{10} e \quad . \tag{238}$$

Hence,

$$\eta = \frac{g_{ab}\,\lambda}{2\pi\,10^{5}\log_{10} e} \quad . \tag{239}$$

Table 1. SPECTROSCOPIC COEFFICIENTS FOR OXYGEN ($a_1 - a_5$) AND WATER ($b_1 - b_3$) [FROM REF. 11]

Center frequency, ν_0 (GHz)	Strength, a_1 (kHz/kPa)	Temperature exponent, a_2	Width, a_3 (GHz/kPa)	Interference, a_4 (1/kPa)	Temperature exponent, a_5	Quantum number identification, K^a
0[e]	0.307 E−3 (ppm/kPa)		0.12 (0.056) E−1			1[+] to 37[+]
50.47381	0.94 E−6	0.969 E+1	0.86 E−2	0.520 E−2	0.179 E+1	37[−]
50.98742	0.244 E−5	0.869 E+1	0.87 E−2	0.550 E−2	0.169 E+1	35[−]
51.50311	0.604 E−5	0.774 E+1	0.89 E−2	0.560 E−2	0.177 E+1	33[−]
52.02124	0.141 E−4	0.684 E+1	0.92 E−2	0.550 E−2	0.181 E+1	31[−]
52.54227	0.308 E−4	0.600 E+1	0.94 E−2	0.569 E−2	0.179 E+1	29[−]
53.06683	0.637 E−4	0.522 E+1	0.97 E−2	0.528 E−2	0.189 E+1	27[−]
53.59570	0.124 E−3	0.448 E+1	0.100 E−1	0.544 E−2	0.183 E+1	25[−]
54.12997	0.2265 E−3	0.381 E+1	0.102 E−1	0.480 E−2	0.199 E+1	23[−]
54.67115	0.3893 E−3	0.319 E+1	0.105 E−1	0.484 E−2	0.190 E+1	21[−]
55.22137	0.6274 E−3	0.262 E+1	0.1079 E−1	0.417 E−2	0.207 E+1	19[−]
55.78382	0.9471 E−3	0.212 E+1	0.1110 E−1	0.375 E−2	0.207 E+1	17[−]
56.26477	0.5453 E−3	0.100 E−1	0.1646 E−1	0.774 E−2	0.890	D1[b] 1[+]
56.36339	0.1335 E−2	0.166 E+1	0.1144 E−1	0.297 E−2	0.229 E+1	15[−]
56.96818	0.1752 E−2	0.126 E+1	0.1181 E−1	0.212 E−2	0.253 E+1	13[−]
57.61249	0.2125 E−2	0.910	0.1221 E−1	0.940 E−3	0.376 E+1	11[−]
58.32389	0.2369 E−2	0.621	0.1266 E−1	−0.550 E−3	−0.111 E+2	D2 9[−]
58.44658	0.1447 E−2	0.827 E−1	0.1449 E−1	0.597 E−2	0.790	3[+]
59.16422	0.2387 E−2	0.386	0.1319 E−1	−0.244 E−2	0.700 E−1	7[−]
59.59098	0.2097 E−2	0.207	0.1360 E−1	0.344 E−2	0.490	5[+]
60.30604	0.2109 E−2	0.207	0.1382 E−1	−0.435 E−2[c]	0.680	D3 5[−]
60.43478	0.2444 E−2	0.386	0.1297 E−1	0.132 E−2	−0.120 E+1	7[+]
61.15057	0.2486 E−2	0.621	0.1248 E−1	−0.360 E−3	0.584 E+1	9[+]
61.80016	0.2281 E−2	0.910	0.1207 E−1	−0.159 E−2	0.286 E+1	11[+]
62.41122	0.1919 E−2	0.126 E+1	0.1171 E−1	−0.266 E−2	0.226 E+1	D4 13[+]
62.48626	0.1507 E−2	0.827 E−1	0.1468 E−1	−0.503 E−2[c]	0.850	3[−]
62.99797	0.1492 E−2	0.166 E+1	0.1139 E−1	−0.334 E−2	0.218 E+1	15[+]
63.56852	0.1079 E−2	0.212 E+1	0.1108 E−1	−0.417 E−2	0.196 E+1	17[+]
64.12778	0.7281 E−3	0.262 E+1	0.1078 E−1	−0.448 E−2	0.200 E+1	19[+]
64.67886	0.4601 E−3	0.319 E+1	0.105 E−1	−0.515 E−2	0.184 E+1	21[+]
65.22412	0.2727 E−3	0.381 E+1	0.102 E−1	−0.507 E−2	0.192 E+1	23[+]
65.76474	0.152 E−3	0.448 E+1	0.100 E−1	−0.567 E−2	0.178 E+1	25[+]
66.30195	0.794 E−4	0.522 E+1	0.97 E−2	−0.549 E−2	0.184 E+1	27[+]
66.83663	0.391 E−4	0.600 E+1	0.94 E−2	−0.588 E−2	0.174 E+1	29[+]
67.36933	0.181 E−4	0.684 E+1	0.93 E−2	−0.560 E−2	0.177 E+1	31[+]
67.90051	0.795 E−5	0.774 E+1	0.89 E−2	−0.580 E−2	0.173 E+1	33[+]
68.43054	0.328 E−5	0.869 E+1	0.87 E−2	−0.570 E−2	0.165 E+1	35[+]
68.95972	0.128 E−5	0.969 E+1	0.86 E−2	−0.530 E−2	0.174 E+1	37[+]
118.75034	0.9341 E−3	0.000	0.1592 E−1	−0.441 E−3	0.890	1[−]

Table 1. (continued)

Center frequency, ν_0 (GHz)	Strength, a_1 (kHz/kPa)	Temperature exponent, a_2	Width, a_3 (GHz/kPa)	Quantum number identification (O_2) Lower	Upper
368.498350	0.679 E−4	0.200 E−1	0.156 E−1	1, 1	2, 3
424.763120	0.638 E−3	0.122 E−1	0.147 E−1	2, 1	2, 3
487.249371	0.235 E−3	0.122 E−1	0.147 E−1	2, 1	3, 3
715.393150	0.996 E−4	0.891 E−1	0.144 E−1	3, 3	4, 5
773.839732	0.571 E−3	0.798 E−1	0.140 E−1	4, 3	4, 5
834.145790	0.180 E−3	0.798 E−1	0.140 E−1	4, 3	5, 5
				Identification (H_2O)	
ν_0	b_1	b_2	b_3	Lower	Upper
• 22.235080	0.105	0.214 E+1	0.281 E−1	5, 2, 3	6, 1, 6
68.052	0.180 E−2	0.875 E+1	0.280 E−1	3, 2, 1 (1)[d]	4, 1, 3
• 183.310091	0.238 E+1	0.653	0.282 E−1	2, 2, 0	3, 1, 3
321.225644	0.460 E−1	0.616 E+1	0.220 E−1	9, 3, 6	10, 2, 9
• 325.152919	0.155 E+1	0.152 E+1	0.290 E−1	4, 2, 2	5, 1, 5
• 380.197372	0.123 E+2	0.102 E+1	0.285 E−1	3, 2, 1	4, 1, 4
386.778	0.400 E−2	0.733 E+1	0.160 E−1	11, 2, 10	10, 3, 7
437.34667	0.630 E−1	0.502 E+1	0.150 E−1	6, 6, 0	7, 5, 3
439.150812	0.921	0.356 E+1	0.175 E−1	5, 5, 0	6, 4, 3
443. 018295	0.191	0.502 E+1	0.148 E−1	6, 6, 1	7, 5, 2
• 448.001075	0.107 E+2	0.137 E+1	0.246 E−1	3, 3, 0	4, 2, 3
470.888947	0.328	0.357 E+1	0.181 E−1	5, 5, 1	6, 4, 2
474.689127	0.124 E+1	0.234 E+1	0.210 E−1	4, 4, 0	5, 3, 3
488.491133	0.256	0.281 E+1	0.222 E−1	7, 1, 7	6, 2, 4
504.219	0.380 E−1	0.669 E+1	0.127 E−1	7, 7, 0	8, 6, 3
505.126	0.120 E−1	0.669 E+1	0.130 E−1	7, 7, 1	8, 6, 2
• 556.936002	0.526 E+3	0.114	0.317 E−1	1, 0, 1	1, 1, 0
• 620.700807	0.521 E+1	0.234 E+1	0.216 E−1	4, 4, 1	5, 3, 2
658.340	0.460	0.776 E+1	0.328 E−1	1, 0, 1 (1)	1, 1, 0
• 752.033227	0.259 E+3	0.336	0.302 E−1	2, 0, 2	2, 1, 1
836.836	0.120 E−1	0.811 E+1	0.170 E−1	11, 2, 9	10, 5, 6
859.810	0.150 E−1	0.799 E+1	0.270 E−1	2, 0, 2 (1)	2, 1, 1
899.380	0.910 E−1	0.784 E+1	0.300 E−1	1, 1, 1 (1)	2, 0, 2
903.280	0.640 E−1	0.835 E+1	0.280 E−1	2, 2, 1 (1)	3, 1, 2
907.773	0.179	0.504 E+1	0.204 E−1	8, 3, 5	9, 2, 8
• 916.169	0.890 E+1	0.137 E+1	0.249 E−1	3, 3, 1	4, 2, 2
970.320	0.940 E+1	0.184 E+1	0.246 E−1	4, 3, 1	5, 2, 4
• 987.910	0.145 E+3	0.180	0.299 E−1	1, 1, 1	2, 0, 2
• 1097.368	0.840 E+3	0.656	0.335 E−1	3, 0, 3	3, 1, 2

Read 0.307 E−3 as 0.307×10^{-3}.

[c] Nonresonant O_2 spectrum (equation (21)).

[b] D1 denotes doublet.

[e] *Rosenkranz*'s [1975] first-order solution for the 60-GHz band shape has a shortcoming: the listed values of $a_4(K = 3^-, 5^-)$ have to be reduced 5% (which is of negligible consequence) to assure that $\alpha(O_2) \geq 0.000$ for $f > 160$ GHz even when $N''_2 = 0$ (equation (21)).

[d] Here (1) denotes first vibrationally excited state.

III. SHELLMAN - MORFITT ROOT FINDING ROUTINE

A. GENERAL OUTLINE

The Shellman-Morfitt root finding routine was developed by C.H. Shellman and D.G. Morfitt to locate ELF VLF LF mode constants of wave propagating in an earth-ionosphere waveguide environment. The theory of the algorithm described in this chapter is based on References 1 and 14.

The complex root finding routine is used to find the zeros of the modal function. The routine will locate all simple zeros of an analytic function in a prescibed rectangular region of the complex z-plane. The principle of the root finding method is based on the following theorem [Ref. 15]:

> Theorem (Argument Principle):
> Let D be a simply connected domain and f(z) be analytic in D except at a finite number of poles. Let Γ be a closed contour in D not passing through any of the zeros or poles of f(z). Then, the accumulated phase change, $\Delta\phi$, of f(z) around Γ traversed in a clockwise direction is given by
>
> $$\Delta\phi = 2\pi (N_z - N_p) \quad , \tag{240}$$
>
> where N_z is the number of zeros and N_p is the number of poles (counting multiplicities) enclosed by Γ.

From the above theorem, if f(z) has only zeros in the region enclosed by Γ , then every constant phase contour associated with a zero crosses Γ.

An analytic function f(z) can be expressed as

$$f(z) = \sqrt{[Re(f)]^2 + [Im(f)]^2}\ \exp(j\theta) \quad , \tag{241}$$

where θ is the phase of f(z) given by

$$\theta = \arg [f(z)] \quad . \tag{242}$$

If f(z) does not have any pole or branch point, then the constant phase curve, $\theta = \theta_c$, radiating from a zero of f(z) must cross the closed contour, Γ, enclosing the zero at least once. In addition, no other zero of f(z) may be on this phase curve. This is illustrated in Figure 5.

A line of constant phase which crosses the contour Γ may be followed until it leads to a zero or until it crosses the contour again. A zero of f(z) can be determined from the intersection of the curves

$$Im(f) = 0 \quad ; \quad (\theta_c = 0 \text{ or } \pi) \tag{243}$$

and

$$Re(f) = 0 \quad ; \quad \left(\theta_c = \frac{\pi}{2} \text{ or } \frac{3\pi}{2}\right) \quad . \tag{244}$$

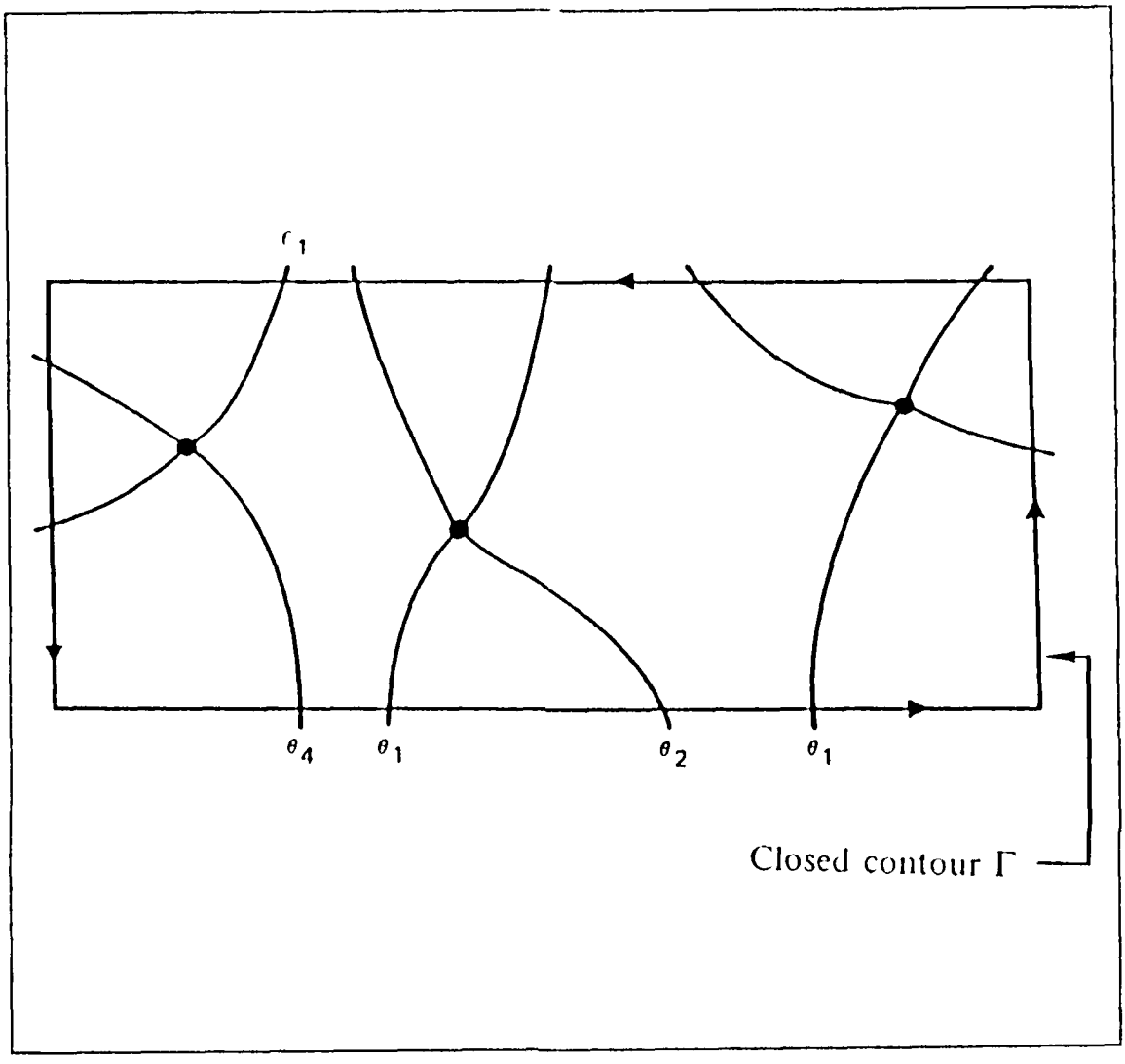

Figure 5. Constant Phase Line of f(z) [From Ref. 1]

B. ROOT SEARCH PROCEDURE

A search rectangle is set up in the complex z-plane so that the simple zeros of f(z) will be located by the routine. The corners of this rectangle are denoted by:

- t_L - value of the real part of z at the left edge of the rectangle.
- t_R - value of the real part of z at the right edge of the rectangle.
- t_T - value of the imaginary part of z at the top edge of the rectangle.
- t_B - value of the imaginary part of z at the bottom of the rectangle.

The search rectangle is divided into small mesh squares of length δ. Restrictions on the size of δ will be addressed later.

A new search rectangle is generated from the specified search rectangle by expressing the edge of the new rectangle in terms of mesh units. One mesh unit is of length δ. Thus

$$J_L = Int\left(\frac{t_L}{\delta}\right) \quad , \tag{245}$$

$$J_R = Int\left(\frac{t_R}{\delta}\right) \quad , \tag{246}$$

$$J_T = Int\left(\frac{t_T}{\delta}\right) \tag{247}$$

and

$$J_B = Int\left(\frac{t_B}{\delta}\right) \quad . \tag{248}$$

where Int(x) denotes the integer part of x. In order that the original search rectangle falls completely within the new search rectangle, the new rectangle is made one mesh unit larger on all sides. That is,

$$J_L = \begin{cases} J_L - 1 & ; \quad t_L \geq 0 \\ J_L - 2 & ; \quad t_L < 0 \end{cases} \quad . \tag{249}$$

$$J_R = \begin{cases} J_R + 2 & ; \quad t_R \geq 0 \\ J_R + 1 & ; \quad t_R < 0 \end{cases} \quad . \tag{250}$$

$$J_T = \begin{cases} J_T + 2 & : \quad t_T > 0 \\ J_T + 1 & : \quad t_T \leq 0 \end{cases} \tag{251}$$

and

$$J_B = \begin{cases} J_B - 1 & ; \quad t_B \geq 0 \\ J_B - 2 & : \quad t_B < 0 \end{cases} \quad . \tag{252}$$

The search rectangle with mesh grid is shown in Figure 6. The plus and minus signs at the corners of the mesh squares are the signs of Im(f). The solid curves represent the phase line, Im(f)=0, while the dashed curves represent the phase line, Re(f)=0. The zeros of f(z) are located at the crossing of the Im(f)=0 and Re(f)=0 curves. A local mesh coordinate system is shown in Figure 7. The lower left-hand corner of the mesh square is taken as the origin of that mesh square's local coordinate system. The value of f(z) evaluated in the local mesh coordinates of the k^{th} mesh square is denoted by $f^{(k)}(\chi_k, \omega_k)$. Thus, the values of f(z) at the corners of mesh square 1 are

$$f^{(1)}(0, 1) = f(J_L \delta + j J_T \delta) \quad , \tag{253}$$

$$f^{(1)}(0, 0) = f[J_L \delta + j (J_T - 1)\delta] \quad , \tag{254}$$

$$f^{(1)}(1, 0) = f[(J_L + 1)\delta + j (J_T - 1)\delta] \tag{255}$$

and

$$f^{(1)}(1, 1) = f[(J_L + 1)\delta + j J_T \delta] \quad . \tag{256}$$

A basic assumption made on f(z) is that Im(f) and Re(f) are linear functions of the local mesh coordinates, χ_k and ω_k. This means that in the mesh square k, f(z) can be expressed as [Ref. 1]

$$f^{(k)}(\chi_k, \omega_k) = a_k + b_k \omega_k + c_k \chi_k + d_k \omega_k \chi_k \quad , \tag{257}$$

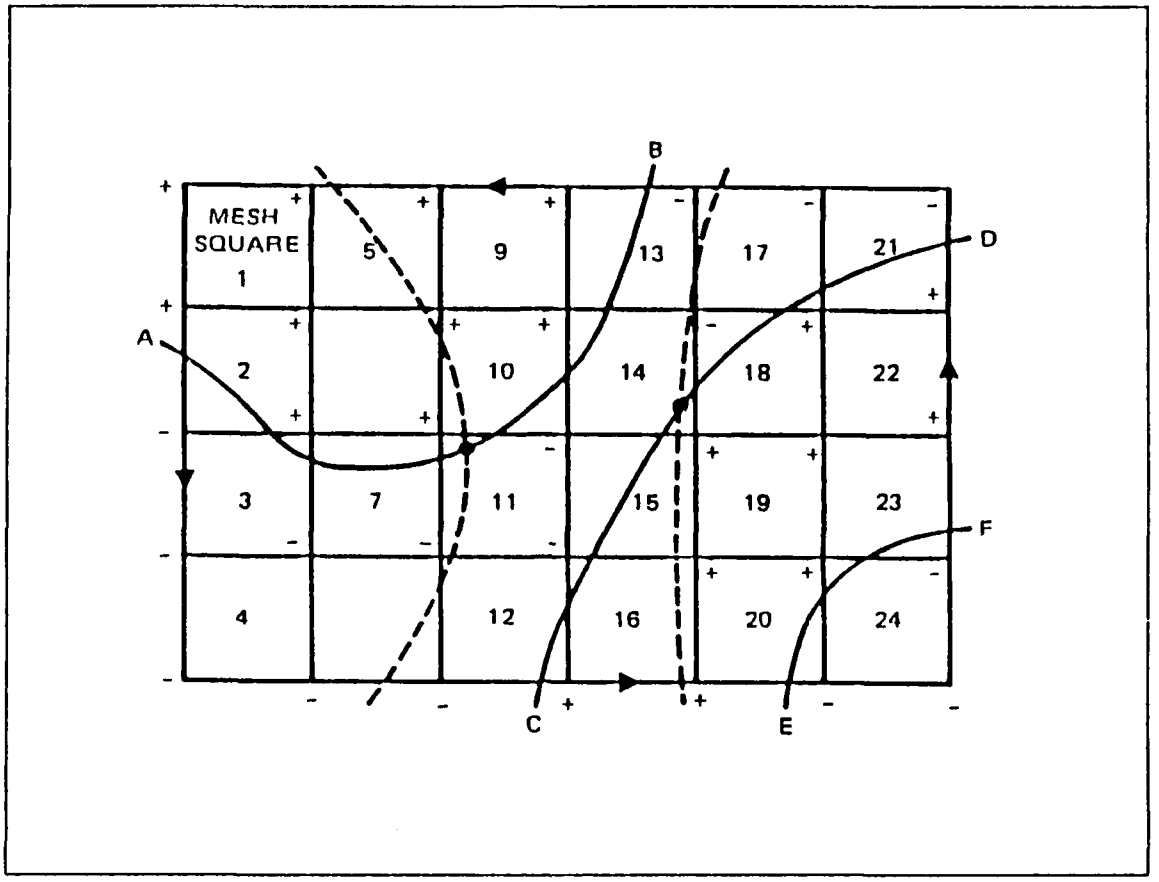

Figure 6. Illustration of search rectangle with mesh grid [From Ref. 1]

where

$$a_k = f^{(k)}(0,0) \quad , \tag{258}$$

$$b_k = f^{(k)}(0,1) - f^{(k)}(0,0) \quad , \tag{259}$$

$$c_k = f^{(k)}(1,0) - f^{(k)}(0,0) \tag{260}$$

and

$$d_k = f^{(k)}(0,0) + f^{(k)}(1,1) - f^{(k)}(0,1) - f^{(k)}(1,0) \quad . \tag{261}$$

This assumption puts an upper bound on the size of the mesh unit, δ. The mesh unit should be sufficiently small to ensure that the linear variation of $\hat{f}(z)$ holds. However, δ should not be excessively small to reduce computer run time.

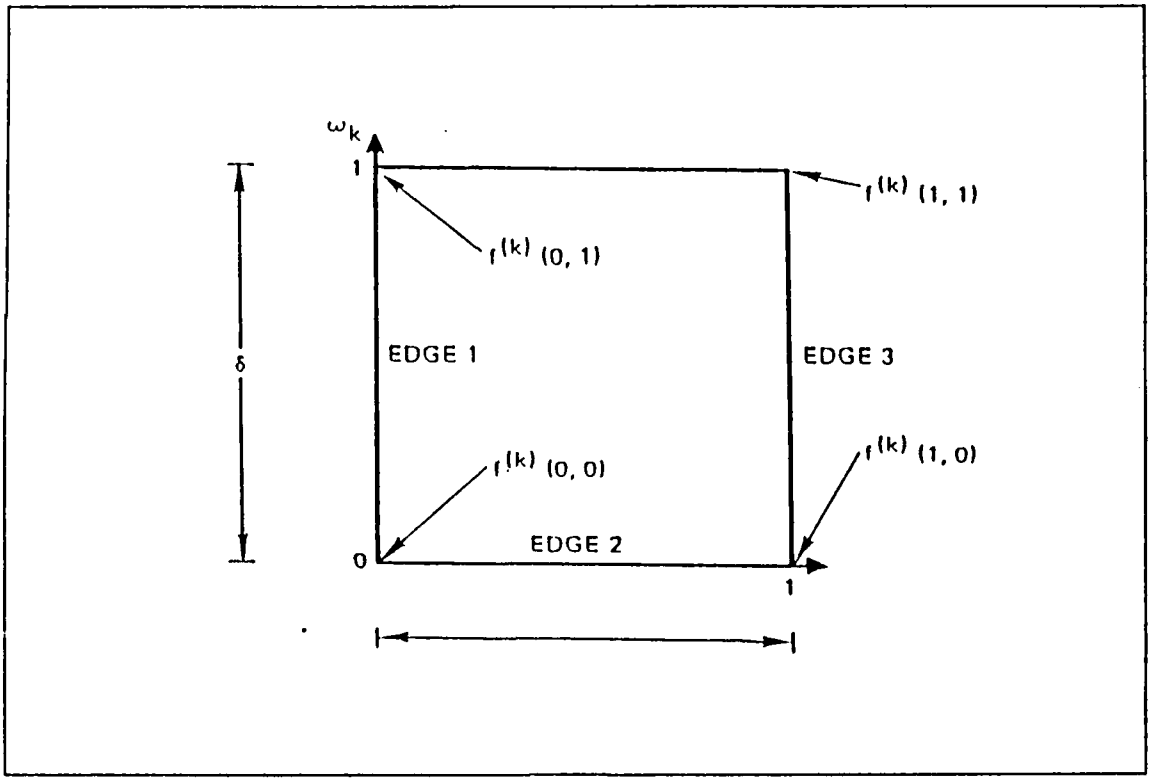

Figure 7. Local mesh coordinate system [From Ref. 1]

The zeros of f(z) are searched by examining the imaginary part of f(z) counterclockwise around the rectangular contour. For the example shown in Figure 6, the edges of the search rectangle are examined for crossing of the phase curve, Im(f) = 0, starting with mesh square 1, edge 1. The values $Im[f^{(1)}(0, 1)]$ and $Im[f^{(1)}(0, 0)]$ are first computed. If they are of the same sign, then there will be no Im(f) = 0 curve passing through edge 1.

Mesh square 2 is investigated next. The values of $Im[f^{(2)}(0, 1)]$ and $Im[f^{(2)}(0, 0)]$ are computed. The value of $Im[f^{(2)}(0, 1)]$ is identical to $Im[f^{(1)}(0, 0)]$. If the signs of $Im[f^{(2)}(0, 1)]$ and $Im[f^{(2)}(0, 0)]$ are opposite as shown in Figure 6, then the Im(f) = 0 curve enters mesh square 2 along edge 1. The crossing point is given by [Ref. 1]

$$\chi_2 = 0 \tag{262}$$

and

$$\omega_2 = -\frac{Im[f^{(2)}(0,0)]}{Im[f^{(2)}(0,1)] - Im[f^{(2)}(0,0)]} \quad . \tag{263}$$

The next step is to determine if a zero is within mesh square 2. The values of $Im[f^{(2)}(1,0)]$ and $Im[f^{(2)}(1,1)]$ are first computed. Two tests must be made:

1. A test is made to determine if there is one or two Im(f)=0 curves entering and leaving the mesh square. If $Im[f^{(k)}(0,0)]$ and $Im[f^{(k)}(1,1)]$ are of the same sign, e.g., minus, and $Im[f^{(k)}(0,1)]$ and $Im[f^{(k)}(1,0)]$ both have opposite signs, e.g., plus, then there are two lines of Im(f)=0 entering and leaving the square. This condition is depicted in mesh square 14 of Figure 6. Otherwise, there is only one line of Im(f)=0 entering and leaving the mesh square. This is illustrated in mesh square 2 of Figure 6.
2. A test has to be performed to determine if there is at least one Re(f)=0 entering and leaving the mesh square. If $Re[f^{(k)}(0,0)]$, $Re[f^{(k)}(0,1)]$, $Re[f^{(k)}(1,0)]$ and $Re[f^{(k)}(1,1)]$ are all of the same sign, then there is no line of Re(f)=0 passing through the mesh square. Otherwise, there is at least one Re(f)=0 curve entering and leaving the mesh square.

Note that the above tests will fail if there are two or more Im(f)=0 or Re(f)=0 crossing the mesh square at the same edge. As shown in Figure 8, two Im(f)=0 crossing the same edge of a mesh square results in a zero being missed. In this situation, the mesh size has to be reduced in order to resolve the two zeros.

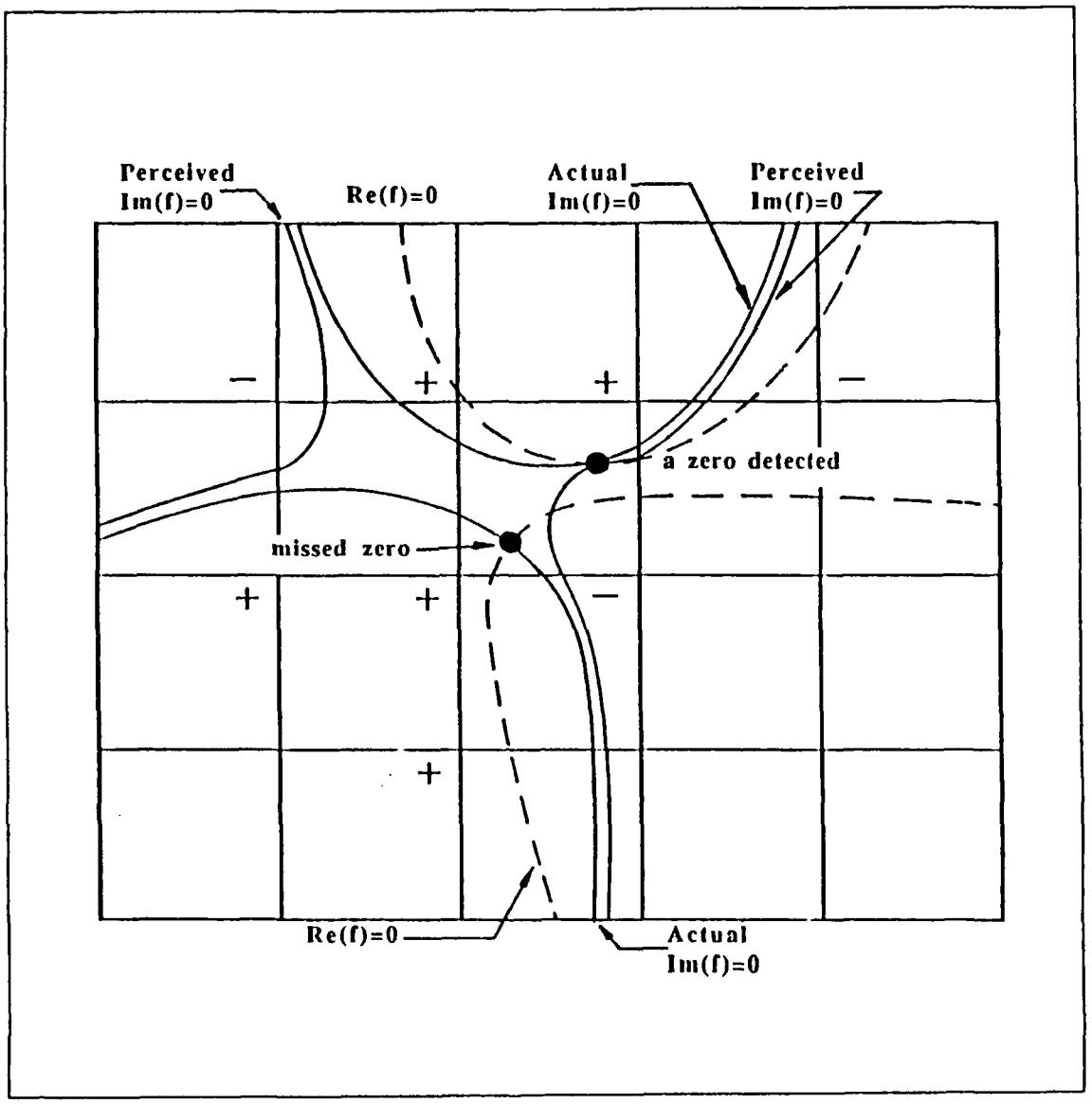

Figure 8. Crossing of two Im(f) = 0 at the same edge of the mesh square

The program (see subroutine fzerox in Chapter V) also checks for the presence of more than one zero on the same phase line. Such a situation may occur as in Figure 9. The program treats such an occurrence as an error and will proceed to reduce the mesh size. The root-search will start all over again.

One can infer that the presence of more than one zero on the same phase line is due to the inability to resolve two phase lines crossing a mesh square at the same edge. These

zeros actually lie on different phase lines and are 'legitimate' zeros. It is the author's opinion that these zeros are acceptable and a mesh-size reduction accompanied by a re-run of the root search routine unnecessary.

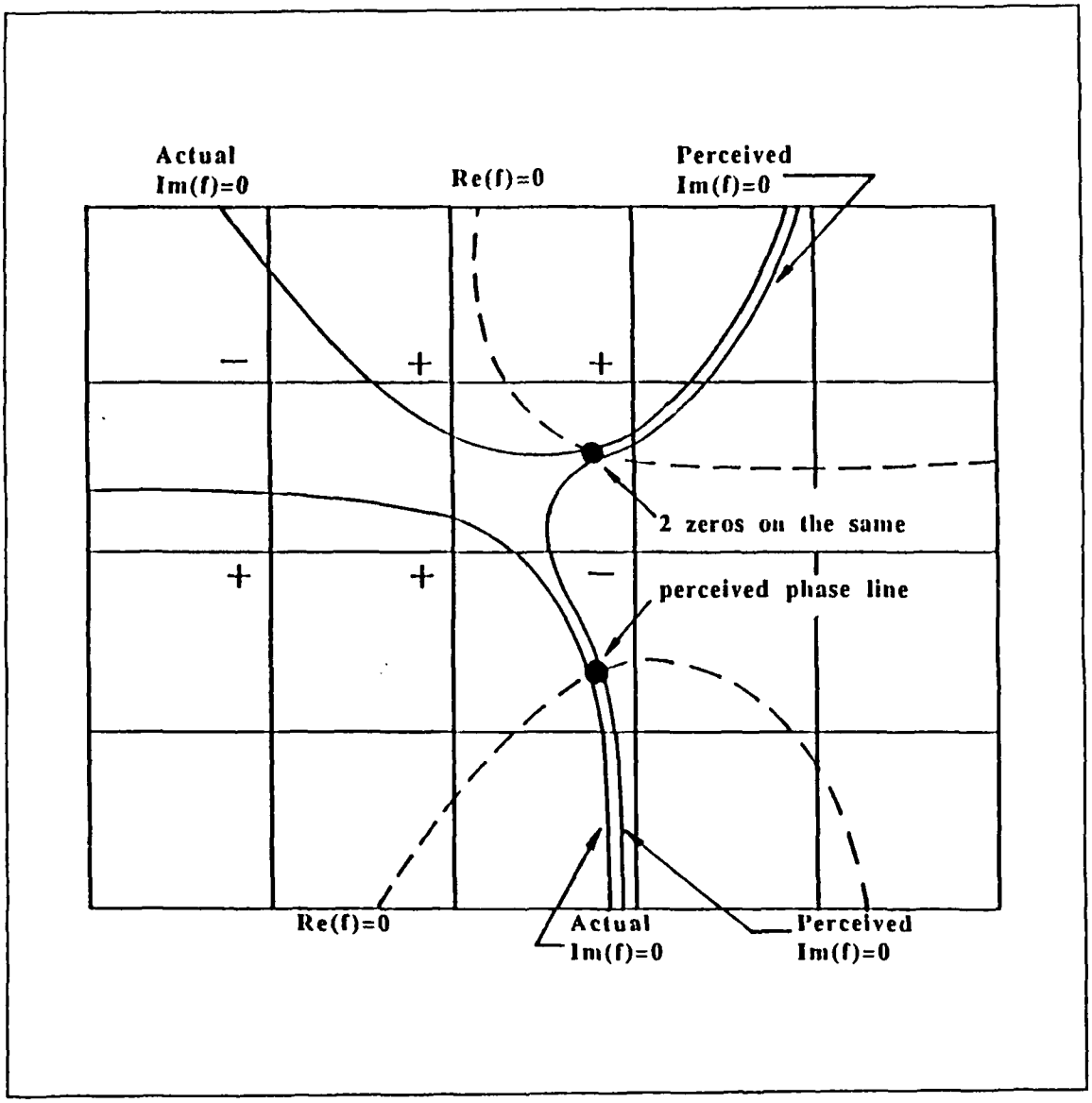

Figure 9. Two zeros found on the same phase line

The line Im(f) = 0 is traced from mesh to mesh until it exits the contour rectangle. For the example in Figure 6, the curve AB is followed through mesh squares 2, 3, 7, 11, 10, 14 and 13. In mesh square 11, both Im(f) = 0 and Re(f) = 0 pass through the mesh

square. The point of intersection can be determined from Equation 257. The mathematical details are presented in section C.

The contour AB is followed out of mesh square 11 into mesh squares 10 and 14. In mesh square 14, there are two Im(f)=0 curves and one Re(f)=0 curve. A crossing point is chosen to be a zero of f(z) if it lies on the Im(f)=0 curve currently being followed. Therefore, when the contour AB is being traced, the zero in mesh square 14 will be ignored. However, this zero will be located when contour CD is being traced.

When contour AB exits the search rectangle at point B, the value of the leading edge (counterclockwise) of the mesh square is noted. In this example, the value of the leading edge is $f^{(13)}(0, 1)$. Identifying the exit points would prevent subsequent re-entering of the search rectangle via these points.

After the contour AB exits at B, the search for zeros of f(z) is continued by looking for more crossings of Im(f)=0 with the search rectangle. Since mesh square 2 was the last mesh square that was checked for such crossings, the next mesh square to be examined will be mesh square 3.

The next crossing of Im(f)=0 with the search rectangle is at mesh square 12. This contour CD is again followed through to mesh 21 where the exit point D is noted. The zero along CD in mesh square 14 is considered as an acceptable zero of f(z) since it lies on the contour CD which is the current contour being traced. The rectangular contour search will continue as described above until the search gets to mesh square 1, edge 4 where it stops.

C. DETERMINATION OF THE COORDINATES OF ROOTS

The root of f(z) is the point of intersection of Im(f)=0 and Re(f)=0. This can be determined from Equation 257.

By equating Im(f) of Equation 257 to zero, the following equations are obtained:

$$\gamma_k = -\frac{Im(a_k) + Im(b_k)\omega_k}{Im(c_k) + Im(d_k)\omega_k} \tag{264}$$

and

$$\omega_k = -\frac{Im(a_k) + Im(c_k)\gamma_k}{Im(b_k) + Im(d_k)\gamma_k} \quad . \tag{265}$$

Similarly, by equating Re(f) to zero,

$$\chi_k = - \frac{Re(a_k) + Re(b_k)\omega_k}{Re(c_k) + Re(d_k)\omega_k} \tag{266}$$

and

$$\omega_k = - \frac{Re(a_k) + Re(c_k)\chi_k}{Re(b_k) + Re(d_k)\chi_k} \quad . \tag{267}$$

Note that Equations 264 and 265 are equivalent; so are Equations 266 and 267. By equating the right hand side of Equation 264 and that of Equation 266, the following quadratic equation in ω_k results:

$$P_1 \omega_k^{\,2} + Q_1 \omega_k + W_1 = 0 \quad , \tag{268}$$

where

$$P_1 = Re\,(b_k)\, Im(d_k) - Im(b_k)\, Re\,(d_k) \quad , \tag{269}$$

$$\begin{aligned} Q_1 = {} & Re\,(a_k)\, Im(d_k) + Re\,(b_k)\, Im(c_k) \\ & - Im(a_k)\, Re\,(d_k) - Im(b_k)\, Re\,(c_k) \end{aligned} \tag{270}$$

and

$$W_1 = Re\,(a_k)\, Im(c_k) - Im(a_k)\, Re\,(c_k) \quad . \tag{271}$$

Similarly, from Equation 265 and 267, the quadratic equation in χ_k is obtained:

$$P_2 \chi_k^{\,2} + Q_2 \chi_k + W_2 = 0 \quad , \tag{272}$$

where

$$P_2 = Re(c_k)\, Im(d_k) - Im(c_k)\, Re(d_k) \quad , \tag{273}$$

$$\begin{aligned} Q_2 = {} & Re(a_k)\, Im(d_k) + Re(c_k)\, Im(b_k) \\ & - Im(a_k)\, Re(d_k) - Im(c_k)\, Re(b_k) \end{aligned} \tag{274}$$

and

$$W_2 = Re(a_k) Im(b_k) - Im(a_k)\, Re(b_k) \quad . \tag{275}$$

According to the program source code, if

$$|P_1| < |P_2| \quad , \tag{276}$$

then the root-finder routine uses Equations 264 and 268 to solve for χ_s and ω_s. If the condition in Equation 276 is not satisfied, then χ_s and ω_s will be determined from Equations 265 and 272.

However, it should be noted that if Equation 276 is true and if $|P_1|$ approaches zero, one of the solutions of Equation 268 will become infinite. By the same token, if Equation 276 is not true and if $|P_2|$ approaches zero, one of the solutions of Equation 272 will become infinite. The program (see subroutine quad in Chapter V) prevents such occurrences by incorporating a test such that the program returns only one solution when $|P_1|$ or $|P_2|$ approaches zero, i.e., Equation 268 or 272 reduces to a linear equation.

On the other hand, unless both $|P_1|$ and $|P_2|$ become very small, the above problem could be avoided if χ_s and ω_s are determined from Equations 265 and 272 when Equation 276 is true; otherwise Equations 264 and 268 are used. This modification is recommended.

A solution of Equations 265 and 272 or 264 and 268 will be valid if it lies within the current mesh square, i.e.,

$$0 \leq \chi_s \leq 1 \tag{277}$$

and

$$0 \leq \omega_s \leq 1 \quad , \tag{278}$$

where $z_s = (\chi_s, \omega_s)$ is the solution .

In addition, the solution must also lie on the line Im(f)=0 currently being traced. The test for this condition is derived below.

From Equation 257, Im(f)=0 and Re(f)=0 are equations of an equilateral hyperbola with vertical and horizontal asymptotes given by

$$\chi_C = -\frac{Im(b_i)}{Im(d_i)} \tag{279}$$

and

$$\omega_C = -\frac{Im(c)}{Im(d)} \quad . \tag{280}$$

Let (χ_E, ω_E) be the point at which $Im(f)=0$ enter the mesh square. If

$$(\chi_E - \chi_C)\,(\chi_S - \chi_C) > 0 \tag{281}$$

and

$$(\omega_E - \omega_C)\,(\omega_S - \omega_C) > 0 \quad . \tag{282}$$

then the solution of $f(z)$ lies on the current line.

Figure 10 illustrates the case where z_i is a proper solution and Figure 11 shows the case where z_i is not a proper solution of $f(z)=0$.

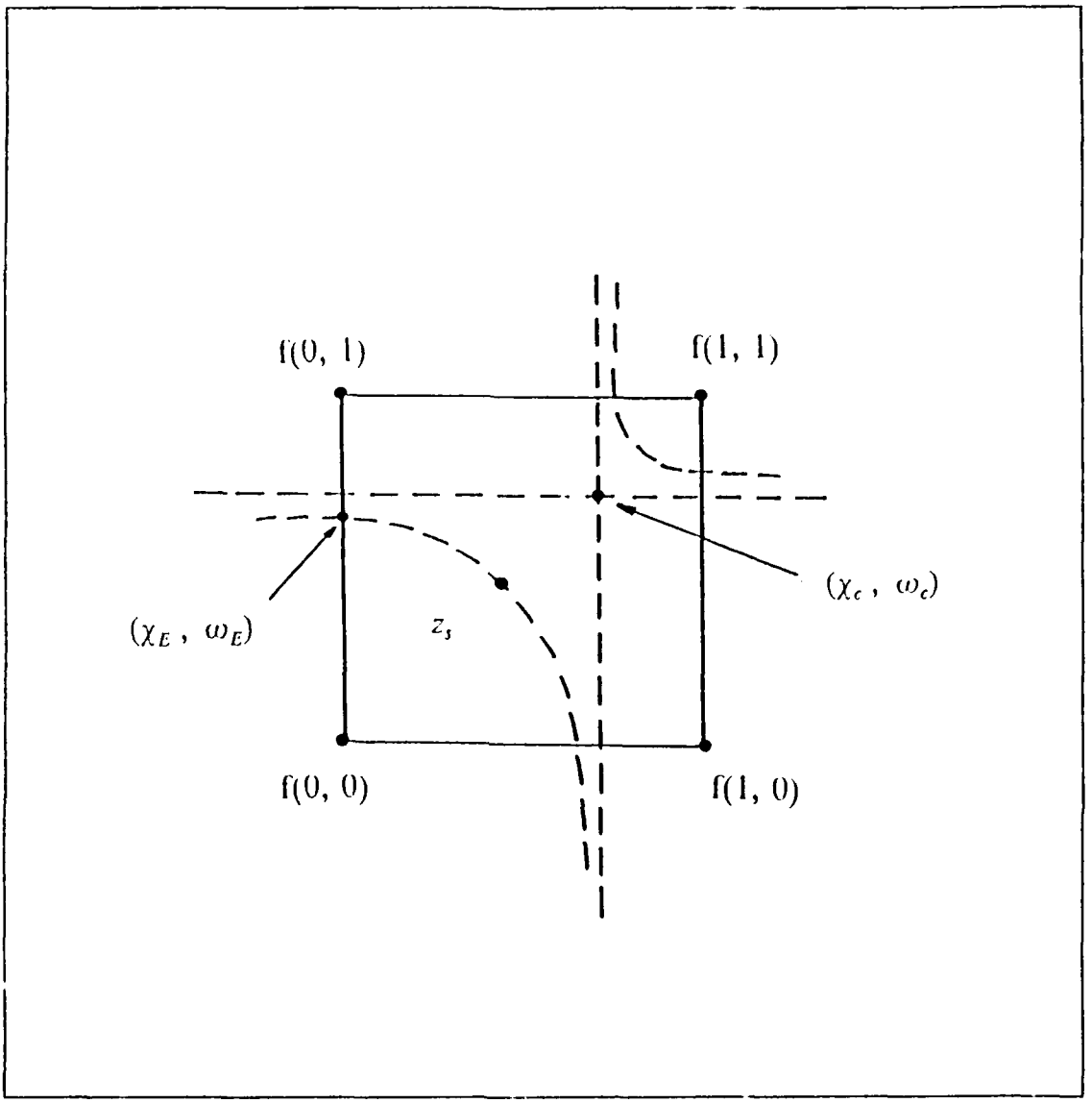

Figure 10. z_s is a proper solution of $f(z) = 0$ [After Ref. 14]

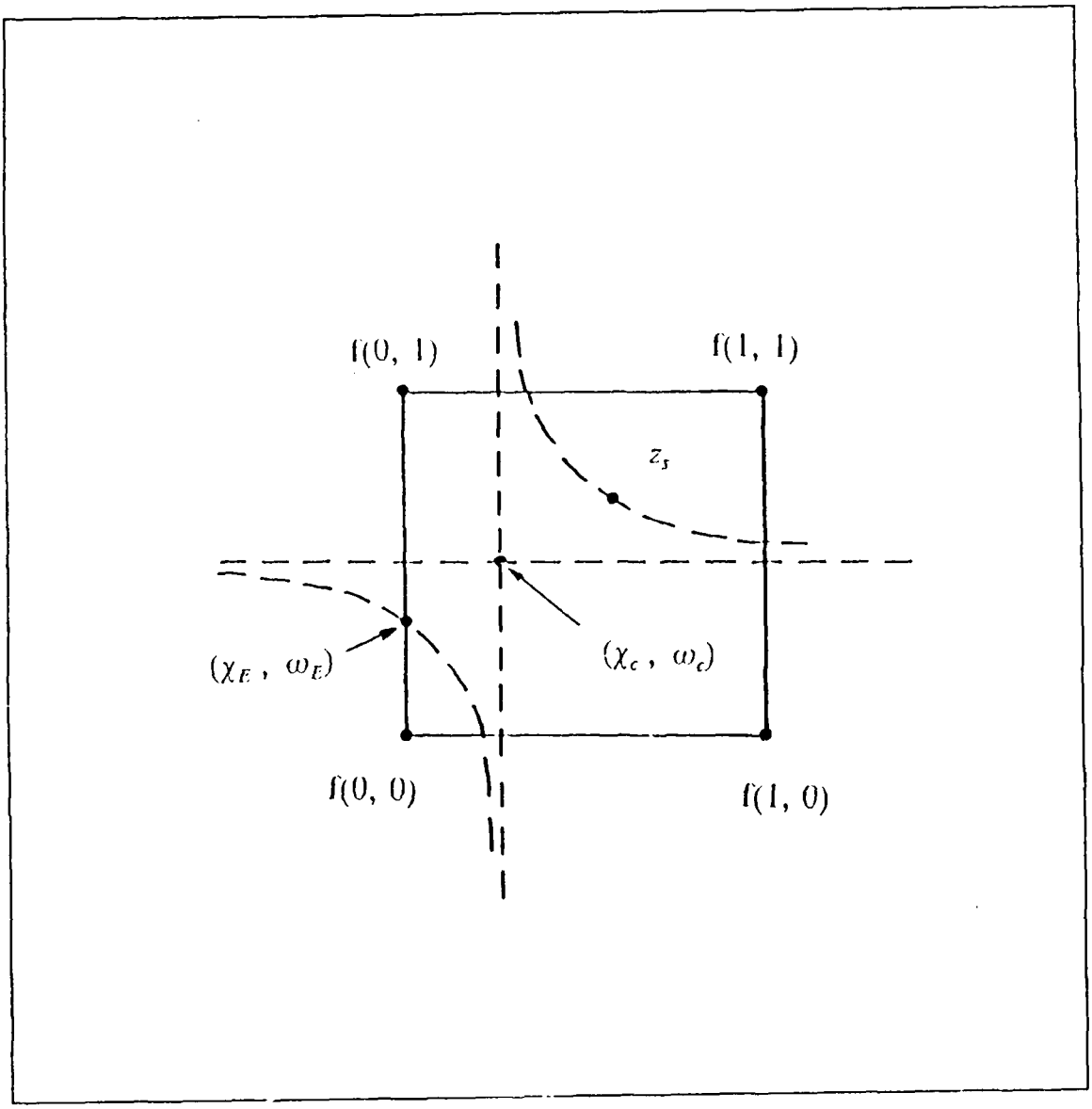

Figure 11. z_s is not a proper solution of $f(z) = 0$ [After Ref. 14]

D. SOLUTION OF THE QUADRATIC EQUATION

Procedures for the solution of the quadratic equation are required for solving Equations 268 and 272.

Consider the quadratic equation of the form

$$ax^2 + 2bx + c = 0 \quad . \tag{283}$$

The solution is

$$\begin{aligned} x &= -\frac{2b \pm \sqrt{4b^2 - 4ac}}{2a} \\ &= \frac{b}{a}\left[-1 \pm \sqrt{1 - \frac{ac}{b^2}}\right] \\ &= \frac{b}{a}\left[-1 \pm \sqrt{1 + \varepsilon}\right] \quad , \end{aligned} \tag{284}$$

where

$$\varepsilon = -\frac{ac}{b^2} \quad . \tag{285}$$

Hence,

$$x_1 = \frac{b}{a}\left[-1 + \sqrt{1 + \varepsilon}\right] \tag{286}$$

and

$$x_2 = \frac{b}{a}\left[-1 - \sqrt{1 + \varepsilon}\right] \quad . \tag{287}$$

If $\varepsilon \ll 1$, then

$$(1 + \varepsilon)^{1/2} = 1 + \frac{1}{2}\varepsilon + \frac{\left(\frac{1}{2} - 1\right)}{2}\varepsilon^2 + \ldots\ldots \quad . \tag{288}$$

Thus,

$$x_1 = \frac{b}{a}\left\{\frac{1}{2}\left(-\frac{ac}{b^2}\right) + \frac{1}{2}\,\frac{\left(\frac{1}{2}-1\right)}{2}\left(-\frac{ac}{b^2}\right)^2 + \frac{\frac{1}{2}\left(\frac{1}{2}-1\right)\left(\frac{1}{2}-2\right)}{3\,.\,2}\left(-\frac{ac}{b^2}\right)^3 + \ldots\ldots\right\} . \tag{289}$$

Factoring out $\left(\frac{-ac}{b^2}\right)$, Equation 289 becomes

$$x_1 = -\frac{1}{2}\frac{c}{b}\left\{1 + \frac{\left(\frac{1}{2}-1\right)}{2}\left[-\frac{ac}{b^2}\right] + \frac{\left(\frac{1}{2}-1\right)\left(\frac{1}{2}-2\right)}{3\,.\,2}\left[-\frac{ac}{b}\right]^2 + \ldots\ldots\right\} . \tag{290}$$

Let

$$t_0 = 1 \ , \tag{291}$$

$$t_1 = \frac{\left(\frac{1}{2}-1\right)}{2}\left[-\frac{ac}{b^2}\right] \tag{292}$$

and

$$t_2 = \frac{\left(\frac{1}{2}-1\right)\left(\frac{1}{2}-2\right)}{3\,.\,2}\left[\frac{ac}{b^2}\right]^2 \ . \tag{293}$$

In general,

$$t_k = t_{k-1}\left(\frac{k-\frac{1}{2}}{k+1}\right)\left[\frac{ac}{b^2}\right] \tag{294}$$

and

$$x_1 = -\frac{1}{2}\frac{c}{b}\{t_0 + t_1 + t_2 + \ldots\ldots + t_n\} \quad . \tag{295}$$

Once x_1 is found, x_2 can be found from Equations 286 and 287. By adding Equations 286 and 287, x_2 is given by

$$x_2 = -2\frac{b}{a} - x_1 \quad . \tag{296}$$

E. NEWTON RAPHSON ITERATION

The zeros of $f(z)$ found by the Shellman and Morfitt routine are only approximate solutions. The Newton Raphson iteration is used to improve the accuracy of the zero locations. The new root, z_{i+1}, is related to the previous root, z_i, by

$$z_{i+1} = z_i + \Delta z_i \quad , \tag{297}$$

where

$$\Delta z_i = -\frac{f(z_i)}{f'(z_i)} \quad . \tag{298}$$

Iteration of Equation 297 is continued until Δz_i is smaller than a pre-assigned tolerance.

IV. SOLUTION OF STOKES' DIFFERENTIAL EQUATION

A. STOKES' EQUATION

When the modified refractivity profile is modelled by a series of piecewise linear segments in the mathematical formulation of wave propagation in a multilayer tropospheric waveguide environment, the height gain function in each layer can be obtained from solution of Stokes' Equation.

$$\left[\frac{\partial^2}{\partial q_i^2} + q_i \right] k_n(q_i) = 0 \quad : \quad n = 1, 2 \ . \tag{299}$$

Solutions of Stokes' Equation are commonly given in terms of Airy functions or in terms of modified Hankel functions of order one-third. Several possible solutions exist and the choice of solution is dependent on numerical and physical considerations. Since $Im(q_i)$ is proportional to the attenuation rate of the electromagnetic signal, physical considerations dictate that $Im(q_i) \geq 0$. In this program, the height gain function is expressed as a linear combination of $k_1(q_i)$ and $k_2(q_i)$ which are linearly independent for $Im(q_i) \geq 0$. The choice of $k_1(q_i)$, $k_2(q_i)$ or equivalently $\{Ai(-q_i e^{2\pi/3}), Ai(-q_i)\}$ is to assure that at least one of the two functions do not become very small numerically in the upper half of the complex q_i-plane. For the top layer, i.e., i = 1, the boundary condition at $z \to \infty$ requires that the height gain function represents an outgoing wave. Hence in the topmost layer, $h_2(q_i)$ or equivalently $Ai(-q_i e^{-2\pi/3})$ is chosen to satisfy the radiation condition.

B. EVALUATION OF AIRY FUNCTIONS

1. General Outline

The algorithm for evaluation of complex Airy functions is adopted from Z. Schulten and D.G.M. Anderson [Ref. 16]. Evaluation of the complex function over the entire z-plane was achieved with a Taylor series and generalised Gaussian quadrature method. A Taylor series is used only for a small region near the origin within an ellipse with foci $(-1.58, 3.95)$ and $(0.28, -2.11)$, major axis of 9.0 and minor axis of 6.4. Outside the ellipse, the Gaussian quadrature approximation is used. The elliptical boundary was chosen to satisfy restrictions imposed by computational methods.

Analysis of the Airy functions need only be done in the upper half complex plane as those in the lower half plane can be computed by the following conjugate relations:

$$Ai(z) = Ai^*(z^*) \tag{300}$$

and

$$\frac{dAi(z)}{dz} = \frac{dAi^*(z^*)}{dz} \quad . \tag{301}$$

Therefore, an algorithm can be developed to compute Ai(z) for $0 \leq \arg z \leq 2\pi/3$ and by conjugacy, Ai(z) for $-2\pi/3 \leq \arg z \leq 0$ can be computed.

For $2\pi/3 < \arg z \leq 4\pi/3$, the following connection formula of Airy functions can be used:

$$Ai(z) = e^{j\pi/3} Ai(ze^{-j2\pi/3}) + e^{-j\pi/3} Ai(ze^{j2\pi/3}) \quad . \tag{302}$$

2. Evaluation by Taylor Series Expansion

For small values of |z |, the Airy functions are evaluated by the series expansion [Ref. 1 and 4].

$$Ai(z) = C_1 f(z) - C_2 g(z) \tag{303}$$

and

$$Ai'(z) = C_1 f'(z) - C_2 g'(z) \quad , \tag{304}$$

where

$$f(z) = \sum_{k=0}^{\infty} 3^k \frac{\Gamma\left(k + \frac{1}{3}\right)}{\Gamma\left(\frac{1}{3}\right)} \frac{z^{3k}}{(3k)!} \quad , \tag{305}$$

$$f'(z) = \sum_{k=1}^{\infty} 3^k \frac{\Gamma\left(k+\frac{1}{3}\right)}{\Gamma\left(\frac{1}{3}\right)} \frac{z^{3k-1}}{(3k-1)!} \quad , \tag{306}$$

$$g(z) = \sum_{k=0}^{\infty} 3^k \frac{\Gamma\left(k+\frac{2}{3}\right)}{\Gamma\left(\frac{2}{3}\right)} \frac{z^{3k+1}}{(3k+1)!} \quad , \tag{307}$$

$$g'(z) = \sum_{k=0}^{\infty} 3^k \frac{\Gamma\left(k+\frac{2}{3}\right)}{\Gamma\left(\frac{2}{3}\right)} \frac{z^{3k}}{(3k)!} \quad . \tag{308}$$

$$C_1 = \left[3^{2/3}\,\Gamma\left(\frac{2}{3}\right)\right]^{-1} \tag{309}$$

and

$$C_2 = \left[3^{1/3}\,\Gamma\left(\frac{1}{3}\right)\right]^{-1} \quad . \tag{310}$$

The number of terms required for convergence of the series is determined by a tolerance factor, ε, such that

$$|a_n| < \varepsilon \left|\sum_{i=0}^{n-1} a_i\right| \quad , \tag{311}$$

where

$$Ai(z) = \sum_{i=0}^{n} a_i \quad . \tag{312}$$

Similiar test for convergence is implemented for $Ai'(z)$. In the program, ε is taken to be the machine epsilon, i.e.,

$$\varepsilon = 2^{-37} \quad . \tag{313}$$

3. Evaluation by Generalised Gaussian Quadrature Method

Integral expressions for Ai(z) is given by [Ref. 16]

$$Ai(z) = \frac{1}{2\sqrt{\pi}} z^{-1/4} e^{-\zeta} \int_0^\infty \frac{\rho(x)\,dx}{\zeta + x} \tag{314}$$

$$\text{for } |z| > 0, \ |\arg z| < \frac{2\pi}{3} \quad ,$$

where

$$\zeta = \frac{2}{3} z^{3/2} \tag{315}$$

and

$$\rho(x) = \pi^{-1/2} \, 2^{-11/6} \, 3^{-2/3} \, x^{-2/3} \, e^{-x} \, Ai\left(\frac{3x}{2}\right) \quad . \tag{316}$$

The function, $\rho(x)$, is non-negative and exponentially decreasing. The integral in Equation 314 can be evaluated by the generalised Gaussian quadratic approximation, i.e.,

$$\int_0^\infty \frac{\rho(x)\,dx}{\zeta + x} \sim \sum_{i=1}^{n} \frac{w_i}{\zeta + x_i} \quad , \tag{317}$$

where w_i is the quadrature weight and x_i is the abscissa. Hence

$$Ai(z) \sim \frac{1}{2} \pi^{-1/2} z^{-1/4} e^{-\zeta} \sum_{i=1}^{n} \frac{w_i}{\zeta + x_i} \tag{318}$$

and

$$Ai'(z) \sim \frac{1}{2}\pi^{-1/2}z^{1/4}e^{-\zeta}\left[\left(\frac{5}{6}-\frac{\zeta}{\zeta}\right)\sum_{i=1}^{n}\frac{w_i}{(\zeta+x_i)}-\frac{\zeta}{\zeta}\sum_{i=1}^{n}\frac{w_i}{(\zeta+x_i)^2}\right] \quad . \quad (319)$$

The quadrature weights, w_i , and abscissae, x_i , had been calculated by Z. Schulten et al. [Ref. 16] and are given in Tables II to IV. These tables had been used for computation of single precision values up to seven significant digits.

Table 2. NUMBER OF TERMS REQUIRED IN QUADRATURE FORMULA [AFTER REF. 16]

z	$\arg z$	$Ai(z)$
$\lvert z \rvert \geqslant 11$	$< \frac{2\pi}{3}$	2 terms
$5 < \lvert z \rvert < 11$	$< \frac{2\pi}{3}$	4 terms
$2.5 < \lvert z \rvert < 5$	$< \frac{\pi}{3}$	4 terms

Table 3. 4-TERM GENERALISED GAUSSIAN INTEGRATION FOR AIRY FUNCTIONS [FROM REF. 16]

i	x_i	w_i
1.	3.9198329554455091	4.7763903057577263(−05)
2.	1.6915619004823504	4.9914306432910959(−03)
3.	5.0275532467263018(−01)	8.6169846993840312(−02)
4.	1.9247060562015692(−02)	9.0879095845981102(−01)

Table 4. 2-TERM GENERALISED GAUSSIAN INTEGRATION FOR AIRY FUNCTIONS [FROM REF. 16]

x_i	w_i
1.0592469382112378	3.1927194042263958(−02)
3.6800601866153044(−02)	9.6807280595773604(−01)

C. EXTENDED COMPLEX ARITHMETIC

The extended complex arithmetic was introduced by Baumgartner in XWVG to handle complex numbers of large magnitude to avoid overflow problem.

It was discussed in Section D of Chapter II that for large values of $|q|$, the magnitude of $k_1(q)$ and $k_2(q)$ may become exponentially large or exponentially small.

Numerical evaluation of the modal function of Equation 166 can easily yield complex numbers with magnitudes as large as 10^{+1000} or as small as 10^{-1000}. Numbers of these magnitudes are outside the numerical limits of most computers.

To overcome this problem, each complex function, $k_1(q)$ (or $k_2(q)$), is represented by

$$k_1 = \hat{k}_1 e^{\phi} \quad , \tag{320}$$

where $\hat{k}_1$ is the complex amplitude and ϕ is the real exponent. In the program, $\hat{k}_1$ is "normalized" such that

$$e^{-1} \leq \max [\, |Re(\hat{k}_1)| \, , \, |Im(\hat{k}_1)| \,] \leq e^{+1} \tag{321}$$

and ϕ has integer values. By evaluating the complex amplitude and real exponent separately, overflow or underflow problems are avoided. Functions expressed in the form as in Equation 320 are known as extended complex numbers. Numerical manipulation such as addition and multiplication involving extended complex numbers are performed in the following manner. If $z_1 = \hat{z}_1 e^{\phi_1}$ and $z_2 = \hat{z}_2 e^{\phi_2}$ are two extended complex number, then their product is

$$\begin{aligned} z &= z_1 z_2 \\ &= \hat{z} e^{\phi} , \end{aligned} \tag{322}$$

where

$$\hat{z} = \hat{z}_1 \hat{z}_2 \tag{323}$$

and

$$\phi = \phi_1 + \phi_2 . \tag{324}$$

The sum of two extended complex numbers is given by

$$\begin{aligned} z &= z_1 + z_2 \\ &= \hat{z} e^{\phi} , \end{aligned} \tag{325}$$

where

$$\hat{z} = \hat{z}_1 + \hat{z}_2 e^{(\phi_2 - \phi_1)} \quad ; \phi_1 \geq \phi_2 \tag{326}$$

and

$$\phi = \phi_1 \quad ; \phi_1 \geq \phi_2 \tag{327}$$

or

$$\hat{z} = \hat{z}_2 + \hat{z}_1 e^{(\phi_1 - \phi_2)} \quad ; \phi_1 < \phi_2 \tag{328}$$

and

$$\phi = \phi_2 \quad ; \phi_1 < \phi_2 . \tag{329}$$

V. DESCRIPTION OF MLAYER PROGRAM ELEMENTS

A short description of the functions of each program element in MLAYER is provided in this Chapter. The program had been tested and ran successfully on the Microsoft FORTRAN version 5.0 compilers and Microsoft C compilers version 5.0. The maximum number of layers and modes are 35 and 150 respectively. These limits are the upper bounds for operation on personal computers with 640 kilobytes of main memory.

A. MAIN

1. Description

Main is the controlling program element for MLAYER. It calls appropriate subroutines to calculate modal eigenvalues, mode sum, path loss and radio horizon distance. Main also calls subroutine wvgstdin to read in data from input file, filein. Three output files are opened, namely, filein.out, filein.eig and filein.plt.

Filein.out provides a documented output of input parameters and a list of modal eigenvalues found in each search rectangle. Filein.out also contains a list of eigenvalues in increasing order of real parts with the corresponding values in the θ-plane and respective attenuation of each mode in decibels per kilometer.

Filein.eig is an exact replica of the input file except that the parameter, myfile, is set to one and it contains a list of eigenvalues found. Once filein.eig is created, it can be used as the input file to re-run MLAYER for various transmitter/receiver range and height configurations.

Filein.plt contains eight columns of data, namely range, transmitter height, receiver height, coherent mode sum, incoherent mode sum, coherent path loss, incoherent path loss and radio horizon distance. The data are arranged in this manner to facilitate graph plotting.

Samples of filein, filein.out, filein.eig and filein.plt are given in Appendix B.
In addition, main also computes the following:

- The derivative of the modified refractivity with respect to z for each layer.
- The derivative of the atmospheric absorption with respect to z for each layer.
- The absorptivity and its derivative with respect to z for each layer.
- The derivative of q with respect to z for each layer.
- The modal attenuation rate for each mode.

- The coefficients required for computation of surface roughness.
- The eigenvalues in the θ-plane. The eigenvalues in the θ-plane are related to those in the $q_{n,l}$-plane by

$$\theta = \sin^{-1}\left[\sqrt{1-\beta^2}\right] . \tag{330}$$

The conversion to θ-plane is done solely for comparison of results with other models where root-search was performed in the θ-plane.

2. Inputs

Input data are read in by subroutine wvgstdin in the following order:

- filein : Pathname of input file.
- mfile : If mfile = 0, read input data and calculate eigenvalues. If mfile = 1, read input data and eigenvalues.
- fqmzin : Initial frequency in megahertz.
- delfq : Frequency increment in megahertz.
- nfreq : Number of frequencies for which modes will be found.
- mpol : If mpol = 0, wave is horizontally polarized. If mpol = 1, wave is vertically polarized.
- aloss : Maximum rate of attenuation in decibels per kilometer of modes that will be found.
- seatmp : Seawater temperature in degrees Celsius.
- seaslt : Seawater salinity in grams of salt per kilogram of seawater.
- iflgab : If iflgab = 0, calculate the height invariant atmospheric absorption. If iflgab = 1, read in array containing values of atmospheric absorption at layer boundaries.
- airtmp : Air temperature in degrees Celsius at reference height, zref. Airtmp is used for calculating the height invariant atmospheric absorption when iflgab = 0.
- rh : Relative humidity in percent at reference height. Used for calculating the height invariant atmospheric absorption when iflgab = 0.
- wgpm3 : Water concentration in grams per cubic meter at reference height. Used for calculating the height invariant atmospheric absorption when iflgab = 0.
- rmsbht : Rms bump height in meters of the sea surface.
- ztinit : Initial height of transmitter in meters.
- delzt : Height increment of transmitter in meters.
- nzt : Number of transmitter heights at which field strength is to be

computed.

- zrinit : Initial height of receiver in meters.
- delzr : Height increment of receiver in meters.
- nzr : Number of receiver heights at which field strength is to be computed.
- xinit : Initial range separation of the transmitter and receiver in kilometers.
- delx : Increment in range separation in kilometers.
- nx : Number of range separation values at which field strength is to be computed.
- zref : Reference height at which air temperature, relative humidity and water concentration are specified.
- nzlayr : Number of linear segments used to model the modified refractivity profile.
- zi(j) : Array containing values of heights in meters at layer boundaries.
- zim(j) : Array containing values of modified refractivity at layer boundaries.
- zigab(j) : Array containing values of atmospheric absorption in decibels per kilometer at layer boundaries.

3. Outputs

The outputs to filein.out (logical file 16) are:

- nrmode : Number of modes found.
- qeigen(j) : Array containing values of modal eigenvalues found in the complex $q_{1,1}$-plane.
- theta : Complex eigenangle referenced to ground level for each mode.
- atnu : Rate of attenuation in decibels per kilometer for each mode.

The outputs to filein.eig (logical file 17) are :

- nrmode : Number of modes found.
- qeigen(j) : Array containing values of modal eigenvalues found in the complex $q_{1,1}$-plane.

The outputs to filein.plt (logical file 15)

- ecms : Coherent mode sum field strength relative to free space in decibels.
- eims : Incoherent mode sum field strength relative to free space in decibels.
- ecpl : Coherent mode sum path loss in decibels.
- eipl : Incoherent mode sum path loss in decibels.

4. **Calling subroutine**

- None

5. **Subroutines called**

- wvgstdin
- chkmod
- seah2o ; commented out
- findmod
- casin
- ao2h2o ; disabled
- modsum
- dhoriz
- function ibstrip

The call to subroutine seah2o was commented out in revision 3.0 of the program. To use the subroutine, remove the comment statement. Subroutine ao2h2o was disabled by setting iflgab to one. To enable ao2h2o, set iflgab to zero.

6. **Common block areas**

- com 1
- com 2
- com 3
- pap 1
- datum

B. SUBROUTINE ABCOEF

1. **Description**

Subroutine abcoef calculates the coefficients, A_l and B_n, of the height gain function given by Equations 25 and 28. Computations of the coefficients are done in extended complex arithmetic. The normalizing integral of Equation 77 is also evaluated. The coefficients are then normalized by the following relation:

$$B_i = \frac{B_i}{\sqrt{\int_c f_m^2[q(z)]dz - j\frac{f_m'^2[q(0)]}{k^2}\left(\frac{k}{\alpha_1}\right)^{2/3}\left(\frac{d_i'}{dq_{1,1}}\right)}} \quad . \tag{331}$$

By noting that

$$\begin{aligned}\frac{d_i'}{d\rho_m} &= \frac{d_i'}{dq_{1,1}} \cdot \frac{dq_{1,1}}{d\rho_m} \\ &= -\frac{d_i'}{dq_{1,1}} \cdot \left(\frac{k}{\alpha_1}\right)^{2/3} \frac{2\rho_m}{k^2} \quad ,\end{aligned} \tag{332}$$

it can be seen that the denominator of Equation 331 is identical to that of Equation 77.

In calculating the coefficients, the decision to integrate up or down is determined by the rate of attenuation given by

$$\text{att} = Re[\rho_m] \times 20 \log e \times 10^3 \quad dB/km \quad . \tag{333}$$

If the attenuation rate is greater than 0.1 dB km, upward integration is performed; otherwise downward integration is carried out.

At the same time, the subroutine also checks for evanescence using Equations 153 through 156 for upward integration and Equations 162 through 165 for downward integration.

2. Calling statement

The subroutine is called by the statement

Call abcoef (zero, m).

3. Inputs

The input variables are

- zero : An eigenvalue in the $q_{1,1}$-plane .
- m : Mode number.

4. Outputs

The output variables are

- acoefa(i,m) : Two dimensional array element of complex amplitude of A in the i^{th} layer and m^{th} mode.
- acoefe(i,m) : Two dimensional array element of real exponent of A in the i^{th} layer and m^{th} mode.

- bcoefa(i,m): Two dimensional array element of complex amplitude of B in the i^{th} layer and m^{th} mode.
- bcoefe(i,m): Two dimensional array element of real exponent of B in the i^{th} layer and m^{th} mode.

5. Calling program element

- modsum

6. Subroutines called

- xcdaj
- xcadd

7. Common block areas

- com 1
- com 2
- pap 1
- pap 2

C. SUBROUTINE ADDX

1. Description

This subroutine adds two extended real numbers according to the following equation:

$$z = z_1 + z_2 \quad . \tag{334}$$

where

$$z = z_a \exp(z_e) \quad . \tag{335}$$

$$z_1 = z_{1a} \exp(z_{1e}) \tag{336}$$

and

$$z_2 = z_{2a} \exp(z_{2e}) \quad . \tag{337}$$

2. Calling statement

The subroutine is called by the statement

Call addx (za, ze, z1a, z1e, z2a, z2e).

3. Inputs

The input variables are

- z1a : Real amplitude of the extended real number, z_1 .
- z1e : Real exponent of the extended real number, z_1 .
- z2a : Real amplitude of the extended real number, z_2 .
- z2e : Real exponent of the extended real number, z_2 .

4. Outputs

The output variables are

- za : Real amplitude of the extended real number, z.
- ze : Real exponent of the extended real number, z.

5. Calling program element

- modsum

6. Subroutine called

- normre

7. Common block area

- none

D. SUBROUTINE AO2H2O

1. Description

This subroutine calculates the atmospheric absorption coefficient in decibels per kilometer due to the quantum mechanical resonances of oxygen molecules and water vapour. Computed values are good for frequencies in the range 1 Ghz to 1000 GHz.

2. Calling statement

The subroutine is called by the statement

Call ao2h2o (atmabs, fhz, tc, rh, zm, wgpm3).

3. Inputs

The input variables are

- fhz : Frequency in Hertz.
- tc : Temperature in degrees Celcius.
- rh : Relative humidity in percentage.
- zm : Height above sea level in meters.

- wgpm3 : Water concentration in grams per cubic meter at reference height.

4. Output

The output variable is

- atmabs : Atmosphetric absorption coefficient in decibels per kilometer.

5. Calling program element

- main

6. Subroutine called

- none

7. Common block area

- none

E. SUBROUTINE CHKMOD

1. Description

This subroutine checks for modal eigenvalues with zero value and discard them. A zero-value eigenvalue may sometimes lead to a divide-by-zero error in the mode sum calculation.

2. Calling statement

The subroutine is called by the statement

Call chkmod (qeigen, nrmode).

3. Inputs

The input variables are

- qeigen(j) : Array containing location of modal eigenvalues in the complex $q_{n,l}$-plane.
- nrmode : Number of modes.

4. Outputs

The output variables are

- qeigen(j) : Array containing location of non-zero eigenvalues in complex $q_{n,l}$-plane.
- nrmode : Number of modes.

5. Calling program element

- main

6. Subroutine called

- none

7. Common block area

- none

F. SUBROUTINE DETR

1. Description

This subroutine evaluates the modal function determinant of Equation 47 in extended complex arithmetic. The algorithm is discussed in Section E of Chapter II.

2. Calling statement

The subroutine is called by the statement

Call detr (deta, dete, nzlayr, d, de, dp1, dp1e, dm1, dm1e, dp2, dp2e, dm2, dm2e).

3. Inputs

The input variables are

- nzlayr : Number of linear segments used to model the modified refractivity profile.
- d : Array containing complex amplitudes of elements along the main diagonal of the modal function determinant.
- de : Array containing real exponents of elements along the main diagonal of the modal function determinant.
- dp1 : Array containing complex amplitudes of elements along the diagonal one above the main diagonal of the modal function determinant.
- dp1e : Array containing real exponents of elements along the diagonal one above the main diagonal of the modal function determinant.
- dm1 : Array containing complex amplitudes of elements along the diagonal one below the main diagonal of the modal function determinant.
- dm1e : Array containing real exponents of elements along the diagonal one below the main diagonal of the modal function determinant.
- dp2 : Array containing complex amplitudes of elements along the diagonal two above the main diagonal of the modal function determinant.
- dp2e : Array containing real exponents of elements along the diagonal two above the main diagonal of the modal function determinant.
- dm2 : Array containing complex amplitudes of elements along the diagonal two below the main diagonal of the modal function determinant.
- dm2e : Array containing real exponents of elements along the diagonal two

below the main diagonal of the modal function determinant.

4. Outputs

The output variables are

- deta : Complex amplitude of the modal function.
- dete : Real exponent of the modal function.

5. Calling program element

- fctvlx

6. Subroutine called

- xcadd

7. Common block area

- none

G. SUBROUTINE DHORIZ

1. Description

The subroutine calculates the radio horizon distance between the transmitter and receiver. The radio horizon distance in kilometers is given by

$$d = \sqrt{2} \cdot \sqrt{\frac{4a}{3}} \left[\sqrt{z_R} + \sqrt{z_T} \right] 10^{-3} \quad , \tag{338}$$

where a is the radius of the earth, and z_R and z_T are the receiver and transmitter heights respectively.

2. Calling statement

The subroutine is called by the statement

Call dhoriz (dhz, zrcvr, zxmtr).

3. Inputs

The input variables are

- zrcvr : Receiver height in meters.
- zxmtr : Transmitter height in meters.

4. Output

The output variable is

- dhz : Radio horizon distance in kilometers.

5. Calling program element

- main

6. Subroutine called

- none

7. Commom block area

- none

H. SUBROUTINE DXDETR

1. Description

This subroutine evaluates the modal function determinant and its derivative in extended complex arithmetic. Values of the modal function determinant and its derivative are required by the Newton-Raphson root-finding routine. The methods for evaluating the modal function determinant and its derivative are discussed in Section E of Chapter II.

2. Calling statement

The subroutine is called by the statement

Call dxdetr (deta, dete, dxdeta, dxdete, nzlayr, d, de, dp1, dp1e, dm1, dm1e, dp2, dp2e, dm2, dm2e, dxd, dxde, dxdp1, dxdp1e, dxdm1, dxdm1e, dxdp2, dxdp2e, dxdm2, dxdm2e).

3. Inputs

The input variables are

- nzlayr : Number of linear segments used to model the modified refractivity profile.
- d : Array containing complex amplitudes of elements along the main diagonal of the modal function determinant.
- de : Array containing real exponents of elements along the main diagonal of the modal function determinant.
- dp1 : Array containing complex amplitudes of elements along the diagonal one above the main diagonal of the modal function determinant.
- dp1e : Array containing real exponents of elements along the diagonal one above the main diagonal of the modal function determinant.
- dm1 : Array containing complex amplitudes of elements along the diagonal one below the main diagonal of the modal function determinant.
- dm1e : Array containing real exponents of elements along the diagonal one below the main diagonal of the modal function determinant.
- dp2 : Array containing complex amplitudes of elements along the diagonal two above the main diagonal of the modal function determinant.

- dp2e : Array containing real exponents of elements along the diagonal two above the main diagonal of the modal function determinant.
- dm2 : Array containing complex amplitudes of elements along the diagonal two below the main diagonal of the modal function determinant.
- dm2e : Array containing real exponents of elements along the diagonal two below the main diagonal of the modal function determinant.
- dxd : Array containing complex amplitudes of the derivatives of the elements along the main diagonal of the modal function determinant.
- dxde : Array containing real exponents of the derivatives of the elements along the main diagonal of the modal function determinant.
- dxdp1 : Array containing complex amplitudes of the derivatives of the elements along the diagonal one above the main diagonal of the modal function determinant.
- dxdp1e : Array containing real exponents of the derivatives of the elements along the diagonal one above the main diagonal of the modal function determinant.
- dxdm1 : Array containing complex amplitudes of the derivatives of the elements along the diagonal one below the main diagonal of the modal function determinant.
- dxdm1e : Array containing real exponents of the derivatives of the elements along the diagonal one below the main diagonal of the modal function determinant.
- dxdp2 : Array containing complex amplitudes of the derivatives of the elements along the diagonal two above the main diagonal of the modal function determinant.
- dxdp2e : Array containing real exponents of the derivatives of the elements along the diagonal two above the main diagonal of the modal function determinant.
- dxdm2 : Array containing complex amplitudes of the derivatives of the elements along the diagonal two below the main diagonal of the modal function determinant.
- dxdm2e : Array containing real exponents of the derivatives of the elements along the diagonal two below the main diagonal of the modal function determinant.

4. Outputs

The output variables are

- deta : Complex amplitude of the modal function.
- dete : Real exponent of the modal function.
- dxdeta : Complex amplitude of the derivative of the modal function.
- dxdete : Real exponent of the derivative of the modal function.

5. Calling program element

- fdfdtx

6. Subroutine called

- xcadd

7. Commom block area

- none

I. SUBROUTINE FCTVLX

1. Description

This subroutine calculates the values of the elements in the matrix of the modal function of Equation 47 and invokes subroutine detr to evaluate the modal function. The subroutine shifts the imaginary part of $q_{1,1}$ by *qshift* so that the real axis will not fall on the mesh line of the search rectangle set up by the Shellman-Morfitt routine. This allows the zeros on the real axis to be located. It is known that zeros near or on the negative real axis contribute significantly to the fields within a duct.

However, the shift implies that the Shellman-Morfitt routine will search for zeros of $\|\underline{\Delta}(t_{1,1})\|$ instead of $\|\underline{\Delta}(q_{1,1})\|$ where

$$t_{1,1} = q_{1,1} - j\,qshift \quad . \tag{339}$$

To compensate for the error, the shift back to $q_{1,1}$ is done in subroutine fndmod for all zeros found.

2. Calling statement

The subroutine is called by the statement

Call fctvlx (q11in, deta, dete).

3. Input

The input variable is

- q11in : Location in the complex $q_{1,1}$-plane where the modal function is to be evaluated.

4. Outputs

The output variable are

- deta : Complex amplitude of the modal function.
- dete : Real exponent of the modal function.

5. **Calling program element**

- fzerox

6. **Subroutines called**

- xcdai
- xcadd
- detr
- surf

7. **Common block areas**

- com1
- com2
- com3
- com4

J. SUBROUTINE FDFDTX

1. **Description**

This subroutine calculates the values of the elements in the matrices of $\|\underline{\Delta}(q_{1,1})\|$ and $\frac{\partial}{\partial q_{1,1}} \|\underline{\Delta}(q_{1,1})\|$ and then invokes subroutine dxdetr to evaluate the modal function and its derivative. The subroutine also shifts the imaginary part of $q_{1,1}$ by *qshift* as in subroutine fctvlx. It is similarly compensated by a "shift-back" in subroutine fndmod.

2. **Calling statement**

The subroutine is called by the statement

Call fdfdtx (q11in, deta, dete, dxdeta, dxdete).

3. **Input**

The input variable is

- q11in : Location in the complex $q_{1,1}$-plane where the modal function and its derivative is to be evaluated.

4. **Outputs**

The output variables are

- deta : Complex amplitude of the modal function.
- dete : Real exponent of the modal function.
- dxdeta : Complex amplitude of the derivative of the modal function.
- dxdete : Real exponent of the derivative of the modal function.

5. Calling program element

- fzerox

6. Subroutines called

- xcdai
- xcadd
- dxdetr
- surf

7. Common block areas

- com1
- com2
- com3
- com4

K. SUBROUTINE FINDFX

1. Description

The incorporation of the effects of surface roughness into the mathematical model results in discontinuity of the modal function along the imaginary $q_{1,1}$-axis . The Shellman-Morfitt routine will fail if the edge of the search rectangle lies on the imaginary axis.

Subroutine findfx will determine if any edge of the search rectangle is on the imaginary axis. If so, a small *offset* of 1×10^{-4} is introduced. If the left edge is on the imaginary axis, then the modal function is evaluated at $Re(q_{1,1}) = + offset$. If the right edge is on the imaginary axis, the modal function is evaluated at $Re(q_{1,1}) = - offset$.

2. Calling statement

The subroutine is called by the statement

Call findfx (jr, ji, f, fe, tleft, tright).

3. Inputs

The input variables are

- jr : Real part of the mesh square coordinates in mesh units.
- ji : Imaginary part of the mesh squares coordinates in mesh units.
- tleft : Real part of $q_{1,1}$ at the left edge of the search rectangle.
- tright : Real part of $q_{1,1}$ at the right edge of the search rectangle.

4. Outputs

The output variables are

- f : Complex amplitude of the modal function.
- fe : Real exponent of the modal function.

5. Calling program element

- fzerox

6. Subroutine called

- fctvlx

7. Common block area

- fmccom

L. SUBROUTINE FNDMOD

1. Description

This subroutine sets up the rectangular region in the complex $q_{\alpha 1}$-plane for the Shellman-Morfitt root finding routine to locate the zeros of the modal function.

The initial search rectangle is set up with

- the left edge of rectangle, tleft = 0.0.
- the right edge of rectangle, tright = tleft + tstep, where tstep is the length of the rectangle.
- the top of the rectangle, ttop given by [Ref. 5]

$$\text{ttop} = \frac{2 \times 10^{-3}\, \text{Aloss}}{k20 \log e}\, Re\left[\left(\frac{k}{\alpha_1}\right)^{2/3}\right] \quad , \tag{340}$$

  where Aloss is the maximum attenuation rate in decibels per kilometer of those modes to be found.

- the bottom of the rectangle, tbot = − tol, where tol is the tolerance to which zeros are to be located.

In order that the zeros on the real axis can be located, a small offset of qshift is introduced in subroutines fdfdtx and fctvlx so as to avoid having a mesh line on the real axis. This offset is corrected in the subroutine fndmod by the statement

$$\text{zeros}(k) = \text{zeros}(k) - j\, qshift \quad . \tag{341}$$

After the initial rectangle has been searched for zeros of the modal function, a new search rectangle is set up to the left of the initial rectangle. If no zero is found in three consecutive search rectangles, the search for roots to the left of the initial rectangle

is stopped. Fndmod next forms search rectangles to the right of the initial rectangles. If no zero is found in three consecutive search rectangles, the search for roots to the right of the initial rectangle is stopped.

Since subroutine fzerox extends the search rectangle by one mesh unit on all sides, fndmod also checks for and eliminates all zeros outside the current search rectangle.

After all the zeros have been found, fndmod sorts them in order of increasing real parts and stores them in the array called zeros.

There are two versions of fndmod, namely, fndmod20.for and fndmod80.for. Fndmod80 sets up a smaller mesh and takes longer time to find the modes. Fndmod80 should be used only if fndmod20 fails to find all modes.

2. Calling subroutine

The subroutine is called by the statement

Call fndmod (qeigen, nrmode, dmdz, detadx, zim, nzlayr, aloss, waveno).

3. Inputs

The input variables are

- dmdz : Array containing values of $\frac{dM}{dz}$.
- detadz : Array containing values of $\frac{d\eta}{dz}$.
- zim : Array containing values of M(z) at layer boundaries.
- nzlayr : Number of linear segments used to model the modified refractivity profile.
- aloss : Maximum attenuation rate (in decibels per kilometer) of modes to be found.
- waveno : Wave number.

4. Outputs

The output variables are

- qeigen : Array containing the zeros of the modal function.
- nrmode : Actual number of modes found.

5. **Calling program element**

- main

6. **Subroutine called**

- fzerox

7. **Common block areas**

- com4
- com5

M. SUBROUTINE FZEROX

1. **Description**

Subroutine fzerox is the main subroutine used for finding the zeros of a complex function using the Shellman-Morfitt routine as described in Chapter III. Fzerox will convert the coordinates of the search rectangle edges into mesh units and proceed with the search for sign changes of $Im(f)=0$ along each edge. The maximum number of crossings of $Im(f)=0$ allowed with any edge of the search rectangle is 100.

Fzerox allows a maximum number, maxnsq, of mesh squares to lie on any one phase curve, $Im(f)=0$. If this number is exceeded, the program will reduce the mesh size by one-half and start over. If the problem persists after the mesh size has been reduced by maxnt times, an error message will be written to the output file and the program stops. In the program, maxnq is set at four times the number of mesh squares along the longest side of the search rectangle.

Fzerox also checks for modes found on the same phase line. If so, the program will reduce the mesh size and start over. If the problem remains after mesh size has been reduced by 2^{maxnt} times, an error message will be written to output file and the program will stop.

2. **Calling statement**

The subroutine is called by the statement

Call Fzerox (tleft, tright, tbot, ttop, tmsho, tol, mprint, zeros).

3. **Inputs**

The input variables are

- tleft : Value of the real part of z at the left edge of search rectangle.
- tright : Value of the real part of z at the right edge of search rectangle.
- tbot : Value of the imaginary part of z at the bottom edge of the search rectangle.

- ttop : Value of the imaginary part of z at the top edge of the search rectangle.
- tmsho : Initial size of the mesh square.
- tol : Tolerance to which zeros are to be found. Zeros located closer than tol cannot be distinguished.
- mprint : A flag for debugging output. If mprint = 0, no debugging will be given. Mprint = 1 will activate debugging printout.

4. Outputs

The output variables are

- zeros : Array containing the complex zeros of f(z) in the specified search rectangle in the complex z-plane.
- nrz : The actual number of complex zeros of f(z) found.

5. Calling program element

- fndmod

6. Subroutines called

- findfx
- quad
- nomshx

7. Common block areas

- newmsh
- tmccom

N. SUBROUTINE HTGAIN

1. Description

This subroutine evaluates the normalized height gain function given by Equation 77.

2. Calling Statement

The subroutine is called by the statement

Call htgain (htga, htge, zero, z, m).

3. Inputs

The input variables are

- zero : Modal eigenvalue in $q_{1,1}$-space for mode m.
- z : Height (in meters) above ground at which height gain is to be evaluated.

- m : Mode index.

4. Outputs

The output variables are

- htga : Complex height gain factor in extended arithmetic.
- htge : Real height gain exponent in extended arithmetic.

5. Calling program element

- modsum

6. Subroutines called

- xcdai
- xcadd

7. Common block areas

- com2
- pap1
- pap2

O. SUBROUTINE MODSUM

1. Description

This subroutine calculates the field strength relative to free space given by Equations 100 and 101.

2. Calling statement

The subroutine is called by the statement

Call modsum (eems, eims, xm, rngfac, zr, zt, qeigen, ncount).

3. Inputs

The input variables are

- xm : Range in meters.
- rngfac : Range factor calculated in the main program.
- zr : Receiver height in meters.
- zt : Transmitter height in meters.
- qeigen : Array containing eigenvalues in $q_{1,1}$-space .
- ncount : Counter set in the main program to avoid unnecessary calulations of acoefa, acoefe, bcoefa and bcoefe. If ncount = 1, subroutine modsum will call subroutine abcoef, otherwise subroutine modsum will compute modesum only.

4. Outputs

The output variables are

- ecms : Coherent field strength relative to free space.
- eims : Incoherent field strength relative to free space.

5. Calling program element

- main

6. Subroutines called

- abcoef
- htgain
- xcadd
- addx

7. Common block areas

- com1
- com2
- pap2

P. SUBROUTINE NOMSHX

1. Description

Subroutine nomshx takes the approximate locations of the complex zeros of f(z) provided by fzerox and improves the accuracies of the zero locations using Newton-Raphson iteration.

2. Calling statement

The subroutine is called by the statement .

Call nomshx (tol, zeros, nrz).

3. Inputs

The input variables are

- tol : The tolerance to which zeros are to be located. Zeros located closer than tol cannot be distinguished.
- zeros : Array containing the approximate locations of the complex zeros of f(z).
- nrz : The number of complex zeros stored in array zeros.

4. **Output**

The output variable is

- zeros : An array containing the iterated values of the complex zeros of f(z).

5. **Calling program element**

- fzerox

6. **Subroutine called**

- fdfdtx

7. **Common block area**

- Newmsh

Q. SUBROUTINE NORME

1. **Description**

This subroutine "normalizes" the complex extended numbers, z = za exp(ze) such that

$$\exp(-1.0) \leq \max[\,|Re(za)|,\ |Im(za)|\,] \leq \exp(1.0) \qquad (342)$$

and ze has integer values.

2. **Calling statement**

The program is called by the statement

Call norme (za, ze).

3. **Inputs**

The input variables are

- za : Complex amplitude of the extended complex number, z.
- ze : Real exponent of the extended complex number, z

4. **Outputs**

The output variables are

- za : Complex amplitude of the "normalized" extended complex number, z.
- ze : Real exponent of the "normalized" extended complex number, z.

5. **Calling program elements**

- xcadd
- xcdait
- xcdaig

6. Subroutine called

- none

7. Common block area

- none

R. SUBROUTINE NORMRE

1. Description

This subroutine "normalizes" the real extended number, $z = za \exp(ze)$, such that

$$\exp(-1.0) \leq |za| \leq \exp(+1.0) \tag{343}$$

and ze has integer values.

2. Calling statement

The subroutine is called by the statement

Call normre (za, ze).

3. Inputs

The input variables are

- za : Real amplitude of the real extended number, z.
- ze : Real exponent of the real extended number, z.

4. Outputs

The output variables are

- za : Real amplitude of the "normalized" real extended number, z.
- ze : Real exponent of the "normalized" real extended number, z.

5. Calling program element

- addx

6. Subroutine called

- none

7. Common block area

- none

S. SUBROUTINE QUAD

1. Description

This subroutine finds the roots of the quadratic equation of the form given by Equation 283. If $|\varepsilon|$ given in Equation 285 is less than 0.3, the roots are computed with Equations 295 and 296. Otherwise Equations 286 and 287 are used. In addition, if $|\frac{a}{2b}| < 10^{-30}$, subroutine quad returns only 1 solution given by Equation 295.

2. Calling statement

The subroutine is called by the statement

Call quad (a, b, c, sol, nrsol, mprint).

3. Inputs

The input variables are

- a : The coefficient of x^2 in the quadratic equation.
- b : The coefficient of 2x in the quadratic equation.
- c : The constant term in the quadratic equation.

4. Outputs

The output variables are

- sol : An array containing the real roots of the quadratic equation.
- nrsol : The number of real roots found.
- mprint : A flag for debugging. If mprint is not equal to zero, values of the coefficients a, b, and c will be written to file.out.

5. Calling program element

- fzerox

6. Subroutine called

- none

7. Common block area

- none

T. SUBROUTINE SEAH2O

1. Description

This subroutine evaluates the real effective relative dielectric constant and the real effective conductivity of seawater as a function of temperature, salinity and frequency. The program is based on the equations presented in section G of Chapter II.

2. **Calling statement**

The subroutine is called by the statement

Call seah2o (sigeff, epseff, t, s, freq).

3. **Inputs**

The input variables are

- t : Temperature of seawater in degree Celcius.
- s : Salinity of seawater in grams of salt per kilogram of seawater.
- freq : Frequency in Hertz.

4. **Outputs**

The output variables are

- sigeff : Real effective conductivity in siemens per meter.
- epseff : Real effective relative dielectric constant.

5. **Calling program element**

- main

6. **Subroutine called**

- none

7. **Common block area**

- none

U. SUBROUTINE SURF

1. **Description**

This subroutine evaluates γ_i and $\frac{d\gamma_i}{dq_{1,1}}$ when surface roughness is included in the model.

2. **Calling statement**

The subroutine is called by the statement

Call surf (q11, gamma, dgamdq).

3. **Input**

The input variable is

- q11 : Location in the complex $q_{1,1}$-plane where the modal function and its derivative are to be evaluated.

4. **Outputs**

The output variables are

- gamma : This is γ_i given by Equation 180 and 192 for horizontal and vertical

polarization respectively.

- dgamdq : This is $\frac{d\gamma}{dq_{in}}$ given by Equations 187 and 193 for horizontal and vertical polarization respectively.

5. Calling program elements

- fctvlx
- fdfdtx

6. Subroutines called

- function ctanh
- function csech2

7. Common block areas

- com1
- com5
- com6

V. SUBROUTINE XAINEG

1. Description

This subroutine evaluates the Airy function, Ai(z), and its derivative, Ai'(z), for complex z in extended complex arithmetic for

$$-\frac{2\pi}{3} \leq \arg(z) \leq 0 \quad . \tag{344}$$

The subroutine will test if z* is within the ellipse with foci (−1.58, 3.95) and (0.28, −2.11), major axis of 9.0 and minor axis of 6.4. If z* is within the ellipse, xaineg will invoke xcdait to compute the Airy function and its derivative with a Taylor series. Otherwise xaineq invokes xcdaig which uses the Gaussian quadrature method.

2. Calling statement

The subroutine is called by the statement

Call xaineg (z, aia, aie, daia, daie).

3. Input

The input variable is

- z : A value in the complex z-plane at which the Airy function and its derivative are to be computed.

4. Outputs

- aia : Complex amplitude of Ai(z) in extended complex arithmetic.
- aie : Real exponent of Ai(z) in extended complex arithmetic.
- daia : Complex amplitude of Ai ' (z) in extended complex arithmetic.
- daie : Real exponent of Ai ' (z) in extended complex arithmetic.

5. Calling program element

- xedai

6. Subroutines called

- xedait
- xedaig

7. Common block area

- none

W. SUBROUTINE XAIPOS

1. Description

This subroutine evaluates the Airy function, Ai(z), and its derivative, Ai'(z) in extended complex arithmetic for

$$0 \leq \arg(z) \leq \frac{2\pi}{3} \quad . \tag{345}$$

The subroutine will test if z is within the ellipse with foci (−1.58, 3.95) and (0.28, −2.11), major axis of 9.0 and minor axis of 6.4. If z is within ellipse, xaipos will invoke xedait to compute the Airy function and its derivative with a Taylor series. Otherwise xaipos invokes xedaig which uses the Gaussian quadrature method.

2. Calling statement

The subroutine is called by the statement

Call xaipos (z, aia, aie, daia, daie).

3. Input

The input variable is

- z : A value in the complex z-plane at which the Airy function and its derivative are to be computed.

4. Outputs

The output variables are

- aia : Complex amplitude of $Ai(z)$ in extended complex arithmetic.
- aie : Real exponent of $Ai(z)$ in extended complex arithmetic.
- daia : Complex amplitude of $Ai'(z)$ in extended complex arithmetic.
- daie : Real exponent of $Ai'(z)$ in extended complex arithmetic.

5. Calling program element

- xcdai

6. Subroutines called

- xcdait
- xcdaig

7. Common block area

- none

X. SUBROUTINE XCDAI

1. Description

The subroutine is the driving program in the evaluation of the Airy function, $Ai(z)$, and its derivative, $Ai'(z)$. If

$$0 < \arg(z) \leq \frac{\pi}{2} , \tag{346}$$

xcdai invokes xaipos to compute $Ai(z)$ and $Ai'(z)$ and invokes xaineg to compute $Ai(ze^{-2\pi i/3})$ and $Ai'(ze^{-2\pi i/3})$. It then uses the connection formula of Airy function in Equation 302 and its derivative to compute $Ai(ze^{2\pi i/3})$ and $Ai'(ze^{2\pi i/3})$.

If

$$-\frac{\pi}{2} \leq \arg(z) \leq 0 , \tag{347}$$

xcdai invokes xaipos to compute $Ai(ze^{2\pi i/3})$ and $Ai'(ze^{2\pi i/3})$. It also invokes xaineg to compute $Ai(z)$ and $Ai'(z)$. It then uses the connection formula to compute $Ai(ze^{-2\pi i/3})$ and $Ai'(ze^{-2\pi i/3})$.

If

$$\frac{2\pi}{3} < \arg(z) \leq \pi \tag{348}$$

or

$$-\pi \leq \arg(z) < -\frac{2\pi}{3} , \tag{349}$$

xedai calls xaipos to compute $Ai(ze^{-2\pi i/3})$ and $Ai'(ze^{-2\pi i/3})$. It also calls xaineg to compute $Ai(ze^{2\pi i/3})$ and $Ai'(ze^{2\pi i/3})$. It then uses the connection formula to compute Ai(z) and Ai'(z).

If

$$\frac{\pi}{2} < \arg(z) \leq \frac{2\pi}{3} , \tag{350}$$

xedai calls xaipos to compute Ai(z) and Ai'(z) and calls xaineg to compute $Ai(ze^{-2\pi i/3})$ and $Ai'(ze^{-2\pi i/3})$. It then uses the connection formula to compute $Ai(ze^{2\pi i/3})$ and $Ai'(ze^{2\pi i/3})$.

If

$$-\frac{2\pi}{3} < \arg(z) < -\frac{\pi}{2} , \tag{351}$$

xedai calls xaipos to compute $Ai(ze^{2\pi i/3})$ and $Ai'(ze^{2\pi i/3})$. It also calls xaineg to compute Ai(z) and Ai'(z). It then uses the connection formula to compute $Ai(ze^{-2\pi i/3})$ and $Ai'(ze^{-2\pi i/3})$.

2. Calling statement

The subroutine is called by the statement

Call xedai (z, aia, aie, daia, daie, aipa, aipe, daipa, daipe, aima, aime, daima, daime).

3. Input

The input variable is

- z : A value in the complex z-plane at which the Airy function and its derivative are to be computed.

4. Outputs

The output variables are

- aia : Complex amplitude of Ai(z) in extended arithmetic.

- aic : Real exponent of Ai(z) in extended complex arithmetic.
- daia : Complex amplitude of Ai'(z) in extended complex arithmetic.
- daic : Real exponent of Ai'(z) in extended complex arithmetic.
- aipa : Complex amplitude of $Ai(ze^{j2\pi/3})$ in extended complex arithmetic.
- aipe : Real exponent of $Ai(ze^{j2\pi/3})$ in extended complex arithmetic.
- daipa : Complex amplitude of $Ai'(ze^{j2\pi/3})$ in extended complex arithmetic.
- daipe : Real exponent of $Ai'(ze^{j2\pi/3})$ in extended complex arithmetic.
- aima : Complex amplitude of $Ai(ze^{-j2\pi/3})$ in extended complex arithmetic.
- aime : Real exponent of $Ai(ze^{-j2\pi/3})$ in extended complex arithmetic.
- daima : Complex amplitude of $Ai'(ze^{-j2\pi/3})$ in extended complex arithmetic.
- daime : Real exponent of $Ai'(ze^{-j2\pi/3})$ in extended complex arithmetic.

5. Calling program element

- fctvlx

6. Subroutines called

- xaipos
- xaineg
- xcadd

7. Common block area

- none

Y. SUBROUTINE XCDAIG

1. Description

The subroutine computes the Airy function, Ai(z), and its derivative, Ai'(z), in extended arithmetic using the Gaussian quadrature method.

2. Calling statement

The subroutine is called by the statement

Call xcdaig (z, aia, aic, daia, daic).

3. Inputs

The input variables is

- z : A value in the complex z-plane at which the Airy function and its derivative are to be computed.

4. Outputs

The output variables are

- aia : Complex amplitude of Ai(z) in extended arithmetic.
- aie : Real exponent of Ai(z) in extended complex arithmetic.
- daia : Complex amplitude of Ai'(z) in extended complex arithmetic.
- daie : Real exponent of Ai'(z) in extended complex arithmetic.

5. Calling program elements

- xaipos
- xaineg

6. Subroutine called

- norme

7. Common block area

- norme

Z. SUBROUTINE XCDAIT

1. Description

The subroutine computes the Airy function, Ai(z), and its derivative, Ai'(z), in extended arithmetic using a Taylor series expansion.

2. Calling statement

The subroutine is called by the statement

Call xcdait (z, aia, aie, daia, daie).

3. Input

The input variable is

- z : A value in the complex z-plane at which the Airy function and its derivative are to be computed.

4. Outputs

The output variables are

- aia : Complex amplitude of Ai(z) in extended arithmetic.
- aie : Real exponent of Ai(z) in extended complex arithmetic.
- daia : Complex amplitude of Ai'(z) in extended complex arithmetic.
- daie : Real exponent of Ai'(z) in extended complex arithmetic.

5. **Calling program elements**

- xaipos
- xaineg

6. **Subroutine called**

- norme

7. **Common block area**

- none

AA. FUNCTION PROGRAMS

1. **Function casin**

Function casin evaluates the complex arcsine of a complex number, z, with the equation

$$\sin^{-1}(z) = -j \ln [(1 - z^2)^{1/2} + jz] \quad . \tag{352}$$

The function is called by the statement

casin (z).

The function is used in the main program to convert the eigenvalues from $q_{1,1}$-plane to θ-plane .

2. **Function csech2**

Function csech2 evaluates the square of the hyperbolic secant of a complex number, z, with the equation

$$\text{sech}^2(z) = \frac{4}{e^{2z} + 2 + e^{-2z}} \quad . \tag{353}$$

The function is called by the statement

csech2 (z).

It is used in subroutine surf for evaluating $\frac{\partial a}{\partial q_{1,1}}$, $\frac{\partial b}{\partial q_{1,1}}$, $\frac{\partial \tilde{a}}{\partial q_{1,1}}$ and $\frac{\partial \tilde{b}}{\partial q_{1,1}}$ (see Section F, Chapter II).

3. **Function ctanh**

Function ctanh evaluates the hyperbolic tangent of a complex number, z, with the equation

$$\tanh(z) = \frac{e^{z} - e^{-z}}{e^{z} + e^{-z}}$$

$$\text{for } |\, Re(z)\,| > \frac{1}{10\sqrt{2}} \qquad (354)$$

$$\text{or } |\, Im(z)\,| > \frac{1}{10\sqrt{2}}$$

or

$$\tanh(z) = z - \frac{1}{3} z^3 + \frac{2}{15} z^5 - \frac{17}{315} z^7 + \frac{62}{2835} z^9 \ldots\ldots$$

$$\text{for } |\, Re(z)\,| \leq \frac{1}{10\sqrt{2}} \qquad (355)$$

$$\text{or } |\, Im(z)\,| \leq \frac{1}{10\sqrt{2}} \,.$$

The function is called by the statement

ctanh (z).

It is used in subroutine surf for evaluating a, b, $\tilde{a}$,$\tilde{b}$ and their derivatives.

4. Function ibstrip

Function ibstrip finds the length of a character string by removing all trailing spaces from the end of the string and returns the number of characters in the stripped string.

The function is called by the statement

ibstrip (inst, outst).

where inst is the input string and outst is the stripped string.

The function is used in the main program to check the length of the filename.

AB. MLAYER SUPPORTING PROGRAMS

MLAYER has several supporting programs that helps in the running of the program. They are

- mlayer.mak
- wvgclean.mak
- wvgstrip.mak
- wvgclean.c

- wvgstrip.for
- wvgstdin.for

1. **Mlayer.mak**

This is the makefile for the creation of mla20 and mla80 programs. Mla20 uses subroutine fndmod20.for to set up the rectangular search region whereas mla80 uses fndmod80.for.

Mlayer.mak compiles and links all program elements and creates mla20.exe and mla80.exe for the execution of MLAYER program with either mla20 or mla80.

To compile and link MLAYER, type

nmake mlayer.mak

Nmake will compare the modification dates of the target files (e.g., object and executable files) with those of the dependent files (e.g., source files). If any of the dependent files has been changed recently, i.e., the modification dates of the dependent files are more recent than the target files, nmake will execute the commands in mlayer.mak to update the target files. Nmake updates only those outdated target files.

To execute MLAYER program, type

mla20 < infile

to execute the mla20 version. Infile is the name of the input file which can be either filein or filein.eig. If filein is used, MLAYER will search for all modes of propagation. If filein.eig is used, MLAYER will compute the modsum and path loss without a search for the modes.

2. **Wvgclean.mak**

This is the makefile for the creation of wvgclean.exe

3. **Wvgstrip.mak**

This is the makefile for the creation of wvgstrip.exe.

4. **Wvgclean.c**

Wvgclean.c adds comment or descriptors to each datum line in filein and filein.eig. This will help in editing.

To execute the program, type

wvgclean < filein.eig > temp

ren temp filein.eig

5. **Wvgstrip.for**

Wvgstrip.for removes comments or descriptors that are added by wvgclean.c.

To execute the program, type

```
wvgstrip < filein.eig > temp
ren temp filein.eig
```

6. Wvgstdin.for

Wvgstdin.for reads input data from filein or filein.eig on execution of the MLAYER program.

VI. DISCUSSIONS AND RECOMMENDATIONS

A. ASSESSMENT OF MLAYER

MLAYER was developed with the intention of providing a program which is capable of locating all propagating modes with attenuation rates below a specified value. However, the price of this capability is the extremely long execution time. For instance, a 2-meter evaporation duct takes approximately 3 hours and 20 minutes (on an IBM PS 2 model 80 with an Intel 80386 processor at 16 MHz) to locate 9 modes with attenuation rates less than 5 decibels per kilometer. A 14-meter evaporation duct takes about 6 hours to locate 94 modes with attenuation rates below 2.1 decibels per kilometer. Samples of output data are found in Appendix B.

Calculations of field strength and path loss with MLAYER were found to agree favourably with experimental measurements [Ref. 17 and 18]. Typically, the model underestimates the measured values by about 10 dB. The sources of discrepancies were probably due to the validity of the surface roughness model and the assumption of lateral homogeneity of the medium.

In the following sections, proposed areas for enhancement of the capabilities of MLAYER are discussed.

B. SURFACE ROUGHNESS MODEL

The surface roughness model used in MLAYER is based on the Kirchhoff approximation which is a single scattering theory. This model is only valid for gently undulating surfaces where shadowing of incident and scattered fields are negligible. When shadowing cannot be neglected, the Kirchhoff approximation tends to overpredict the scattered energy which leads to erroneous results.

Shadowing occurs when incoming or outgoing rays are blocked by the rough surface. This leaves some area of the surface in shadow. This effect is associated with multiple scattering. Therefore, to account for shadowing, multiple scattering interactions must be included in the model.

A more accurate model called the phase perturbation technique was introduced by Winebrenner and Ishimaru [Ref. 19]. The phase perturbation theory incorporates all the multiple scatterings required for shadowing of the incident field. The theory is based on the extinction theorem which is a consequence of Green's theorem [Ref. 20]. In Reference 19, numerical results of the phase perturbation bistatic scattering cross section were

compared with exact numerical results. In the region examined, it was found that the results of the phase perturbation technique agree with the exact results except at low grazing angles.

The phase perturbation technique is valid for a wider range of applications. It was shown in Reference 19 that the reflection and backscattering coefficients reduce to that of the Kirchoff approximation when $l/\lambda \gtrsim 1$, i.e., for gently undulating surfaces, where l is the length and λ is the wavelength of the incident wave.

C. LATERAL HOMOGENEITY OF REFRACTIVITY PROFILE

In MLAYER, the refractive index is assumed to vary only with height. Although this assumption appears to be adequate most of the time [Ref. 17], there are incidents where the validity of lateral homogeneity was cited as a possible reason for discrepancies between observations and predicted results [Ref. 18 and 21].

For refractivity profile that varies along the path, the laterally inhomogeneous structures can be approximated by several homogeneous sections. The exchange of energy between the propagating modes at the boundary of two sections are analyzed by mode-conversion techniques [Ref. 22].

D. FIELD CONTRIBUTION FROM THE SOURCE

In the formulation of the propagation model, MLAYER neglects the contribution from the direct wave of the source. This approximation is good for ranges near or beyond the horizon where the major field contributions are from the reflected waves. For ranges well within the horizon, the contribution from the direct wave is significant and should not be ignored. Hence, for wave propagation in the interference region, the coefficients, A_i and B_i, of Equations 31 and 32 must be obtained from the solutions of Equation 46. At the same time, the surface wave field contribution from the integral of the contour, C_2 , in Equation 73 may become significant.

VII. CONCLUSION

MLAYER is a useful research tool for conducting case studies over a large dynamic range of frequencies. Calculation of field strength and path loss are in agreement with observations for frequencies from 63 Mhz to 94 GHz [Ref. 17 and 18]. It can serve as a yardstick against which results of other quicker but less accurate models such as IREPS [Ref. 23] and EREPS [Ref. 24] are compared. In addition, the multiple (as opposed to trilinear) piecewise linear refractivity profile makes it possible to model the simultaneous occurrence of an evaporation duct and elevated ducts.

Finally, modifications of MLAYER to incorporate conditions of horizontal heterogeneity of refractivity, effects of source contribution and an improved modelling of surface roughness as discussed in Chapter VI are recommended to fully exploit its capabilities. These are opportunities opened for further studies.

APPENDIX A. REPRESENTATION OF $k_1(q)$ AND $k_2(q)$ IN TERMS OF MODIFIED HANKEL FUNCTION OF ORDER ONE-THIRD

The Airy function is related to the modified Bessel function of the third kind of order one-third by the following equation [Ref. 4]:

$$Ai(q) = \frac{1}{\pi}\left(\frac{q}{3}\right)^{1/2} K_{1/3}\left(\frac{2}{3}q^{3/2}\right) \quad , \tag{356}$$

where

$$K_{1/3}(q) = j\frac{\pi}{2}\, e^{j\pi/6}\, H_{1/3}^{(1)}\left(qe^{j\pi/2}\right) \tag{357}$$

or

$$K_{1/3}(q) = -j\frac{\pi}{2}\, e^{-j\pi/6}\, H_{1/3}^{(2)}\left(qe^{-j\pi/2}\right) \quad . \tag{358}$$

In Equations 357 and 358, $H_{1/3}^{(1)}(.)$ and $H_{1/3}^{(2)}(.)$ are Hankel functions of the first and second kind of order one-third respectively. Substituting Equation 357 into Equation 356 leads to

$$\begin{aligned} Ai(q) &= \frac{1}{\pi}\left(\frac{q}{3}\right)^{1/2} j\frac{\pi}{2}\, e^{j\pi/6}\, H_{1/3}^{(1)}\left(\frac{2}{3}q^{3/2}\, e^{j\pi/2}\right) \\ &= \frac{j}{2}\left(\frac{q}{3}\right)^{1/2} e^{j\pi/6}\, H_{1/3}^{(1)}\left(\frac{2}{3}q^{3/2}\, e^{j\pi/2}\right) \quad . \end{aligned} \tag{359}$$

Thus,

$$\begin{aligned} Ai\left(-qe^{j2\pi/3}\right) &= \frac{j}{2}\left(\frac{q}{3}\right)^{1/2}\left(e^{-j\pi}\right)^{1/2}\left(e^{j2\pi/3}\right)^{1/2} e^{j\pi/6} \\ &\quad \times H_{1/3}^{(1)}\left(\frac{2}{3}\, q^{3/2} e^{-j3\pi/2}\, e^{j\pi}\, e^{j\pi/2}\right) \\ &= \frac{j}{2}\left(\frac{q}{3}\right)^{1/2} H_{1/3}^{(1)}\left(\frac{2}{3}\, q^{2/3}\right) \quad . \end{aligned} \tag{360}$$

From Equation 142,

$$k_1(q) = -j\,2(12)^{1/6}\,Ai(-q\,e^{j2\pi/3}) \quad . \tag{361}$$

Substituting Equation 360 into Equation 361 gives

$$\begin{aligned} k_1(q) &= (12)^{1/6}\left(\frac{q}{3}\right)^{1/2} H_{1/3}^{(1)}\left(\frac{2}{3}\,q^{3/2}\right) \\ &= \left(\frac{2}{3}\,q^{3/2}\right)^{1/3} H_{1/3}^{(1)}\left(\frac{2}{3}\,q^{3/2}\right) \\ &= h_1(q) \quad . \end{aligned} \tag{362}$$

where $h_1(q)$ is the modified Hankel function of the first kind of order one-third and is defined as [Ref. 5]

$$h_1(q) \equiv \left(\frac{2}{3}\,q^{3/2}\right)^{1/3} H_{1/3}^{(1)}\left(\frac{2}{3}\,q^{3/2}\right) \quad . \tag{363}$$

To derive an expression for $k_2(q)$, the Airy function, $Ai(-q)$, can be expressed as [Ref. 4]

$$Ai(-q) = \frac{1}{2}\left(\frac{q}{3}\right)^{1/2}\left[e^{j\pi/6} H_{1/3}^{(1)}\left(\frac{2}{3}\,q^{3/2}\right) + e^{-j\pi/6} H_{1/3}^{(2)}\left(\frac{2}{3}\,q^{3/2}\right)\right] \tag{364}$$

From Equation 143,

$$k_2(q) = 2(12)^{1/6}\,e^{j\pi/6}\,Ai(-q) \quad . \tag{365}$$

Substituting Equation 364 into 365 leads to

$$
\begin{aligned}
k_2(q) &= (12)^{1/6}\, e^{j\pi/6} \left(\frac{q}{3}\right)^{1/2} \left[e^{j\pi/6}\, H_{1/3}^{(1)}\left(\frac{2}{3}\, q^{3/2}\right) \right. \\
&\quad \left. + e^{-j\pi/6}\, H_{1/3}^{(2)}\left(\frac{2}{3}\, q^{3/2}\right) \right] \\
&= \left(\frac{2}{3}\, q^{3/2}\right)^{1/3} \left[e^{j\pi/3}\, H_{1/3}^{(1)}\left(\frac{2}{3}\, q^{3/2}\right) + H_{1/3}^{(2)}\left(\frac{2}{3}\, q^{3/2}\right) \right] \qquad (366) \\
&= \left(\frac{2}{3}\, q^{3/2}\right)^{1/3} H_{1/3}^{(2)}\left(\frac{2}{3}\, q^{3/2}\right) \\
&\quad - e^{j4\pi/3} \left(\frac{2}{3}\, q^{3/2}\right)^{1/3} H_{1/3}^{(1)}\left(\frac{2}{3}\, q^{3/2}\right) \\
&= h_2(q) - e^{j4\pi/3}\, h_1(q) \quad ,
\end{aligned}
$$

where $h_2(q)$ is the modified Hankel function of the second kind of order one-third and is defined as [Ref. 5]

$$
h_2(q) \equiv \left(\frac{2}{3}\, q^{3/2}\right)^{1/2} H_{1/3}^{(2)}\left(\frac{2}{3}\, q^{3/2}\right) \quad . \qquad (367)
$$

For large $|q|$, the Hankel function can be approximated by the leading term of its asymptotic expansion. That is [Ref. 4],

$$
H_{1/3}^{(1)}(q) \sim \left(\frac{2}{\pi q}\right)^{1/2} \exp\left[j\left(q - \frac{\pi}{6} - \frac{\pi}{4}\right)\right] \quad : \quad -\pi < \arg(q) < 2\pi \qquad (368)
$$

and

$$
H_{1/3}^{(2)}(q) \sim \left(\frac{2}{\pi q}\right)^{1/2} \exp\left[-j\left(q - \frac{\pi}{6} - \frac{\pi}{4}\right)\right] \quad : \quad -2\pi < \arg(q) < \pi \quad . \qquad (369)
$$

Therefore,

$$k_1(q) \sim 12^{1/6}\left(\frac{q}{3}\right)^{1/2}\left(\frac{2}{\pi}\right)^{1/2}\left(\frac{2}{3}q^{3/2}\right)^{-1/2}\exp\left[j\left(\frac{2}{3}q^{3/2}-\frac{5\pi}{12}\right)\right]$$

$$\sim 12^{1/6}\pi^{-1/2}q^{-1/4}\exp\left[j\left(\frac{2}{3}q^{3/2}-\frac{5\pi}{12}\right)\right] \quad ; \tag{370}$$

$$\frac{-2\pi}{3} < \arg(q) < \frac{4\pi}{3} \quad .$$

To obtain the asymptotic expansion for $k_2(q)$, it is more convenient to express $k_2(q)$ in terms of $H_{1/3}^{(2)}(\cdot)$. From Equations 356 and 358,

$$Ai(q) = \frac{1}{\pi}\left(\frac{q}{3}\right)^{1/2}\left(-j\frac{\pi}{2}\right)e^{-j\pi/6}H_{1/3}^{(2)}\left(\frac{2}{3}q^{3/2}e^{-j\pi/2}\right)$$

$$= \frac{-j}{2}\left(\frac{q}{3}\right)^{1/2}e^{-j\pi/6}H_{1/3}^{(2)}\left(\frac{2}{3}q^{3/2}e^{-j\pi/2}\right) \quad . \tag{371}$$

Thus,

$$Ai(-q) = -\frac{j}{2}\left(\frac{q}{3}\right)^{1/2}e^{-j\pi/2}e^{-j\pi/6}H_{1/3}^{(2)}\left(\frac{2}{3}q^{3/2}e^{-j3\pi/2}e^{-j\pi/2}\right)$$

$$= -\frac{1}{2}\left(\frac{q}{3}\right)^{1/2}e^{-j\pi/6}H_{1/3}^{(2)}\left(\frac{2}{3}q^{3/2}e^{-j2\pi}\right) \quad . \tag{372}$$

Substitute Equation 372 into 365 gives

$$k_2(q) = -\left(\frac{2}{3}q^{3/2}\right)^{1/2}H_{1/3}^{(2)}\left(\frac{2}{3}q^{3/2}e^{-j2\pi}\right) \quad . \tag{373}$$

From Equation 369 and 373, the asymptotic expansion for $k_2(q)$ is

$$k_2(q) \sim -\left(\frac{2}{3}\, q^{3/2}\right)^{1/3} \left(\frac{2}{\pi}\right)^{1/2} \left(\frac{2}{3}\, q^{3/2}\, e^{-j2\pi}\right)^{-1/2}$$

$$\exp\left[-j\left(\frac{2}{3}\, q^{3/2}\, e^{-j2\pi} - \frac{5\pi}{12}\right)\right] \tag{374}$$

$$\sim 12^{1/6}\, \pi^{-1/2}\, q^{-1/4}\, \exp\left[-j\left(\frac{2}{3}\, q^{3/2} - \frac{5\pi}{12}\right)\right] \quad ;$$

$$0 < \arg(q) < 2\pi \quad .$$

APPENDIX B. SAMPLE PRINTOUT OF INPUT AND OUTPUT FILES

**********Sample printout for a 2 m evaporation duct input file**********

```
9ghz02m
 0
 9600.00      FQMZIN
 0.000000     DELFQ
 1.000000     NFREQ
 0.000000     MPOL
 5.000000     ALOSS
 15.000000    SEATMP
 35.000000    SEASLT
 1.000000     IFLAGB
 0.000000     AIRTMP
 0.000000     RH
 0.000000     WGPM3
 0.250000     RMSBHT
 48.000000    ZTINIT
 0.000000     DELZT
 1.000000     NZT
 46.0000000   ZRINIT
 7.0000000    DELZR
 2.0000000    NZR
 18.5000      XINIT
 9.250000     DELX
 3.000000     NX
 0.000000     ZREF
 16           NZLAYR
 0.000000     zi[ 0]
 0.000000     zim[ 0]
 0.000000     zigab[ 0]
 0.020000     zi[ 1]
 -0.400000    zim[ 1]
 0.000000     zigab[ 1]
 0.040000     zi[ 2]
 -0.550000    zim[ 2]
 0.000000     zigab[ 2]
 0.079000     zi[ 3]
 -0.700000    zim[ 3]
 0.000000     zigab[ 3]
 0.158000     zi[ 4]
 -0.850000    zim[ 4]
 0.000000     zigab[ 4]
 0.251000     zi[ 5]
 -0.940000    zim[ 5]
 0.000000     zigab[ 5]
 0.631000     zi[ 6]
 -1.100000    zim[ 6]
 0.000000     zigab[ 6]
 1.259000     zi[ 7]
```

```
-1.170000   zim[ 7]
0.000000    zigab[ 7]
2.000000    zi[ 8]
-1.180000   zim[ 8]
0.000000    zigab[ 8]
3.981000    zi[ 9]
-1.090000   zim[ 9]
0.000000    zigab[ 9]
5.012000    zi[ 10]
-1.010000   zim[ 10]
0.000000    zigab[ 10]
7.943000    zi[ 11]
-0.750000   zim[ 11]
0.000000    zigab[ 11]
12.589000   zi[ 12]
-0.270000   zim[ 12]
0.000000    zigab[ 12]
19.953000   zi[ 13]
0.550000    zim[ 13]
0.000000    zigab[ 13]
25.119000   zi[ 14]
1.140000    zim[ 14]
0.000000    zigab[ 14]
31.623000   zi[ 15]
1.900000    zim[ 15]
0.000000    zigab[ 15]
50.000000   zi[ 16]
4.069000    zim[ 16]
0.000000    zigab[ 16]
```

*********Sample printout for 9ghz02.eig*********

```
9ghz02m
 1
 9600.000    FQMZIN
 0.000000    DELFQ
 1           NFREQ
 0           MPOL
 5.000000    ALOSS
 15.000000   SEATMP
 35.000000   SEASLT
 1           IFLAGB
 0.000000    AIRTMP
 0.000000    RH
 0.000000    WGPM3
 0.250000    RMSBHT
 48.000000   ZTINIT
 0.000000    DELZT
 1           NZT
 46.000000   ZRINIT
 7.000000    DELZR
 2           NZR
 18.500000   XINIT
 9.250000    DELX
 3           NX
```

```
0.000000    ZREF
16          NZLAYR
0.000000    zi[ 0]
0.000000    zim[ 0]
0.000000    zigab[ 0]
0.020000    zi[ 1]
-0.400000   zim[ 1]
0.000000    zigab[ 1]
0.040000    zi[ 2]
-0.550000   zim[ 2]
0.000000    zigab[ 2]
0.079000    zi[ 3]
-0.700000   zim[ 3]
0.000000    zigab[ 3]
0.158000    zi[ 4]
-0.850000   zim[ 4]
0.000000    zigab[ 4]
0.251000    zi[ 5]
-0.940000   zim[ 5]
0.000000    zigab[ 5]
0.631000    zi[ 6]
-1.100000   zim[ 6]
0.000000    zigab[ 6]
1.259000    zi[ 7]
-1.170000   zim[ 7]
0.000000    zigab[ 7]
2.000000    zi[ 8]
-1.180000   zim[ 8]
0.000000    zigab[ 8]
3.981000    zi[ 9]
-1.090000   zim[ 9]
0.000000    zigab[ 9]
5.012000    zi[ 10]
-1.010000   zim[ 10]
0.000000    zigab[ 10]
7.943000    zi[ 11]
-0.750000   zim[ 11]
0.000000    zigab[ 11]
12.589000   zi[ 12]
-0.270000   zim[ 12]
0.000000    zigab[ 12]
19.953000   zi[ 13]
0.550000    zim[ 13]
0.000000    zigab[ 13]
25.119000   zi[ 14]
1.140000    zim[ 14]
0.000000    zigab[ 14]
31.623000   zi[ 15]
1.900000    zim[ 15]
0.000000    zigab[ 15]
50.000000   zi[ 16]
4.069000    zim[ 16]
0.000000    zigab[ 16]
9           nrmode
(-1.269556983588969E-001,1.637613838717031E-001)   [ 1]
(-9.291194300692691E-002,1.251243717867209E-001)   [ 2]
```

```
(-4.143216670274859E-002,8.947793427709196E-002)   [3]
(8.240706115401963E-003,6.917378956118456E-002)    [4]
(5.551160395245244E-002,5.324818113693566E-002)    [5]
(7.682611348504449E-002,6.708823745503940E-002)    [6]
(1.394420773218969E-001,9.725689299213881E-002)    [7]
(2.102775842495503E-001,1.357828223763695E-001)    [8]
(2.864589183106626E-001,1.658090146540282E-001)    [9]


**********Sample printout for 9ghz02m.out**********

1


   frequency =     9600.0000 mhz
   horizontal polarization
   maximum mode attenuation rate =        5.0000 db/km

   seawater temperature =       15.0000 degrees celsius
   seawater salinity =       35.0000 grams salt/kg seawater
   dielectric constant of seawater =       80.8869
   conductivity of seawater =        4.6400 si/m
   rms surface bump height =         .2500 meters
   iflagb =   1
   air temperature =         .0000 degrees celsius
   relative himidity =          .0000 percent
   liquid water concentration in air =          .0000 grams/meter**3

   m(        .0000 ) =         .0000 m-units
   gab(        .0000 ) =         .0000 db/km

                  tropospheric modified refractivity profile

     z          m(z)          gab(z)          dm/dz          d(gab)/dz
  (meters)    (m-units)      (db/km)      (m-units/meter)  ((db/km)/meter)

      .0000        .0000       .00000D+00     -20.0000        .00000D+00
      .0200       -.4000       .00000D+00      -7.5000        .00000D+00
      .0400       -.5500       .00000D+00      -3.8462        .00000D+00
      .0790       -.7000       .00000D+00      -1.8987        .00000D+00
      .1580       -.8500       .00000D+00       -.9677        .00000D+00
      .2510       -.9400       .00000D+00       -.4211        .00000D+00
      .6310      -1.1000       .00000D+00       -.1115        .00000D+00
     1.2590      -1.1700       .00000D+00       -.0135        .00000D+00
     2.0000      -1.1800       .00000D+00        .0454        .00000D+00
     3.9810      -1.0900       .00000D+00        .0776        .00000D+00
     5.0120      -1.0100       .00000D+00        .0887        .00000D+00
     7.9430       -.7500       .00000D+00        .1033        .00000D+00
    12.5890       -.2700       .00000D+00        .1114        .00000D+00
    19.9530        .5500       .00000D+00        .1142        .00000D+00
    25.1190       1.1400       .00000D+00        .1169        .00000D+00
    31.6230       1.9000       .00000D+00        .1180        .00000D+00
    50.0000       4.0690       .00000D+00
```

```
******   start search for modal eigenvalues   ******

     tmesh=     1.67984D-03     tol=     1.00000D-04


     zeros found in expanded search rectangle defined by
     tleft=     0.00D+00     tright=     2.69D-01
     ttop =     1.68D-01     tbot  =    -1.00D-04


               qeigen(  1) =    8.24071D-03   6.91738D-02
               qeigen(  2) =    5.55116D-02   5.32482D-02
               qeigen(  3) =    2.10278D-01   1.35783D-01
               qeigen(  4) =    1.39442D-01   9.72569D-02
               qeigen(  5) =    7.68261D-02   6.70882D-02


     zeros found in expanded search rectangle defined by
     tleft=    -2.69D-01     tright=     0.00D+00
     ttop =     1.68D-01     tbot  =    -1.00D-04


               qeigen(  1) =   -1.26956D-01   1.63761D-01
               qeigen(  2) =   -9.29119D-02   1.25124D-01
               qeigen(  3) =   -4.14322D-02   8.94779D-02


     zeros found in expanded search rectangle defined by
     tleft=    -5.38D-01     tright=    -2.69D-01
     ttop =     1.68D-01     tbot  =    -1.00D-04


     zeros found in expanded search rectangle defined by
     tleft=    -8.06D-01     tright=    -5.38D-01
     ttop =     1.68D-01     tbot  =    -1.00D-04


     zeros found in expanded search rectangle defined by
     tleft=     2.69D-01     tright=     5.38D-01
     ttop =     1.68D-01     tbot  =    -1.00D-04


               qeigen(  1) =    2.86459D-01   1.65809D-01


     zeros found in expanded search rectangle defined by
     tleft=     5.38D-01     tright=     8.06D-01
     ttop =     1.68D-01     tbot  =    -1.00D-04
```

```
zeros found in expanded search rectangle defined by
tleft=     8.06D-01     tright=     1.08D+00
ttop =     1.68D-01     tbot  =    -1.00D-04


******  modal eigenvalues  nrmode=   9  ******

mode eigenvalue                  theta                          atnu db/km
   1 -1.26956D-01 1.63761D-01  1.16912D-03 2.38566D-03   4.8743D+00
   2 -9.29119D-02 1.25124D-01  1.03533D-03 2.05835D-03   3.7243D+00
   3 -4.14322D-02 8.94779D-02  9.86784D-04 1.54436D-03   2.6633D+00
   4  8.24071D-03 6.91738D-02  1.15188D-03 1.02280D-03   2.0589D+00
   5  5.55116D-02 5.32482D-02  1.50185D-03 6.03859D-04   1.5849D+00
   6  7.68261D-02 6.70882D-02  1.74517D-03 6.54734D-04   1.9969D+00
   7  1.39442D-01 9.72569D-02  2.29575D-03 7.21529D-04   2.8948D+00
   8  2.10278D-01 1.35783D-01  2.80081D-03 8.25696D-04   4.0415D+00
   9  2.86459D-01 1.65809D-01  3.24286D-03 8.70843D-04   4.9353D+00

**********Sample printout for 9ghz02m.plt**********

   3    1    2
  frequency =    9600.0000 mhz
  18.5    48.0    46.0      52.90      61.21      84.54      76.23    56.5
  18.5    48.0    53.0      69.58      73.08      67.86      64.36    58.6
  27.8    48.0    46.0       2.17      38.48     138.80     102.48    56.5
  27.8    48.0    53.0      19.57      43.39     121.39      97.57    58.6
  37.0    48.0    46.0       3.41      22.15     140.05     121.31    56.5
  37.0    48.0    53.0       2.69      25.91     140.77     117.55    58.6

**********Sample printout for a 14 m evaporation duct input file*********

9ghz14m
 0
 9600.00     FQMZIN
 0.000000    DELFQ
 1           NFREQ
 0           MPOL
 2.100000    ALOSS
 15.000000   SEATMP
 35.000000   SEASLT
 1           IFLAGB
 0.000000    AIRTMP
 0.000000    RH
 0.000000    WGPM3
 0.250000    RMSBHT
 25.000000   ZTINIT
 0.000000    DELZT
 1           NZT
```

```
3.0000000   ZRINIT
7.0000000   DELZR
2           NZR
18.5000     XINIT
9.250000    DELX
3           NX
0.000000    ZREF
20          NZLAYR
0.000000    zi[ 0]
0.000000    zim[ 0]
0.000000    zigab[ 0]
0.040000    zi[ 1]
-3.900000   zim[ 1]
0.000000    zigab[ 1]
0.100000    zi[ 2]
-5.340000   zim[ 2]
0.000000    zigab[ 2]
0.200000    zi[ 3]
-6.400000   zim[ 3]
0.000000    zigab[ 3]
0.398000    zi[ 4]
-7.460000   zim[ 4]
0.000000    zigab[ 4]
0.794000    zi[ 5]
-8.490000   zim[ 5]
0.000000    zigab[ 5]
1.585000    zi[ 6]
-9.470000   zim[ 6]
0.000000    zigab[ 6]
3.162000    zi[ 7]
-10.350000  zim[ 7]
0.000000    zigab[ 7]
6.310000    zi[ 8]
-11.040000  zim[ 8]
0.000000    zigab[ 8]
12.589000   zi[ 9]
-11.320000  zim[ 9]
0.000000    zigab[ 9]
14.000000   zi[ 10]
-11.330000  zim[ 10]
0.000000    zigab[ 10]
25.119000   zi[ 11]
-10.870000  zim[ 11]
0.000000    zigab[ 11]
39.811000   zi[ 12]
-9.750000   zim[ 12]
0.000000    zigab[ 12]
50.119000   zi[ 13]
-8.820000   zim[ 13]
0.000000    zigab[ 13]
63.096000   zi[ 14]
-7.560000   zim[ 14]
0.000000    zigab[ 14]
79.433000   zi[ 15]
-5.880000   zim[ 15]
0.000000    zigab[ 15]
```

```
 100.000000 zi[ 16]
 -3.670000  zim[ 16]
 0.000000   zigab[ 16]
 125.693000 zi[ 17]
 -0.800000  zim[ 17]
 0.000000   zigab[ 17]
 158.489000 zi[ 18]
 2.920000   zim[ 18]
 0.000000   zigab[ 18]
 199.526000 zi[ 19]
 7.690000   zim[ 19]
 0.000000   zigab[ 19]
 209.526000 zi[ 20]
 8.870000   zim[ 20]
 0.000000   zigab[ 20]
```

**********Sample printout for 9ghz14m.eig**********

```
9ghz14m
 1
 9600.000   FQMZIN
 0.000000   DELFQ
 1          NFREQ
 0          MPOL
 2.100000   ALOSS
 15.000000  SEATMP
 35.000000  SEASLT
 1          IFLAGB
 0.000000   AIRTMP
 0.000000   RH
 0.000000   WGPM3
 0.250000   RMSBHT
 25.000000  ZTINIT
 0.000000   DELZT
 1          NZT
 3.000000   ZRINIT
 7.000000   DELZR
 2          NZR
 18.500000  XINIT
 9.250000   DELX
 3          NX
 0.000000   ZREF
 20         NZLAYR
 0.000000   zi[ 0]
 0.000000   zim[ 0]
 0.000000   zigab[ 0]
 0.040000   zi[ 1]
 -3.900000  zim[ 1]
 0.000000   zigab[ 1]
 0.100000   zi[ 2]
 -5.340000  zim[ 2]
 0.000000   zigab[ 2]
 0.200000   zi[ 3]
 -6.400000  zim[ 3]
 0.000000   zigab[ 3]
```

```
0.398000    zi[ 4]
-7.460000   zim[ 4]
0.000000    zigab[ 4]
0.794000    zi[ 5]
-8.490000   zim[ 5]
0.000000    zigab[ 5]
1.585000    zi[ 6]
-9.470000   zim[ 6]
0.000000    zigab[ 6]
3.162000    zi[ 7]
-10.350000  zim[ 7]
0.000000    zigab[ 7]
6.310000    zi[ 8]
-11.040000  zim[ 8]
0.000000    zigab[ 8]
12.589000   zi[ 9]
-11.320000  zim[ 9]
0.000000    zigab[ 9]
14.000000   zi[ 10]
-11.330000  zim[ 10]
0.000000    zigab[ 10]
25.119000   zi[ 11]
-10.870000  zim[ 11]
0.000000    zigab[ 11]
39.811000   zi[ 12]
-9.750000   zim[ 12]
0.000000    zigab[ 12]
50.119000   zi[ 13]
-8.820000   zim[ 13]
0.000000    zigab[ 13]
63.096000   zi[ 14]
-7.560000   zim[ 14]
0.000000    zigab[ 14]
79.433000   zi[ 15]
-5.880000   zim[ 15]
0.000000    zigab[ 15]
100.000000  zi[ 16]
-3.670000   zim[ 16]
0.000000    zigab[ 16]
125.893000  zi[ 17]
-0.800000   zim[ 17]
0.000000    zigab[ 17]
158.489000  zi[ 18]
2.920000    zim[ 18]
0.000000    zigab[ 18]
199.526000  zi[ 19]
7.690000    zim[ 19]
0.000000    zigab[ 19]
209.526000  zi[ 20]
8.870000    zim[ 20]
0.000000    zigab[ 20]
94          nrmode
(-1.141392174382303E-001,2.381981532549529E-002)   [ 1]
(-9.791475196101274E-002,2.146753762359050E-002)   [ 2]
(-8.353759867176463E-002,1.997153241435371E-002)   [ 3]
(-7.039783167095078E-002,1.889606906408722E-002)   [ 4]
```

(-5.814228837496516E-002,1.806765450625147E-002) [5]
(-4.656628790733621E-002,1.728118397954079E-002) [6]
(-3.585330645452212E-002,1.663363181205510E-002) [7]
(-2.527742000231397E-002,1.628348275301875E-002) [8]
(-1.546901363155011E-002,1.571655186158130E-002) [9]
(-5.541956071147925E-003,1.540239335815212E-002) [10]
(3.551321843705835E-003,1.518851207972415E-002) [11]
(1.275397200580210E-002,1.460556299546134E-002) [12]
(2.182707485088627E-002,1.455854335720260E-002) [13]
(3.011306010124748E-002,1.427613140712134E-002) [14]
(3.842803342065884E-002,1.365892306660126E-002) [15]
(4.694372655547260E-002,1.365320803509313E-002) [16]
(5.485441606530146E-002,1.365090923924493E-002) [17]
(6.227012336327741E-002,1.336276100865187E-002) [18]
(7.029778501629384E-002,1.282089227646639E-002) [19]
(7.803056175576653E-002,1.285572220605075E-002) [20]
(8.555171301174155E-002,1.287860792288040E-002) [21]
(9.226312048960586E-002,1.278978888881959E-002) [22]
(9.940292680300993E-002,1.210154187763285E-002) [23]
(1.068485002790371E-001,1.208486102139816E-002) [24]
(1.138252208858628E-001,1.195444121483925E-002) [25]
(1.207736300828756E-001,1.220952877564303E-002) [26]
(1.270094738812559E-001,1.222384497715726E-002) [27]
(1.334153343077380E-001,1.139138734459426E-002) [28]
(1.403978164901863E-001,1.116571468633296E-002) [29]
(1.467611452238766E-001,1.129961336802001E-002) [30]
(1.534013614885507E-001,1.116543866415548E-002) [31]
(1.596149004805981E-001,1.136779885138012E-002) [32]
(1.652780520579286E-001,1.153156478829780E-002) [33]
(1.709514646617846E-001,1.066116492781759E-002) [34]
(1.772646284812436E-001,1.023671860551962E-002) [35]
(1.836482895835790E-001,1.049763117145163E-002) [36]
(1.891728805710848E-001,1.025773869961451E-002) [37]
(1.951501729145819E-001,1.007563477610222E-002) [38]
(2.006781595657978E-001,1.041321459422345E-002) [39]
(2.059566903740310E-001,1.043172189566190E-002) [40]
(2.106263141043572E-001,9.926428640075490E-003) [41]
(2.157518751516274E-001,8.798215719693539E-003) [42]
(2.213117492755677E-001,9.015024671611194E-003) [43]
(2.273294238073336E-001,8.321071087819404E-003) [44]
(2.303987147631242E-001,1.185554142465963E-003) [45]
(2.318960198770044E-001,8.464799970637166E-003) [46]
(2.348881611845628E-001,7.882321847941567E-003) [47]
(2.402844396949530E-001,8.719487457459410E-003) [48]
(2.455147471247609E-001,9.692237120376304E-003) [49]
(2.499562362348160E-001,1.010888147000029E-002) [50]
(2.545987673232816E-001,1.010149239614689E-002) [51]
(2.600542439477720E-001,1.049907356151861E-002) [52]
(2.662691013974199E-001,1.044438363485770E-002) [53]
(2.726418617644147E-001,1.092098859083637E-002) [54]
(2.787900254603262E-001,1.175196099261803E-002) [55]
(2.849476164544477E-001,1.227969492073188E-002) [56]
(2.913747922726816E-001,1.246149094591169E-002) [57]
(2.980151522337324E-001,1.329730594318235E-002) [58]
(3.042875049575047E-001,1.319657577519411E-002) [59]
(3.113767357254904E-001,1.314377702678184E-002) [60]

```
(3.187819780335167E-001,1.333680648010814E-002)    [61]
(3.264578839391167E-001,1.384739430048439E-002)    [62]
(3.338112497216490E-001,1.464186747417008E-002)    [63]
(3.410941266084628E-001,1.490152638527356E-002)    [64]
(3.487677270086091E-001,1.524482539938137E-002)    [65]
(3.563811238953353E-001,1.551353021082856F-002)    [66]
(3.643646265942290E-001,1.538942161737147E-002)    [67]
(3.729775181063331E-001,1.559989625580370E-002)    [68]
(3.814931085621074E-001,1.618605966683290E-002)    [69]
(3.898891425944480E-001,1.689462812245438E-002)    [70]
(3.980319033943261E-001,1.714047724320524E-002)    [71]
(4.067283853697590E-001,1.729643131530817E-002)    [72]
(4.154949433609382E-001,1.751352926449171E-002)    [73]
(4.246400421526860E-001,1.750551050950182E-002)    [74]
(4.341831113214738E-001,1.789042401852184E-002)    [75]
(4.435147531419498E-001,1.866150403101799E-002)    [76]
(4.525289981946153E-001,1.909787541066863E-002)    [77]
(4.618630098407780E-001,1.919260738082309E-002)    [78]
(4.716181770152394E-001,1.927318684881558E-002)    [79]
(4.815020432944205E-001,1.952391397029549E-002)    [80]
(4.917304699196995E-001,1.972766534431011E-002)    [81]
(5.020225407049786E-001,2.044077417123271E-002)    [82]
(5.118252276793764E-001,2.102681780869346E-002)    [83]
(5.218948685680153E-001,2.102179462275660E-002)    [84]
(5.324815199710420E-001,2.111602176832850E-002)    [85]
(5.432604196740195E-001,2.136847129075478E-002)    [86]
(5.541811165125796E-001,2.172276354461229E-002)    [87]
(5.651832495410506E-001,2.227384315438282E-002)    [88]
(5.758688247777175E-001,2.293313938401881E-002)    [89]
(5.866533408029618E-001,2.286336319718634E-002)    [90]
(5.981376451733623E-001,2.292879795570507E-002)    [91]
(6.097267273995461E-001,2.326416356305734E-002)    [92]
(6.213712082142159E-001,2.370559660462316E-002)    [93]
(6.330414592077247E-001,2.426761624643026E-002)    [94]


**********Sample printout for 9ghz14m.out**********

1

   frequency =    9600.0000 mhz
   horizontal polarization
   maximum mode attenuation rate =       2.1000 db/km

   seawater temperature =      15.0000 degrees celsius
   seawater salinity =      35.0000 grams salt/kg seawater
   dielectric constant of seawater =      80.8869
   conductivity of seawater =       4.6400 si/m
   rms surface bump height =        .2500 meters
   iflagb =   1
   air temperature =        .0000 degrees celsius
   relative himidity =         .0000 percent
   liquid water concentration in air =        .0000 grams/meter**3

   m(       .0000 ) =        .0000 m-units
   gab(       .0000 ) =        .0000 db/km
```

tropospheric modified refractivity profile

z (meters)	m(z) (m-units)	gab(z) (db/km)	dm/dz (m-units/meter)	d(gab)/dz ((db/km)/meter)
.0000	.0000	.00000D+00	-97.5000	.00000D+00
.0400	-3.9000	.00000D+00	-24.0000	.00000D+00
.1000	-5.3400	.00000D+00	-10.6000	.00000D+00
.2000	-6.4000	.00000D+00	-5.3535	.00000D+00
.3980	-7.4600	.00000D+00	-2.6010	.00000D+00
.7940	-8.4900	.00000D+00	-1.2389	.00000D+00
1.5850	-9.4700	.00000D+00	-.5580	.00000D+00
3.1620	-10.3500	.00000D+00	-.2192	.00000D+00
6.3100	-11.0400	.00000D+00	-.0446	.00000D+00
12.5890	-11.3200	.00000D+00	-.0071	.00000D+00
14.0000	-11.3300	.00000D+00	.0414	.00000D+00
25.1190	-10.8700	.00000D+00	.0762	.00000D+00
39.8110	-9.7500	.00000D+00	.0902	.00000D+00
50.1190	-8.8200	.00000D+00	.0971	.00000D+00
63.0960	-7.5600	.00000D+00	.1028	.00000D+00
79.4330	-5.8800	.00000D+00	.1075	.00000D+00
100.0000	-3.6700	.00000D+00	.1108	.00000D+00
125.8930	-.8000	.00000D+00	.1141	.00000D+00
158.4890	2.9200	.00000D+00	.1162	.00000D+00
199.5260	7.6900	.00000D+00	.1180	.00000D+00
209.5260	8.8700	.00000D+00		

****** start search for modal eigenvalues ******

tmesh= 5.84278D-04 tol= 5.84278D-05

zeros found in expanded search rectangle defined by
tleft= 1.87D-01 tright= 2.80D-01
ttop = 2.45D-02 tbot = -5.84D-05

qeigen(1) =	1.89173D-01	1.02577D-02
qeigen(2) =	2.10626D-01	9.92643D-03
qeigen(3) =	2.30399D-01	1.18555D-03
qeigen(4) =	2.34888D-01	7.88232D-03
qeigen(5) =	2.78790D-01	1.17520D-02
qeigen(6) =	2.72642D-01	1.09210D-02
qeigen(7) =	2.66269D-01	1.04444D-02
qeigen(8) =	2.60054D-01	1.04991D-02
qeigen(9) =	2.54599D-01	1.01015D-02
qeigen(10) =	2.49956D-01	1.01089D-02
qeigen(11) =	2.45515D-01	9.69224D-03
qeigen(12) =	2.40284D-01	8.71949D-03
qeigen(13) =	2.31896D-01	8.46480D-03

```
          qeigen( 14) =    2.27329D-01   8.32107D-03
          qeigen( 15) =    2.21312D-01   9.01502D-03
          qeigen( 16) =    2.15752D-01   8.79822D-03
          qeigen( 17) =    2.05957D-01   1.04317D-02
          qeigen( 18) =    2.00678D-01   1.04132D-02
          qeigen( 19) =    1.95150D-01   1.00756D-02

zeros found in expanded search rectangle defined by
tleft=     9.35D-02     tright=     1.87D-01
ttop =     2.45D-02     tbot  =    -5.84D-05

          qeigen(  1) =    9.94029D-02   1.21015D-02
          qeigen(  2) =    1.13825D-01   1.19544D-02
          qeigen(  3) =    1.70951D-01   1.06612D-02
          qeigen(  4) =    1.83648D-01   1.04976D-02
          qeigen(  5) =    1.77265D-01   1.02367D-02
          qeigen(  6) =    1.65278D-01   1.15316D-02
          qeigen(  7) =    1.59615D-01   1.13678D-02
          qeigen(  8) =    1.53401D-01   1.11654D-02
          qeigen(  9) =    1.46761D-01   1.12996D-02
          qeigen( 10) =    1.40398D-01   1.11657D-02
          qeigen( 11) =    1.33415D-01   1.13914D-02
          qeigen( 12) =    1.27009D-01   1.22238D-02
          qeigen( 13) =    1.20774D-01   1.22095D-02
          qeigen( 14) =    1.06849D-01   1.20849D-02

zeros found in expanded search rectangle defined by
tleft=     0.00D+00     tright=     9.35D-02
ttop =     2.45D-02     tbot  =    -5.84D-05

          qeigen(  1) =    3.55132D-03   1.51885D-02
          qeigen(  2) =    3.84280D-02   1.36589D-02
          qeigen(  3) =    9.22631D-02   1.27898D-02
          qeigen(  4) =    8.55517D-02   1.28786D-02
          qeigen(  5) =    7.80306D-02   1.28557D-02
          qeigen(  6) =    7.02978D-02   1.28209D-02
          qeigen(  7) =    6.22701D-02   1.33628D-02
          qeigen(  8) =    5.48544D-02   1.36509D-02
          qeigen(  9) =    4.69437D-02   1.36532D-02
          qeigen( 10) =    3.01131D-02   1.42761D-02
          qeigen( 11) =    2.18271D-02   1.45585D-02
          qeigen( 12) =    1.27540D-02   1.46056D-02

zeros found in expanded search rectangle defined by
tleft=    -9.35D-02     tright=     0.00D+00
ttop =     2.45D-02     tbot  =    -5.84D-05

          qeigen(  1) =   -8.35376D-02   1.99715D-02
          qeigen(  2) =   -4.65663D-02   1.72812D-02
          qeigen(  3) =   -5.54196D-03   1.54024D-02
```

```
          qeigen(  4) =   -1.54690D-02   1.57166D-02
          qeigen(  5) =   -2.52774D-02   1.62835D-02
          qeigen(  6) =   -3.53533D-02   1.66336D-02
          qeigen(  7) =   -5.81423D-02   1.80677D-02
          qeigen(  8) =   -7.03978D-02   1.88961D-02

zeros found in expanded search rectangle defined by
tleft=    -1.87D-01     tright=    -9.35D-02
ttop =     2.45D-02     tbot  =    -5.84D-05

          qeigen(  1) =   -9.79148D-02   2.14675D-02
          qeigen(  2) =   -1.14139D-01   2.38198D-02

zeros found in expanded search rectangle defined by
tleft=    -2.80D-01     tright=    -1.87D-01
ttop =     2.45D-02     tbot  =    -5.84D-05

zeros found in expanded search rectangle defined by
tleft=    -3.74D-01     tright=    -2.80D-01
ttop =     2.45D-02     tbot  =    -5.84D-05

zeros found in expanded search rectangle defined by
tleft=     2.80D-01     tright=     3.74D-01
ttop =     2.45D-02     tbot  =    -5.84D-05

          qeigen(  1) =    3.72978D-01   1.55999D-02
          qeigen(  2) =    3.64365D-01   1.53894D-02
          qeigen(  3) =    3.56381D-01   1.55135D-02
          qeigen(  4) =    3.48768D-01   1.52448D-02
          qeigen(  5) =    3.41094D-01   1.49015D-02
          qeigen(  6) =    3.33811D-01   1.46419D-02
          qeigen(  7) =    3.26458D-01   1.38474D-02
          qeigen(  8) =    3.18782D-01   1.33368D-02
          qeigen(  9) =    3.11377D-01   1.31438D-02
          qeigen( 10) =    3.04288D-01   1.31966D-02
          qeigen( 11) =    2.98015D-01   1.32973D-02
          qeigen( 12) =    2.91375D-01   1.24615D-02
          qeigen( 13) =    2.84948D-01   1.22797D-02

zeros found in expanded search rectangle defined by
tleft=     3.74D-01     tright=     4.67D-01
ttop =     2.45D-02     tbot  =    -5.84D-05

          qeigen(  1) =    4.61863D-01   1.91926D-02
```

```
          qeigen(  2) =    4.52529D-01   1.90979D-02
          qeigen(  3) =    4.43515D-01   1.86615D-02
          qeigen(  4) =    4.34183D-01   1.78904D-02
          qeigen(  5) =    4.24640D-01   1.75055D-02
          qeigen(  6) =    4.15495D-01   1.75135D-02
          qeigen(  7) =    4.06728D-01   1.72964D-02
          qeigen(  8) =    3.98032D-01   1.71405D-02
          qeigen(  9) =    3.89889D-01   1.68946D-02
          qeigen( 10) =    3.81493D-01   1.61861D-02

 zeros found in expanded search rectangle defined by
 tleft=     4.67D-01     tright=     5.61D-01
 ttop =     2.45D-02     tbot  =    -5.84D-05


          qeigen(  1) =    5.54181D-01   2.17228D-02
          qeigen(  2) =    5.43260D-01   2.13685D-02
          qeigen(  3) =    5.32482D-01   2.11160D-02
          qeigen(  4) =    5.21895D-01   2.10218D-02
          qeigen(  5) =    5.11825D-01   2.10268D-02
          qeigen(  6) =    5.02023D-01   2.04408D-02
          qeigen(  7) =    4.91730D-01   1.97277D-02
          qeigen(  8) =    4.81502D-01   1.95239D-02
          qeigen(  9) =    4.71618D-01   1.92732D-02

 zeros found in expanded search rectangle defined by
 tleft=     5.61D-01     tright=     6.54D-01
 ttop =     2.45D-02     tbot  =    -5.84D-05


          qeigen(  1) =    6.44509D-01   2.47339D-02
          qeigen(  2) =    6.33041D-01   2.42676D-02
          qeigen(  3) =    6.21371D-01   2.37056D-02
          qeigen(  4) =    6.09727D-01   2.32642D-02
          qeigen(  5) =    5.98138D-01   2.29288D-02
          qeigen(  6) =    5.86653D-01   2.28634D-02
          qeigen(  7) =    5.75869D-01   2.29331D-02
          qeigen(  8) =    5.65183D-01   2.22738D-02

 zeros found in expanded search rectangle defined by
 tleft=     6.54D-01     tright=     7.48D-01
 ttop =     2.45D-02     tbot  =    -5.84D-05


2 modes found on same phase line
          qeigen(  1) =    6.68467D-01   2.47500D-02
          qeigen(  2) =    6.56153D-01   2.47347D-02

 zeros found in expanded search rectangle defined by
 tleft=     7.48D-01     tright=     8.41D-01
```

ttop = 2.45D-02 tbot = -5.84D-05

2 modes found on same phase line

****** modal eigenvalues nrmode= 94 ******

mode	eigenvalue		theta		atnu db/km
1	-1.14139D-01	2.38198D-02	3.47000D-04	3.36133D-03	2.0384D+00
2	-9.79148D-02	2.14675D-02	3.37466D-04	3.11498D-03	1.8371D+00
3	-8.35376D-02	1.99715D-02	3.39522D-04	2.88036D-03	1.7091D+00
4	-7.03978D-02	1.88961D-02	3.49316D-04	2.64885D-03	1.6170D+00
5	-5.81423D-02	1.80677D-02	3.66463D-04	2.41421D-03	1.5461D+00
6	-4.65663D-02	1.72812D-02	3.89814D-04	2.17081D-03	1.4788D+00
7	-3.58533D-02	1.66336D-02	4.23955D-04	1.92120D-03	1.4234D+00
8	-2.52774D-02	1.62835D-02	4.84349D-04	1.64625D-03	1.3935D+00
9	-1.54690D-02	1.57166D-02	5.67769D-04	1.35548D-03	1.3450D+00
10	-5.54196D-03	1.54024D-02	7.28131D-04	1.03582D-03	1.3181D+00
11	3.55132D-03	1.51885D-02	9.68348D-04	7.68051D-04	1.2998D+00
12	1.27540D-02	1.46056D-02	1.25460D-03	5.70059D-04	1.2499D+00
13	2.18271D-02	1.45585D-02	1.53413D-03	4.64688D-04	1.2459D+00
14	3.01131D-02	1.42761D-02	1.76251D-03	3.96631D-04	1.2217D+00
15	3.84280D-02	1.36589D-02	1.96946D-03	3.39607D-04	1.1689D+00
16	4.69437D-02	1.36532D-02	2.16626D-03	3.08626D-04	1.1684D+00
17	5.48544D-02	1.36509D-02	2.33540D-03	2.86226D-04	1.1682D+00
18	6.22701D-02	1.33628D-02	2.48351D-03	2.63474D-04	1.1435D+00
19	7.02978D-02	1.28209D-02	2.63465D-03	2.38289D-04	1.0972D+00
20	7.80306D-02	1.28557D-02	2.77370D-03	2.26958D-04	1.1001D+00
21	8.55517D-02	1.28786D-02	2.90271D-03	2.17257D-04	1.1021D+00
22	9.22631D-02	1.27898D-02	3.01313D-03	2.07852D-04	1.0945D+00
23	9.94029D-02	1.21015D-02	3.12585D-03	1.89575D-04	1.0356D+00
24	1.06849D-01	1.20849D-02	3.23999D-03	1.82645D-04	1.0342D+00
25	1.13825D-01	1.19544D-02	3.34337D-03	1.75087D-04	1.0230D+00
26	1.20774D-01	1.22095D-02	3.44356D-03	1.73620D-04	1.0448D+00
27	1.27009D-01	1.22238D-02	3.53092D-03	1.69523D-04	1.0461D+00
28	1.33415D-01	1.13914D-02	3.61798D-03	1.54177D-04	9.7483D-01
29	1.40398D-01	1.11657D-02	3.71101D-03	1.47335D-04	9.5552D-01
30	1.46761D-01	1.12996D-02	3.79399D-03	1.45841D-04	9.6698D-01
31	1.53401D-01	1.11654D-02	3.87856D-03	1.40966D-04	9.5550D-01
32	1.59615D-01	1.13678D-02	3.95622D-03	1.40704D-04	9.7282D-01
33	1.65278D-01	1.15316D-02	4.02569D-03	1.40268D-04	9.8683D-01
34	1.70951D-01	1.06612D-02	4.09370D-03	1.27526D-04	9.1235D-01
35	1.77265D-01	1.02367D-02	4.16832D-03	1.20257D-04	8.7602D-01
36	1.83648D-01	1.04976D-02	4.24268D-03	1.21161D-04	8.9835D-01
37	1.89173D-01	1.02577D-02	4.30584D-03	1.16655D-04	8.7782D-01
38	1.95150D-01	1.00756D-02	4.37319D-03	1.12820D-04	8.6224D-01
39	2.00678D-01	1.04132D-02	4.43471D-03	1.14982D-04	8.9113D-01
40	2.05957D-01	1.04317D-02	4.49259D-03	1.13703D-04	8.9271D-01
41	2.10626D-01	9.92643D-03	4.54304D-03	1.06994D-04	8.4947D-01
42	2.15752D-01	8.79822D-03	4.59766D-03	9.37065D-05	7.5292D-01
43	2.21312D-01	9.01502D-03	4.65652D-03	9.48020D-05	7.7148D-01
44	2.27329D-01	8.32107D-03	4.71922D-03	8.63419D-05	7.1209D-01

45	2.30399D-01	1.18555D-03	4.75019D-03	1.22215D-05	1.0146D-01
46	2.31896D-01	8.46480D-03	4.76638D-03	8.69643D-05	7.2439D-01
47	2.34888D-01	7.88232D-03	4.79691D-03	8.04647D-05	6.7454D-01
48	2.40284D-01	8.71949D-03	4.85181D-03	8.80035D-05	7.4619D-01
49	2.45515D-01	9.69224D-03	4.90448D-03	9.67707D-05	8.2943D-01
50	2.49956D-01	1.01089D-02	4.94869D-03	1.00029D-04	8.6509D-01
51	2.54599D-01	1.01015D-02	4.99440D-03	9.90411D-05	8.6445D-01
52	2.60054D-01	1.04991D-02	5.04766D-03	1.01853D-04	8.9848D-01
53	2.66269D-01	1.04444D-02	5.10756D-03	1.00134D-04	8.9380D-01
54	2.72642D-01	1.09210D-02	5.16837D-03	1.03472D-04	9.3458D-01
55	2.78790D-01	1.17520D-02	5.22643D-03	1.10108D-04	1.0057D+00
56	2.84948D-01	1.22797D-02	5.28389D-03	1.13802D-04	1.0509D+00
57	2.91375D-01	1.24615D-02	5.34313D-03	1.14206D-04	1.0664D+00
58	2.98015D-01	1.32973D-02	5.40378D-03	1.20498D-04	1.1379D+00
59	3.04288D-01	1.31966D-02	5.46027D-03	1.18348D-04	1.1293D+00
60	3.11377D-01	1.31438D-02	5.52345D-03	1.16527D-04	1.1248D+00
61	3.18782D-01	1.33368D-02	5.58872D-03	1.16857D-04	1.1413D+00
62	3.26458D-01	1.38474D-02	5.65564D-03	1.19895D-04	1.1850D+00
63	3.33811D-01	1.46419D-02	5.71907D-03	1.25368D-04	1.2530D+00
64	3.41094D-01	1.49015D-02	5.78111D-03	1.26222D-04	1.2752D+00
65	3.48768D-01	1.52448D-02	5.84578D-03	1.27702D-04	1.3046D+00
66	3.56381D-01	1.55135D-02	5.90923D-03	1.28557D-04	1.3276D+00
67	3.64365D-01	1.53894D-02	5.97497D-03	1.26126D-04	1.3170D+00
68	3.72978D-01	1.55999D-02	6.04515D-03	1.26366D-04	1.3350D+00
69	3.81493D-01	1.61861D-02	6.11381D-03	1.29642D-04	1.3852D+00
70	3.89889D-01	1.68946D-02	6.18078D-03	1.33851D-04	1.4458D+00
71	3.98032D-01	1.71405D-02	6.24497D-03	1.34403D-04	1.4668D+00
72	4.06728D-01	1.72964D-02	6.31279D-03	1.34169D-04	1.4802D+00
73	4.15495D-01	1.75135D-02	6.38044D-03	1.34413D-04	1.4988D+00
74	4.24640D-01	1.75055D-02	6.45021D-03	1.32898D-04	1.4981D+00
75	4.34183D-01	1.78904D-02	6.52228D-03	1.34320D-04	1.5310D+00
76	4.43515D-01	1.86615D-02	6.59206D-03	1.38626D-04	1.5970D+00
77	4.52529D-01	1.90979D-02	6.65873D-03	1.40447D-04	1.6344D+00
78	4.61863D-01	1.91926D-02	6.72700D-03	1.39711D-04	1.6425D+00
79	4.71618D-01	1.92732D-02	6.79763D-03	1.38840D-04	1.6494D+00
80	4.81502D-01	1.95239D-02	6.86847D-03	1.39196D-04	1.6708D+00
81	4.91730D-01	1.97277D-02	6.94101D-03	1.39179D-04	1.6883D+00
82	5.02023D-01	2.04408D-02	7.01331D-03	1.42723D-04	1.7493D+00
83	5.11825D-01	2.10268D-02	7.08148D-03	1.45402D-04	1.7994D+00
84	5.21895D-01	2.10218D-02	7.15075D-03	1.43959D-04	1.7990D+00
85	5.32482D-01	2.11160D-02	7.22286D-03	1.43161D-04	1.8071D+00
86	5.43260D-01	2.13685D-02	7.29558D-03	1.43428D-04	1.8287D+00
87	5.54181D-01	2.17228D-02	7.36854D-03	1.44363D-04	1.8590D+00
88	5.65183D-01	2.22738D-02	7.44134D-03	1.46577D-04	1.9062D+00
89	5.75869D-01	2.29331D-02	7.51138D-03	1.49509D-04	1.9626D+00
90	5.86653D-01	2.28634D-02	7.58133D-03	1.47679D-04	1.9566D+00
91	5.98138D-01	2.29288D-02	7.65513D-03	1.46674D-04	1.9622D+00
92	6.09727D-01	2.32642D-02	7.72892D-03	1.47398D-04	1.9909D+00
93	6.21371D-01	2.37056D-02	7.80238D-03	1.48781D-04	2.0287D+00
94	6.33041D-01	2.42676D-02	7.87532D-03	1.50898D-04	2.0768D+00

**********Sample printout for 9ghz14m.plt*********

```
 3    1    2
frequency =     9600.0000 mhz
```

18.5	25.0	3.0	3.71	-.11	133.73	137.55	27.7
18.5	25.0	10.0	-8.31	.94	145.74	136.49	33.6
27.8	25.0	3.0	1.66	-.54	139.30	141.50	27.7
27.8	25.0	10.0	-1.61	.84	142.57	140.12	33.6
37.0	25.0	3.0	.08	-.58	143.38	144.04	27.7
37.0	25.0	10.0	.85	.90	142.61	142.56	33.6

LIST OF REFERENCES

1. G.B. Baumgartner Jr, "XWVG : A waveguide program for trilinear tropospheric ducts," Technical Document 610, Naval Ocean Systems Center, San Diego, CA 92152, June 1983.

2. R. Pappert, "Field strength and path loss in a multilayer tropospheric waveguide environment," Technical Note 1366, Naval Ocean Systems Center, San Diego, CA 92152, October 1984.

3. C.L. Pekeris, "Accuracy of the earth-flattening approximation in the theory of microwave propagation," *Physical Review* , Vol. 70, No. 7 and 8, pp. 518-522, October 1946.

4. Milton Abramowitz and Irene A. Stegun, *Handbook of Mathematical Functions* , Dover Publications, Inc., New York, NY 10014, December 1972.

5. Sherman Marcus and William D. Stuart, "A model to calculate EM fields in tropospheric duct environments at frequencies through SHF," Electromagnetic Compatibility Analysis Center Report ESD-TR-81-102, Annapolis, MD 21402, September 1981.

6. R. Pappert and C. Goodhart, "Waveguide calculations of signal levels in tropospheric ducting environments," Technical Note 3129, Naval Electronics Laboratory Center, San Diego, CA 92152, February 1976.

7. Franz E. Hohn, *Elementary Matrix Algebra* , 3rd Edition, Macmillan Company, New York, NY 10022, 1973.

8. P. Beckman and A. Spizzichino, *The Scattering of Electromagnetic Waves from Rough Surfaces* , Macmillan, New York, NY 10022, 1963.

9. C.H. Collie, J.B. Hasted and D.M. Ritson, "The dielectric properties of water and heavy water," *Proc Phys Soc London* , Vol. 60, pp. 145-160, 1948.

10. Lawrence A. Klein and Calvin T. Swift, "An improved model for the dielectric constant of sea water at microwave frequencies," *IEEE Trans. on Antennas and Propagation* , Vol. 25, No. 1, pp. 104-111, January 1977.

11. Hans J. Liebe, "Modelling attenuation and phase of radio waves in air at frequencies below 1000 GHz," *Radio Science* , Vol. 16, No. 6, pp. 1183-1199, November-December 1981.

12. Lamont V. Blake, *Radar Range-Performance Analysis* , Artech House Inc., Norwood, MA 02062, 1986.

13. Donald E. Kerr, *Propagation of Short Radio Waves* , Peter Peregrinus Ltd., London, United Kingdom, 1987.

14. D.G. Morfitt and C.H. Shellman, "MODESRCH, An improved computer program for obtaining ELF VLF LF mode constants in an earth-ionosphere waveguide," Interim Report 77T, Naval Ocean Systems Center, San Diego, CA 92152, October 1976.

15. Lester A. Rubenfeld, *A First Course in Applied Complex Variables* , John Wiley & Sons Inc., 1985.

16. Z. Schulten and D.G.M. Anderson, "An algorithm for the evaluation of the complex Airy functions," *Journal of Computational Physics* , Vol. 31, No. 60-75, pp. 60-75, 1979.

17. Herbert V. Hitney, Juergen H. Richter, Richard A. Pappert, Kenneth D. Anderson and Gerald B. Baumgartner, Jr., "Tropospheric radio propagation assessment," *Proceedings of the IEEE* , Vol. 73, No. 2, pp.265-283, February 1985.

18. K.D. Anderson, "Low-altitude millimeter-wave propagation in the evaporation duct," Technical Report 1300, Naval Ocean Systems Center, San Diego, CA 92152, July 1989.

19. S.L. Broschat, E.I. Thorsos, A. Ishimaru, "The phase perturbation techniques vs. an exact numerical method for random rough surface scattering," *Journal of Electromagnetic Waves and Applications* , Vol. 3, No. 3, pp. 237-256, 1989.

20. Darrell R. Jackson, Dale P. Winebrenner and Akira Ishimaru, "Comparison of perturbation theories for rough-surface scattering," *J. Acoust. Soc. Am.* , No. 83(3), pp. 961-969, March 1988.

21. V. Blanchetiere-Ciarletti, J. Lavergnat, M. Sylvain and A. Weill, "Experimental observation of horizontal refractivity gradients during periods of multipath propagation," *Radio Science* , Vol. 24, No. 6, pp. 705-724, November-December 1989.

22. Se Hyun Cho and James R. Wait, "Electromagnetic wave propagation in a laterally non-uniform troposphere," *Radio Science* , Volume 13, Number 2, pp. 253, March-April 1978.

23. H.V. Hitney and R.A. Paulus, "Integrated refractive effects prediction system (IREPS), interim user's manual," Technical Document 238, Naval Ocean Systems Center, San Diego, CA 92152, March 1979.

24. H.V. Hitney, A.E. Barrios and G.E. Lindem, "Enginner's refractive effects prediction system (EREPS), revision 1.00 user's manual," Technical Document 1342, Naval Ocean Systems Center, San Diego, CA 92152, July 1988.

INITIAL DISTRIBUTION LIST

		No. Copies
1.	Defense Technical Information Center Cameron Station Alexandria, VA 22304-6145	2
2.	Library, Code 0142 Naval Postgraduate School Monterey, CA 93943-5002	2
3.	Research Administration, Code 012 Naval Postgraduate School Monterey, CA 93943-5000	1
4.	Chairman, Code EC Department of Electrical and Computer Engineering Naval Postgraduate School Monterey, CA 93943-5000	1
5.	Professor Hung-Mou Lee, Code EC Lh Naval Postgraduate School Monterey, CA 93943-5000	10
6.	Professor Richard W. Adler, Code EC Ab Naval Postgraduate School Monterey, CA 93943-5000	2
7.	Herbert V. Hitney Code 543 Naval Ocean Systems Center 271, Catalina Blvd San Diego, CA 92152-5000	1
8.	Director, Defence Materials Organisation LEO Building Paya Lebar Airport Airport Road Singapore 1953 Republic of Singapore	4
9.	Kuo-Huei Yen No. 12, Constitution Rd Lin-ya Area Kaoshiung R.O.C., Taiwan	1

10. Lean-Weng Yeoh
#04-161, Blk 123
Serangoon North Ave 1
Singapore 1955
Republic of Singapore

4